

©[2019]

Raheel Fondekar

ALL RIGHTS RESERVED

# **PLASMODIUM c-GMP DEPENDENT PROTEIN KINASE INHIBITORS**

By

RAHEEL FONDEKAR

A thesis submitted to the

School of Graduate Studies

Rutgers, The State University of New Jersey

in partial fulfilment of the requirements

for the degree of

Master of Science

Graduate Program in Medicinal Chemistry

Written under the direction of

David J. Augeri, PhD

and approved by

---

---

---

New Brunswick, New Jersey

October 2019

# ABSTRACT OF THE THESIS

PLASMODIUM c-GMP DEPENDENT

PROTEIN KINASE INHIBITORS

By RAHEEL FONDEKAR

Thesis Director:

David J. Augeri, PhD

Malaria is an infectious parasitic disease affecting vertebrates such as birds and animals including humans. It is caused by unicellular eukaryotes belonging to the genus *Plasmodium* and is transmitted by the bite of the female *Anopheles* mosquitoes. *Plasmodium* are obligate parasites which means they require a vertebrate host and the insect vector to complete their lifecycle. According to one estimate, malaria may have claimed the lives of approximately half the people to have ever walked the face of the earth. The disease-causing *Plasmodium* species have been around for more than a million years. Malaria asserts a deep and harrowing socio-economic effect on malaria-endemic countries. This can be inferred from the fact that most of the malaria-endemic countries are under-developed. Hence, malaria is regarded as the world's most devastating parasitic infection. The disease is endemic to countries close to the equator as the pathogen and the insect vector thrive particularly well in tropical climates. Five species of *Plasmodium* are known to infect humans – *P. falciparum*, *P. vivax*, *P. ovale*, *P. malariae* and *P. knowlesi*. Together, *P. falciparum* and *P. vivax* account for more than 90% of the human infections. The sporozoites of the parasite, introduced into the host body by the bite of the vector, find their way to the liver where they infect hepatocytes. They undergo multiplication and growth

and exit hepatocytes as merozoites. Subsequently, the merozoites begin invading erythrocytes where they feast on the haemoglobin. After undergoing multiplication, the merozoites exit erythrocytes thus causing rupture and destruction of these cells. This phenomenon is attributed to high fever and chills associated with malaria patients.

Malaria eradication relies heavily on pathogen and vector control. Vector control essentially aims to prevent spread of the disease by eliminating *Anopheles* mosquitoes. Pathogen control, on the other hand, is essential for disease treatment and prophylaxis. It is typically accomplished with the use of antimalarial drugs. The most effective antimalarial drug therapy as of today is artemisinin combination therapies (ACTs). However, with the recent rise in artemisinin resistance reported in several countries in Southeast Asia, the urgency to develop new antimalarial drugs is rapidly increasing. In addition, the parasites have long-developed resistance to most of the existing antimalarials like chloroquine, quinine and mefloquine which makes the fight against malaria even more grave.

*Plasmodium* c-GMP dependent protein kinase (PKG) has been extensively researched in recent times as a potential means of pathogen control. The enzyme has been found to have a crucial role in each of the lifecycle stages of the parasite. Studies have shown that parasitic invasion of the hepatocytes, growth related schizogony in the erythrocytes and gametogenesis occurring in the mosquito cycle can all be linked to *Plasmodium* PKG. This makes parasitic PKG a very attractive target not only for malaria treatment, but also for prophylaxis. Trisubstituted pyrrole (TSP) has been identified as a potent and selective inhibitor of parasitic PKG. As a result, PKG inhibitors were synthesized to optimize the activity and selectivity of TSP and to generate a much-needed SAR in order to map the floor of the binding pocket of the enzyme. The optimization process involved introduction of a wide range of substituents at different locations of the TSP structure. A few new scaffolds were also investigated to evaluate activity and further SAR knowledge. In the biological assay performed, TSP (18 nM) and several potent analogues were identified.

## ACKNOWLEDGEMENTS

I would like to extend my sincere gratitude and heartfelt appreciation to my thesis advisor, Dr David Augeri, RUBRIC, Rutgers, The State University of New Jersey, for always being there for me with the best advice and for supporting me unconditionally.

I would also like to thank Dr Longqin Hu, Professor and Department Chair, Department of Medicinal Chemistry, Rutgers University and Dr Edmond LaVoie, Professor, Department of Medicinal Chemistry, Rutgers University, for providing me with the right guidance in attaining my Master's degree.

I would like to extend my appreciation to Elissa Glinn, Administrative Coordinator, Department of Medicinal Chemistry, Rutgers University, for always helping me out with the most cheerful smile.

I would also like to thank our collaborators, Dr Purnima Bhanot, Associate Professor, Rutgers New Jersey Medical School, who is the PI for this program and Dr John Siekierka, Professor, Montclair State University, for performing the biological assays.

I would like to sincerely thank my RUBRIC colleagues, Dr. Jacques Roberge, Mr. John Gilleran, Dr. Bin Cao, Mr. Anthony Bencivenga, Dr. Qisheng Xin and Dr. Qi Qao, Rutgers University, for teaching me the best and most efficient techniques of organic synthesis.

I would like to thank my father, Santosh Fondekar, for providing me with his infinite wisdom and in particular, for always making time to talk to me when I needed him. I would like to thank my mother, Smita Fondekar, for the limitless motivation and positivity that has helped me conquer my toughest challenges. Last, but not least, I would like to thank my sister, Tanya Fondekar, who has been there for me professionally and personally and provided me with oodles of love and encouragement throughout my graduate school life.

## DEDICATION

*I would like to dedicate this thesis to my MOTHER, my FATHER, my SISTER and my ADVISOR, all of whom have supported me professionally and emotionally in order to make my graduate school experience an extremely memorable one.*

# TABLE OF CONTENTS

ABSTRACT.....	ii
ACKNOWLEDGEMENT.....	iv
DEDICATION.....	v
TABLE OF CONTENTS.....	vi
LIST OF TABLES.....	vii
LIST OF FIGURES.....	viii
LIST OF SCHEMES.....	ix
ABBREVIATIONS.....	xi
MALARIA.....	1
PLASMODIUM c-GMP DEPENDENT PROTEIN KINASE (PKG).....	21
PYRROLES.....	38
TRISUBSTITUTED PYRROLE (TSP) AND ITS ANALOGUES.....	51
PLASMODIUM FALCIPARUM PROTEIN KINASE G INHIBITORS.....	64
REFERENCES.....	116
APPENDIX.....	121

## LIST OF TABLES

<b>Table 1.</b>	Biological activity of <i>Plasmodium falciparum</i> PKG Inhibitors.....	65
-----------------	---	----



## LIST OF FIGURES

<b>Figure 1.</b>	Lifecycle of <i>Plasmodium</i> .....	3
<b>Figure 2.</b>	Antimalarial Drugs.....	9
<b>Figure 3.</b>	Antimalarial Drugs.....	13
<b>Figure 4.</b>	Expression of <i>Pb</i> PKG in sporozoites and hepatic stages of <i>P. berghei</i> .....	24
<b>Figure 5.</b>	Impact of TSP on liver stage parasitaemia.....	26
<b>Figure 6.</b>	Target validation of TSP by employing a transgenic TSP-resistant enzyme, PKG T <sub>619</sub> Q-HA, using PKG-HA as control.....	28
<b>Figure 7.</b>	PKG regulates the secretion of micronemal proteins and formation and/or release of merozoites.....	31
<b>Figure 8.</b>	Imidazopyridine-based PKG inhibitors.....	34
<b>Figure 9.</b>	Thiazole-based PKG inhibitors.....	36
<b>Figure 10.</b>	Dipole Moment of Pyrrole and Furan.....	38
<b>Figure 11.</b>	Pyrrole-based natural products and drugs.....	39
<b>Figure 12.</b>	Structure and numbering of 1 <i>H</i> -Pyrrole.....	47
<b>Figure 13.</b>	Optimization of kinase inhibitors leading to the discovery of TSP.....	52

## LIST OF SCHEMES

<b>Scheme 1.</b>	Knorr Synthesis of Pyrroles.....	40
<b>Scheme 2.</b>	Paal-Knorr Synthesis of Pyrroles.....	41
<b>Scheme 3.</b>	Hantzsch Synthesis of Pyrroles.....	41
<b>Scheme 4.</b>	Piloty Synthesis of Pyrroles.....	42
<b>Scheme 5.</b>	Regioselective Ruthenium-Catalyzed Synthesis of Pyrroles.....	43
<b>Scheme 6.</b>	Proposed Mechanisms for the Ruthenium-Catalyzed Synthesis of Pyrroles.....	43
<b>Scheme 7.</b>	Palladium-Catalyzed Oxidative Heck/Oxidative Amination Cascade for the Synthesis of Pyrroles.....	44
<b>Scheme 8.</b>	Proposed Mechanism for the Palladium-Catalyzed Synthesis of Pyrroles...	45
<b>Scheme 9.</b>	Synthesis of Pyrroles by Rhodium-Catalyzed Transannulations of 1,2,3- Triazoles.....	45
<b>Scheme 10.</b>	Proposed Mechanisms for the Rhodium-Catalyzed Synthesis of Pyrroles...	46
<b>Scheme 11.</b>	Electrophilic Aromatic Substitutions of Pyrroles.....	47
<b>Scheme 12.</b>	Vilsmeier-Haack Formylation of Pyrroles.....	48
<b>Scheme 13.</b>	Friedel-Crafts Acylation of Pyrroles.....	49
<b>Scheme 14.</b>	H <sub>2</sub> O <sub>2</sub> oxidation of Pyrroles at neutral pH.....	49
<b>Scheme 15.</b>	H <sub>2</sub> O <sub>2</sub> oxidation of Pyrroles at acidic pH.....	50
<b>Scheme 16.</b>	Hydrogenation of Pyrroles to Pyrrolidines.....	50
<b>Scheme 17.</b>	Synthesis of $\alpha$ -bromoketone <b>88</b> .....	54
<b>Scheme 18.</b>	Synthesis of analogues <b>94A</b> , <b>94B</b> and <b>94C</b> .....	54
<b>Scheme 19.</b>	Synthesis of analogue <b>100</b> .....	55
<b>Scheme 20.</b>	Synthesis of analogues <b>105A</b> and <b>105B</b> .....	56
<b>Scheme 21.</b>	Synthesis of $\alpha$ -bromoketone <b>106</b> .....	56
<b>Scheme 22.</b>	Synthesis of analogue <b>112</b> .....	57
<b>Scheme 23.</b>	Synthesis of analogue <b>114</b> .....	57

<b>Scheme 24.</b>	Synthesis of analogues <b>115</b> , <b>116</b> and <b>117</b> .....	58
<b>Scheme 25.</b>	Synthesis of analogues <b>118</b> and <b>119</b> .....	58
<b>Scheme 26.</b>	Synthesis of analogues <b>121A</b> and <b>121B</b> .....	59
<b>Scheme 27.</b>	Synthesis of analogue <b>125</b> .....	59
<b>Scheme 28.</b>	Synthesis of analogue <b>130</b> .....	60
<b>Scheme 29.</b>	Synthesis of analogue <b>134</b> .....	61
<b>Scheme 30.</b>	Synthesis of bromo diaryl ketone <b>135</b> .....	61
<b>Scheme 31.</b>	Synthesis of analogue <b>139</b> .....	62
<b>Scheme 32.</b>	Synthesis of indole analogue <b>148</b> .....	63

## ABBREVIATIONS

1,2 DME	1,2-dimethoxyethane
AcOH	Acetic acid
Boc	<i>t</i> -Butoxycarbonyl
Br <sub>2</sub>	Bromine
Cbz	Benzyloxycarbonyl
CHCl <sub>3</sub>	Chloroform
CNS	Central Nervous System
DMF	N,N-dimethylformamide
DMSO	Dimethyl sulphoxide
EtOH	Ethanol
HCl	Hydrochloric acid
H <sub>2</sub>	Hydrogen
H <sub>2</sub> SO <sub>4</sub>	Sulphuric acid
K <sub>2</sub> CO <sub>3</sub>	Potassium carbonate
LAH	Lithium aluminium hydride
LDA	Lithium diisopropylamide
LiHMDS	Lithium bis(trimethylsilyl)amide
mCPBA	<i>meta</i> -Chloroperoxybenzoic acid

MeCN	Acetonitrile
MeOH	Methanol
NaBH <sub>4</sub>	Sodium borohydride
Na <sub>2</sub> CO <sub>3</sub>	Sodium carbonate
NaH	Sodium hydride
NaHMDS	Sodium bis(trimethylsilyl)amide
NaOH	Sodium hydroxide
NBS	N-bromosuccinimide
NH <sub>3</sub>	Ammonia
NH <sub>4</sub> OAc	Ammonium acetate
Pd/C	Palladium on carbon
POCl <sub>3</sub>	Phosphorus oxychloride
rt	Room temperature
TMEDA	N,N,N',N'-Tetramethylethane-1,2-diamine
Zn(CN) <sub>2</sub>	Zinc cyanide

## I. MALARIA

### A. INTRODUCTION AND OVERVIEW

Malaria is a parasitic infection transmitted by mosquitoes that has afflicted humans over the millennia. The name malaria is derived from “mala aria”, which in Medieval Italian means “bad air”, as the foul-smelling air in marshy areas was attributed as the cause of the disease.<sup>1</sup> It has also been referred to as *ague* and *intermittent fever* in other parts of the world. The synonym *marsh fever* is based on early knowledge that malaria was associated with swamps and poorly drained areas. Although malaria can be traced to ancient times, it developed into a rampant disease with the advent of farming. Mosquitoes flourished in stagnant water that was in abundance at that time as clearing of land for farming gave rise to ponds. Mosquitoes belonging to the genus *Anopheles* are the insect vectors of this disease. The influx of humans towards agricultural lands contributed to the spread of the disease. Firstly, humans provided the necessary reservoir required by the parasites to grow and multiply. Secondly, they served as blood meals for the mosquitoes, whose survival is clearly imperative for the spread of the disease.

Malaria was widely recognized in ancient Rome by the 4<sup>th</sup> century, BCE. Hippocrates made observations of the intermittent fevers and classified the fever according to periodicity: *tritaios pyretos* (fever every two days or tertian fever) and *tetartaios pyretos* (fever every three days or quartan fever).<sup>2</sup> It is believed that malaria might have contributed to the fall of the Roman Empire and was so pervasive in Rome that it was unpopularly known as the “Roman fever”.<sup>3</sup> Areas in southern Italy, the Pontine Marshes and the city of Rome provided breeding grounds for mosquitoes. Irrigated gardens, swamp-like grounds and drainage problems from road construction led to the increase of standing water.

It was in 1880 that a French army doctor named Charles Louis Alphonse Laveran observed parasites in the red blood cells of infected people for the first time.<sup>3</sup> He proposed that the parasite was responsible for malaria and named it *Oscillaria malariae*. This was the first time

a protist was identified as the cause of the disease and he was later conferred the Nobel Prize for Physiology in 1907. In 1885, the parasite *Oscillaria malariae* was re-examined by biologists, Ettore Marchiafa and Angello Celli, and grouped into a new genus termed *Plasmodium* due to its similarity to multinucleate cells of slime moulds having the same name. Over the next three decades, it was established that four species of *Plasmodium* infect humans: *Plasmodium falciparum*, *Plasmodium vivax*, *Plasmodium ovale* and *Plasmodium malariae*. Around 1965, a fifth species known as *Plasmodium knowlesi* was identified. This species was found to affect long-tailed macaques and indirectly infect humans. The female *Anopheles* mosquito was identified to be the vector for the disease. There are more than 400 different species of the *Anopheles* mosquito, 30 of which are malaria vectors of major importance.<sup>4</sup> All of the important vector species infect by bite between dusk and dawn.

Approximately fifty percent of the world's population live in malaria-endemic regions. The disease is widespread in the tropical and subtropical zones that exist in a broad band around the equator. This includes much of sub-Saharan Africa, Asia and Latin America.<sup>4</sup> Groups of people most susceptible to the disease are infants, pregnant women, HIV/AIDS patients, non-immune refugees and travellers entering endemic regions. Once endemic in the United States and southern Europe, malaria was eradicated from most temperate countries in the 20<sup>th</sup> century.<sup>5</sup> The socio-economic liability of malaria in endemic regions is colossal. An estimated \$12 billion in economic revenue is lost annually in Africa as a result of malaria due to increased healthcare costs, inability of infected locals to work and negative effects on tourism.

Described as an acute febrile illness, symptoms usually appear within 10-15 days of a bite by an infected mosquito in a non-immune individual.<sup>4</sup> The first observed symptoms are generally fever, headache, joint pain and chills. These are usually experienced in many other disease conditions and hence, it is difficult to diagnose malaria purely on the basis of symptoms. The disease may soon progress to jaundice, haemolytic anaemia, and haemoglobinuria. If not treated within 24 hours, *P. falciparum* malaria can progress to cerebral malaria which is characterized by neurological symptoms like convulsions and coma, often leading to death.

## B. LIFECYCLE OF THE PARASITE

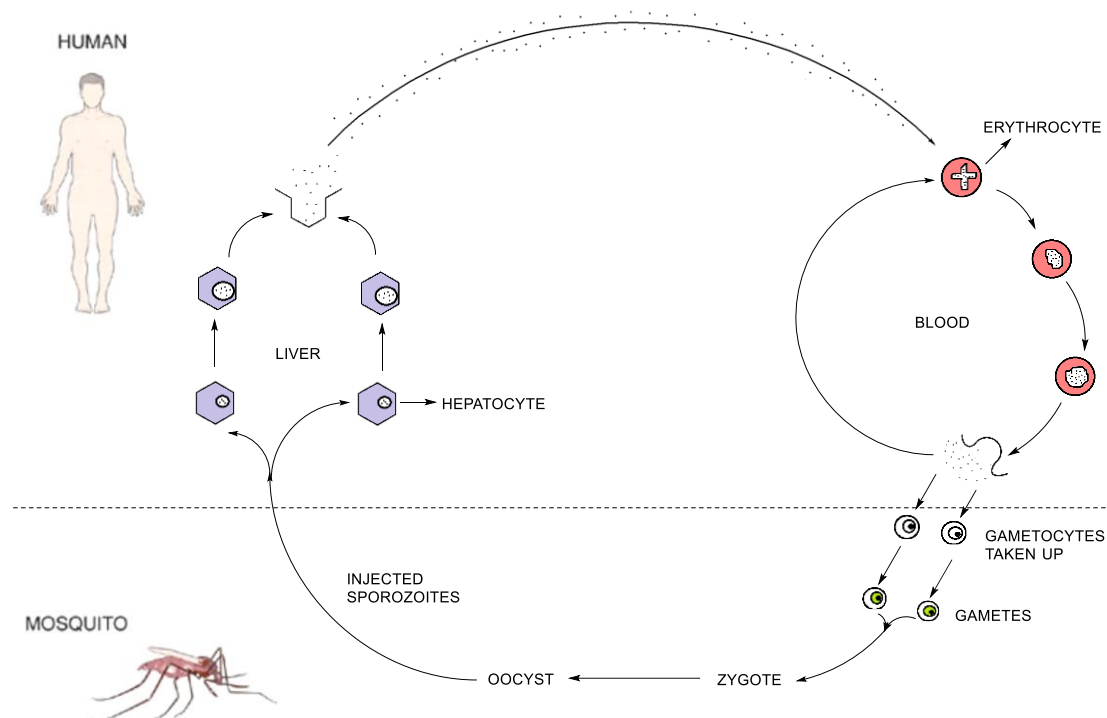


**Figure 1.** Lifecycle of *Plasmodium* <sup>6</sup>

*Plasmodium* is a genus of unicellular eukaryotic protozoa that are obligate parasites of vertebrates and insects. Belonging to the phylum Apicomplexa, they represent a taxonomic group of single cell organisms with secretory organelles at one end of the cell. These organelles, termed as micronemes, are an adaptation that the parasite applies in penetration of the host cell.

The lifecycle of the parasite (**Figure 1**) consists of a sexual cycle, which takes place in the female *Anopheles* mosquito, and an asexual cycle, which occurs in humans.<sup>6</sup> Sporozoites of the parasite get injected into the human bloodstream after an infected mosquito bite. Around 20-100 sporozoites are inoculated in the host's blood after a single mosquito bite. Within 30 minutes, these sporozoites disappear from the bloodstream and invade the hepatic parenchymal cells producing parasitophorous vacuoles. These vacuoles allow the parasite to develop in the hepatocytes while being protected from the host's immune response. The parasite undergoes 13-14 rounds of mitosis and meiosis to give rise to a schizont. The schizont is a multinucleated



stage from which thousands of haploid daughter cells called merozoites emerge. After 10-14 days, the infected hepatocytes rupture and release a batch of fresh merozoites. Some of the merozoites might enter other hepatocytes to give resting forms of the parasite known as hypnozoites (not in case of *P. falciparum*). These hypnozoites are dormant forms of the parasite and can be reactivated months or years later to continue an exoerythrocytic cycle of multiplication.

Most of the merozoites infect erythrocytes. The parasite binds to the erythrocyte and forms a parasitophorous vacuole. The infection occurs in a highly synchronous fashion with roughly all of the parasites throughout the blood in the same stage of development. They enter the erythrocytes and form motile intracellular parasites termed trophozoites. The trophozoites undergo development and multiplication. The host haemoglobin is transported to the parasite's food vacuole, where it is digested providing a source of amino acids. Free haem toxic to the parasite, is polymerized to the non-toxic haemozoin by the parasitic enzyme *haem polymerase*. Following DNA replication and multiple mitotic divisions, the parasite transforms into a schizont again. Each schizont then produces a fresh batch of 10-20 merozoites that exit the ruptured erythrocytes. These merozoites infect fresh erythrocytes and repeat the erythrocytic cycle. The debris from the ruptured erythrocytes is one of the causes of severe fever and chills.

Some merozoites develop into the male and female gametocytes. These are ingested by a mosquito when it bites an infected human. The gametocytes undergo gametogenesis to develop into gametes, which 'mate' and produce a zygote in the insect's mid-gut. The zygote develops into a motile ookinete which lodges into the basal lamina of the mid-gut epithelium and settles as an immotile oocyst. The oocyst undergoes cell division and meiosis to produce thousands of haploid sporozoites. The sporozoites eventually migrate to the mosquito's salivary gland and the cycle begins again when the mosquito bites a new human host.

### C. DIAGNOSIS

Prompt and accurate diagnosis of malaria is part of effective disease management. The signs and symptoms of malaria are quite general. Clinically, malaria is suspected on the basis of very high fever or a history of fever. There is no combination of signs or symptoms that makes malaria easily detectable.<sup>7</sup> This is exactly the reason why healthcare providers insist on parasitological diagnosis. The two methods used routinely for parasitological diagnosis of malaria are light microscopy analysis and immunochromatographic Rapid Diagnostic Tests (RDTs). The latter detect parasite-specific antigens or enzymes that are either genus or species specific.

A proficient pathologist should be able to identify the malarial parasite upon examination of blood smears under the microscope. If light microscopy analysis does not provide conclusive diagnosis, the patient must be directed to take RDTs. RDTs for detecting *Pf*HRP2 (*P. falciparum* Histidine-Rich Protein 2) can be useful in false negative cases.<sup>7</sup> In such cases, patients might have received incomplete antimalarial treatment, and as a result, their blood films turn up negative. This is particularly likely if the patient was recently administered a dose of an artemisinin derivative. If the blood film analysis is negative in patients with symptoms compatible with severe malaria, a series of blood films should be examined after 6–12-hours, or an RDT (preferably one detecting *Pf*HRP2) should be performed. If both the slide examination and the RDT results are negative, then malaria is extremely unlikely, and other causes of the illness should be sought and treated. If both the results turn out to be positive, the patient should be immediately treated with a suitable antimalarial combination therapy.

Before determining a suitable antimalarial therapy for a patient diagnosed with malaria, the disease must first be categorized as either uncomplicated or severe malaria.<sup>8</sup>

#### 1. Uncomplicated malaria

This type of malaria elicits classical symptoms during the malarial attack for 6-10 hours. It consists of three stages: a cold stage, a hot stage and a sweating stage. The cold stage is characterized by cold sensations and shivering. The hot stage consists of fever, headaches and

vomiting. Seizures may also be observed in young children during this stage. Finally, the sweating stage is marked by excessive perspiration, tiredness and the body returning back to normal body temperature. These attacks occur every two days with the tertian parasites (*P. falciparum*, *P. vivax* and *P. ovale*) and every three days with the quartan parasite (*P. malariae*). Physical check-ups may reveal an enlarged spleen, jaundice and an enlarged liver.

## 2. Severe malaria

Severe malaria occurs when infections are complicated by serious organ failure or severe anomalies in the patient's circulatory system.<sup>8-9</sup> The manifestations of severe malaria are cerebral malaria (abnormal behaviour, unconsciousness, convulsions or coma), haemolytic anaemia, haemoglobinuria, acute respiratory distress syndrome (ARDS), thrombocytopenia, renal impairment, hyperparasitaemia (more than 5% of the erythrocytes are infected by malaria parasites), metabolic acidosis and hypoglycaemia. Severe malaria is a medical emergency and should be treated urgently and aggressively.

## D. GENETIC RESISTANCE TO MALARIA

Disease-causing microorganisms evolve and mutate in order to protect themselves against drugs and other agents. Similarly, the human body, when placed under severe stress due to a malaria parasite, develops certain resistive mechanisms to ward off a pathogen. As a result, such genetic resistance is predominantly seen in populations residing in endemic regions. Six of the most important mutations are sickle cell anaemia or sickle cell disease, glucose-6-phosphate dehydrogenase (G6PD) deficiency, various thalassaemias, increased nitric oxide (NO) production, haemoglobin C and pyruvate kinase deficiency.<sup>1</sup> Each mutation, in its own way, can disable the pathogen and hence, these variations are referred to as acquired immunity. However, each mutation has certain adverse effects and as such, this form of immunity is not always desirable. Additionally, antimalarial drugs might produce drastic life-threatening complications in such individuals.

It is said that increased levels of glutathione in the erythrocytes of G6PD patients prevent the parasite from maturing. Alternatively, G6PD patients suffering from malaria cannot be administered certain antimalarials as they elicit haemolytic anaemia and prehepatic jaundice. Heterozygotes with sickling disease are usually asymptomatic and are 90% less likely of succumbing to death by *P. falciparum* malaria.<sup>10</sup> Homozygotes on the other hand, inherit two copies of the haemoglobin S gene and suffer from severe sickling disease which is implicated in serious life-threatening complications. Erythrocytes lack mitochondria and are therefore, heavily dependent on pyruvate kinase for their ATP needs. As a result, the parasite finds it difficult to grow and reproduce in the erythrocytes of patients with pyruvate kinase deficiency.

#### E. DRUG THERAPY

Antimalarial drugs constitute an integral and indispensable component in the fight against malaria. Of protozoan origin, the biochemistry of *Plasmodium* is similar to that of mammals, making parasite selectivity a critical aspect. Like mammalian cells, *Plasmodium* are eukaryotes and lack cell walls. They are motile and cannot synthesize carbohydrates from small molecules.

Research on antimalarial drugs received an impetus during World War II.<sup>1</sup> Between 1941 and 1946, more than 15,000 compounds were synthesized and screened for the treatment of malaria by the United States, Australia and Great Britain. Research in this field witnessed an upsurge again during the Vietnam War, especially because of growing resistance to most of the antimalarials at that time. From 1968 to 1978, more than 250,000 compounds were investigated as part of a US Army research initiative.<sup>11</sup>

The following list of antimalarials drugs provides a brief account of some of the most effective and relevant medications used currently.

1. Quinine ((R)-(6-methoxyquinolin-4-yl)((1S,2S,4S,5R)-5-vinylquinuclidin-2-yl)methanol)

Quinine (**Figure 2**) is a cinchona alkaloid derived from the bark of trees belonging to the genus *Cinchona*. These trees are indigenous to the tropical Andean forests of western South America. Quinine has been used for the treatment of ‘fevers’ since the 16<sup>th</sup> century, when Jesuit missionaries brought the bark to Europe from Peru.<sup>6</sup> It is a blood schizonticide and has no effect on sporozoites, hypnozoites (*P. vivax*) and gametocytes, together referred to as exoerythrocytic forms. Its mechanism of action has not yet been fully resolved, but it is theorized to inhibit the protozoal enzyme *haem polymerase*, similarly to chloroquine. ‘Cinchonism’ characterized by nausea, dizziness, tinnitus, headache and blurring of vision, is a common adverse effect of quinine if the plasma concentration exceeds 30-60  $\mu\text{mol/L}$ . Other unwanted effects include retinopathy, thrombocytopenia, cardiac dysrhythmias, hypotension and CNS disturbances leading to delirium and coma. Its use as an antimalarial reduced significantly after the discovery and emergence of chloroquine in the 1940s. However, the use of quinine has been re-established with the emergence and spread of chloroquine-resistant and more recently, multiple drug resistant strains of malarial parasites.

2. Mefloquine ((S)-(2,8-bis(trifluoromethyl)quinolin-4-yl)((R)-piperidin-2-yl)methanol)

Mefloquine, a quinoline-methanol like quinine, was formulated at the Walter Reed Army Institute of Research (WRAIR) during the Vietnam War.<sup>1</sup> The drug was marketed worldwide by Hoffmann-LaRoche under the trade name Lariam®. This marked the first Public-Private Venture between the US Department of Defense and a pharmaceutical company. Mefloquine is a very potent blood schizonticide and is chemically similar to quinine with the quinuclidine ring of quinine replaced with a substituted piperidine (**Figure 2**). It is said to exert its antimalarial effect by forming toxic haem complexes that damage parasitic food vacuoles.<sup>6,9</sup> It is also active against the gametocytes of *P. vivax*, *P. ovale* and *P. malariae*. Mefloquine is used

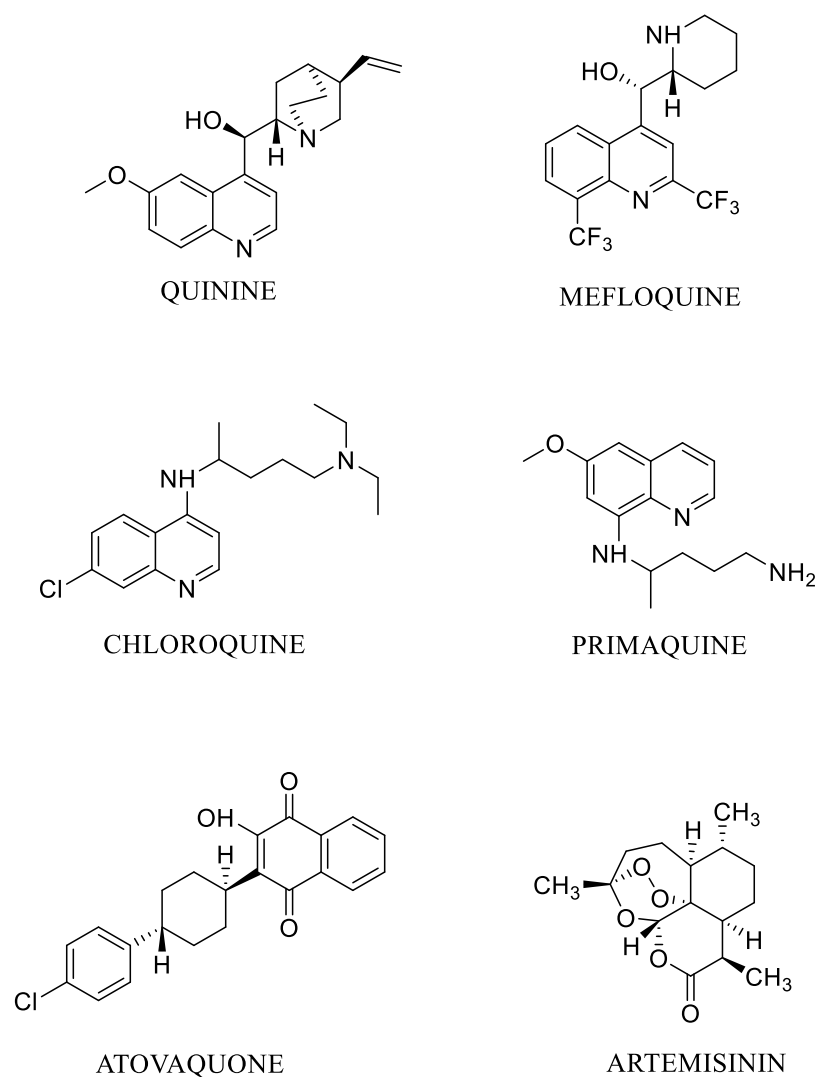


**Figure 2.** Antimalarial drugs

in combination with artemisinin and its derivatives for the treatment of malaria induced by multi-drug resistant *P. falciparum*.

### 3. Chloroquine (N4-(7-chloroquinolin-4-yl)-N1,N1-diethylpentane-1,4-diamine)

Until recently, chloroquine was the most widely used anti-malarial. It was discovered in 1934 by Johann Andersag while working at Bayer AG and was marketed under the trade name Resochin®. Chloroquine (**Figure 2**) is used as a blood schizonticide against all four human-infecting plasmodial species (where resistance is not an issue).<sup>6, 9</sup> It has no effect on the exoerythrocytic forms of the parasite. It is uncharged at neutral pH and can therefore diffuse

freely into the parasitic lysosome. At the acidic pH of the lysosome, it is converted to a protonated, membrane-impermeable adduct that is trapped inside the parasite's food vacuole. Its chief antimalarial action derives from an inhibition of *haem polymerase*, the enzyme that polymerises toxic free haem to haemozoin. Inhibition of the biocrystallization of haem poisons the parasite and prevents it from utilising the amino acids from haemoglobin proteolysis. Adverse effects include retinopathy, haemolysis in G6PD deficient patients, porphyria and exacerbation of psoriasis. The majority of the strains of *P. falciparum* are now resistant to chloroquine in most parts of the world.<sup>12</sup> This resistance appears to result from enhanced efflux of the drug from the parasitic vesicles due to mutations in the plasmodium transporter gene *pfcr*. Historically, chloroquine is one of the least expensive, extensively tested and least toxic antimalarial drugs.

Amodiaquine, also a 4-aminochloroquinoline is a noteworthy antimalarial belonging to this chemotype. Its mechanism of action is similar to that of chloroquine. It is administered in areas of chloroquine resistance and is reported to cause less pruritus than chloroquine in some patients.<sup>9</sup>

#### 4. Primaquine (N4-(6-methoxyquinolin-8-yl)pentane-1,4-diamine)

Primaquine, a vital drug in the treatment of malaria, is an analogue of pamaquine, the first 8-aminoquinoline antimalarial drug. Primaquine (**Figure 2**) lacks the diethyl substituents on the amino moiety as present in pamaquine. Primaquine is highly effective against the liver hypnozoites of *P. vivax* and can, thereby, effect radical cure of *P. vivax* induced malaria.<sup>6</sup> It also has gametocytocidal activity against all four human infesting species, in particular *P. falciparum*, and is the most effective antimalarial drug for preventing transmission of the disease.<sup>1, 6</sup> It does not affect the sporozoites and has little to no action against the erythrocytic stage of the parasite. Primaquine's mechanism of action is not entirely clear but, it is believed to disrupt the parasite's mitochondria by blocking oxidative metabolism. Primaquine is contraindicated in patients with G6PD deficiency as it can lead to haemolytic anaemia.

Etaquine and tafenoquine are newer analogues in this series. They are more active and slowly metabolized as compared to primaquine.

5. Atovaquone (2-((1*r*,4*r*)-4-(4-chlorophenyl)cyclohexyl)-3-hydroxynaphthalene-1,4-dione)

It is a hydroxynaphthoquinone drug (**Figure 2**) used prophylactically to prevent malaria and to treat cases resistant to other drugs.<sup>6</sup> It is active against the erythrocytic stages of the parasite. Atovaquone inhibits the parasite mitochondrial electron transport chain in the respiratory cycle, possibly by mimicking the natural substrate ubiquinone. It is usually used in combination with the antifolate drug, proguanil, because they act synergistically. Resistance to atovaquone has swiftly developed from a single point mutation in the gene coding for cytochrome b.

6. Artemisinin ((3*R*,5*aS*,6*R*,8*aS*,9*R*,12*S*,12*aR*)-3,6,9-trimethyloctahydro-12*H*-3,12-epoxy [1,2]dioxepino[4,3-*i*]isochromen-10(3*H*)-one) and related compounds

Artemisinin is a sesquiterpene lactone derived from the Chinese herb *qing hao*, a traditional Chinese therapy used for over 1000 years to treat high fever.<sup>6,9</sup> The scientific name of the herb is *Artemisia annua*. In 1972, the Chinese chemist, Tu Youyou, discovered and isolated Artemisinin from the leaves of the herb. Artemisinin contains an unusual peroxide bridge as shown in **Figure 2** and, this endoperoxide 1,2,4-trioxane ring is responsible for the drug's mechanism of action. Upon administration, artemisinin is converted to its active metabolite, dihydroartemisinin. This metabolite is said to inhibit the parasite's Ca-dependent ATPase and, it is possible that the endoperoxide bridge of this drug has to be activated in the presence of intracellular iron before it exerts its effects. It is rapidly active against the erythrocytic stage of the parasite and is considered to be the most effective blood schizonticide. It has no effect on the hepatic forms of the parasite. Artesunate, a water-soluble derivative, and the semi-synthetic analogues, artemether and artether, have higher activity as they are better absorbed. Chemically, artesunate is a hemisuccinate derivative of the active metabolite, dihydroartemisinin, whereas artemether is the methyl ether of dihydroartemisinin. Clinical evidence of artemisinin drug resistance in Southeast Asia was first reported in 2008.<sup>13-14</sup>



#### 7. Pyrimethamine (5-(4-chlorophenyl)-6-ethylpyrimidine-2,4-diamine)

Chemically a diaminopyrimidine, pyrimethamine (**Figure 3**) is a slow acting blood schizonticide and is used in the treatment of uncomplicated malaria.<sup>9</sup> It inhibits the enzyme dihydrofolate reductase (DHFR) in the parasite which ultimately prevents the biosynthesis of purines and pyrimidines, and thereby arrests the processes of DNA replication, cell division and reproduction. It is particularly useful for the treatment of chloroquine-resistant *P. falciparum* malaria when combined with a sulphonamide such as sulphadoxine. Pyrimethamine-resistant strains are prevalent worldwide.

#### 8. Proguanil (1-[amino-(4-chloroanilino)methylidene]-2-propan-2-ylguanidine)

Chemically a biguanide as shown in **Figure 3**, proguanil is essentially a prodrug that is converted to its active metabolite, cycloguanil.<sup>9</sup> Cycloguanil functions as an inhibitor of DHFR and thereby, blocks the biosynthesis of purines and pyrimidines, in particular deoxythymidylate. It is a slow-acting blood schizonticide and is always used in combination with atovaquone or chloroquine. Proguanil is mostly used as a prophylactic therapy for people from non-endemic areas travelling to malaria-endemic regions.

#### 9. Sulphadoxine (4-(((5,6-dimethoxypyrimidin-4-yl)methyl)sulfonyl)aniline)

It is chemically a sulphonamide, and this class of drugs acts as a specific inhibitor of the enzyme dihydropteroate synthetase. This enzyme lies upstream to DHFR in the biosynthetic pathway of nucleotide bases. Sulphadoxine (**Figure 3**) is a structural analogue to p-aminobenzoic acid (PABA) and competes with PABA to inhibit its conversion to dihydrofolic acid. It is a long-acting blood schizonticide and is not effective when used alone.<sup>1</sup> It is always formulated in combination with pyrimethamine and this combination is marketed under the brand name Fansidar®.

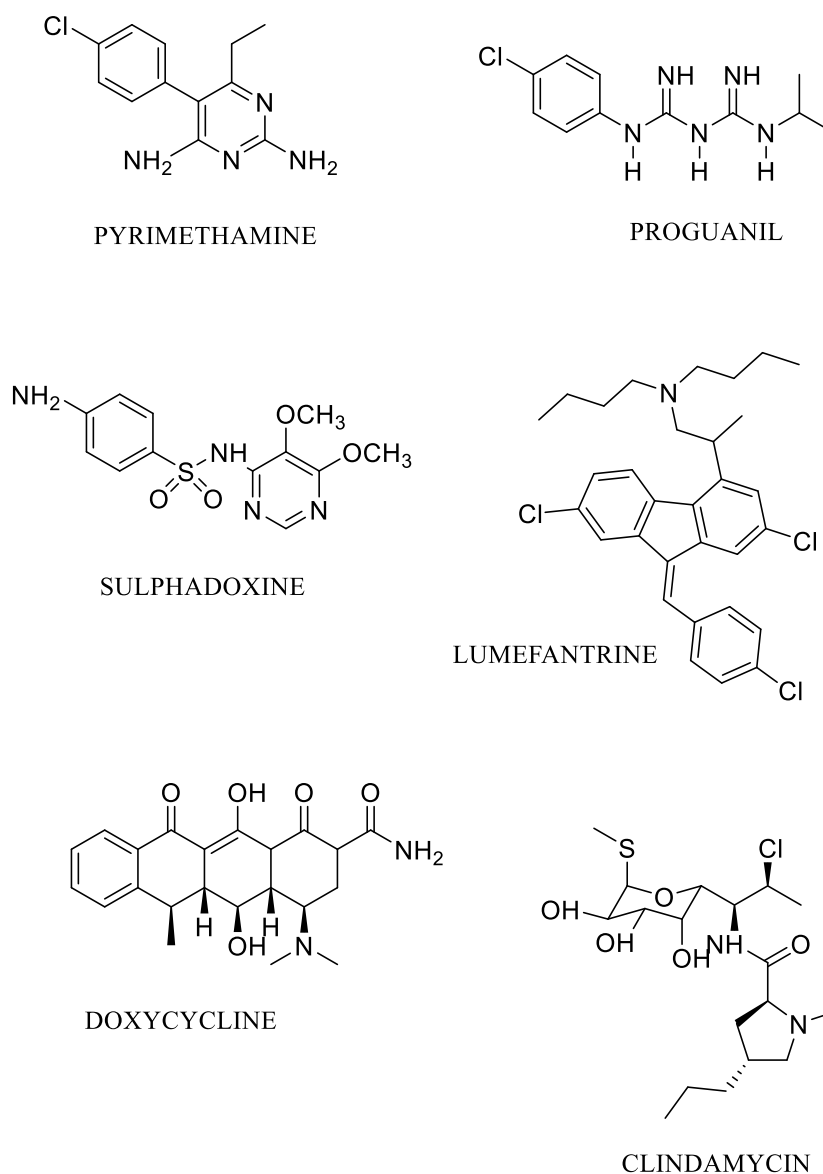


**Figure 3.** Antimalarial drugs

10. Lumefantrine ((Z)-N-butyl-N-(2-(2,7-dichloro-9-(4-chlorobenzylidene)-9H-fluoren-4-yl)propyl)butan-1-amine)

This aryl amino alcohol drug is a relatively new analogue of the drug halofantrine. Halofantrine was often used in the past but is rarely used today.<sup>6</sup> Lumefantrine (**Figure 3**) is a blood schizonticide that is never used alone. It is typically used in combination with artemether. Its pharmacological action is brought about by a possible interference in the parasite's detoxification process of haem. It is also said to be effective against hepatic merozoites before they invade the erythrocytes.

11. Doxycycline ((4R,4aR,5S,5aR,6R)-4-(dimethylamino)-5,12-dihydroxy-6-methyl-1,11-dioxo-1,2,3,4,4a,5,5a,6,11,12a-decahydrotetracene-2-carboxamide)

As seen with other tetracyclines, doxycycline is effective by binding to the parasite's 30S ribosomal subunit. This prevents the 30S and 50S subunits from binding and thus inhibits the process of protein synthesis.<sup>1,9</sup> Although doxycycline (**Figure 3**) is a good antibacterial, its use for malaria is limited to prophylaxis against strains of *P. falciparum* that are resistant to chloroquine and sulphadoxine-pyrimethamine. Like other tetracyclines, it can chelate calcium and, it is usually not administered to children.

12. Clindamycin ((2S,4R)-N-((1S,2S)-2-chloro-1-((2R,3R,4S,5R,6R)-3,4,5-trihydroxy-6-(methylthio)tetrahydro-2H-pyran-2-yl)propyl)-1-methyl-4-propylpyrrolidine-2-carboxamide)

7-chloro-lincomycin or clindamycin as shown in **Figure 3** is a semi-synthetic derivative of lincomycin.<sup>15</sup> These drugs belong to a class of antibiotics known as lincosamides. Clindamycin was introduced in the 1960s as an alternative to lincomycin with an improved side effect profile. It inhibits parasitic protein synthesis by binding to the 50S ribosomal subunit. Popularly used for bacterial infections, clindamycin can be used as an antimalarial only when given in combination with quinine. Clindamycin (marketed as Cleocin®) is never prescribed as a monotherapy for the treatment of malaria. The combination of quinine and clindamycin is useful in cases of chloroquine resistant *P. falciparum* malaria and for treating uncomplicated *P. falciparum* malaria in pregnant women. A major adverse effect of clindamycin is the ability of the drug to destroy probiotic bacteria residing in human intestines. These probiotic bacteria are essential to the body to ward off pathogens such as *Clostridioides difficile*. Termination of such beneficial probiotic bacteria by clindamycin makes the body susceptible to *C. difficile* pseudomembranous colitis infections.

There are different clinical combination therapy regimens for treating malaria. The regimen chosen is dependent on the classification of the disease.

a. Treatment of uncomplicated *P. falciparum* malaria <sup>16</sup>

Children and adults with uncomplicated *P. falciparum* malaria (except pregnant women in their first trimester) must be treated for a period of three days with one of the following recommended Artemisinin Combination Therapies (ACTs): artemether and lumefantrine, artesunate and amodiaquine, artesunate and mefloquine or artesunate and sulphadoxine-pyrimethamine (SP). Pregnant women with uncomplicated *P. falciparum* malaria during the first trimester must be treated with a combination therapy of quinine + clindamycin for a period of seven days.

b. Treatment of uncomplicated malaria caused by *P. vivax*, *P. malariae*, *P. ovale* or *P. knowlesi* <sup>17</sup>

Children and adults with uncomplicated *P. vivax*, *P. malariae*, *P. ovale* or *P. knowlesi* malaria (except pregnant women in their first trimester) are treated with an ACT. Chloroquine may be used in areas with chloroquine-susceptible infections. Pregnant women in their first trimester must be treated with quinine. To prevent relapse, children and adults (except pregnant women, infants aged less than six months, women breastfeeding infants less than six months and people with G6PD deficiency) suffering from *P. vivax* or *P. ovale* malaria must be treated with a 14-day course of primaquine. Pregnant and breastfeeding women should consider weekly chemoprophylaxis with chloroquine until delivery and breastfeeding are complete, following which, they should be treated with primaquine. Individuals with G6PD deficiency must follow up with a single weekly dose of primaquine for 8 weeks under close medical supervision.

c. Treatment of severe malaria <sup>18</sup>

Children and adults suffering from severe malaria (including infants, pregnant women in all trimesters and lactating women) must be treated with intravenous or intramuscular artesunate

for at least 24 hours and until they can tolerate oral medication. Once both the criteria are met, complete treatment with 3 days of an ACT is recommended.

## F. PREVENTIVE MEASURES

In diseases such as malaria, prevention is key. These measures not only reduce the number of cases or incidence of the disease, but if implemented correctly, they can potentially eliminate the disease from our planet. As seen earlier, the mosquito is the definitive host for the parasite. The only objective of infecting humans is to facilitate the parasite to infect more mosquitoes so that sexual recombination can occur.<sup>6</sup> Hence, it is extremely crucial to control the transmission of the disease. This may be achieved in several ways:

### 1. Vaccination

The complex nature of the parasite and its interactions with the human red blood cells provide a large number of sites for the immune system to elicit its response.<sup>1</sup> An ideal vaccine should, at a minimum, be effective against both *P. falciparum* and *P. vivax*, the two species responsible for 90% of malarial cases. RTS,S/AS01 also known as Mosquirix is an injectable vaccine that provides partial protection against malaria in young children. It contains surface proteins from the sporozoite stage, meaning it is designed for the immune system to kill the parasite as it enters the patient's blood from the mosquito before the parasite infects the liver. As the number of immune individuals increases, there will be fewer human "reservoirs" in which the parasite can multiply. WHO has announced that the RTS,S vaccine would be rolled out in pilot projects in selected areas of 3 countries in sub-Saharan Africa: Ghana, Kenya and Malawi. The initial phase of this programme was due to begin in early 2019.<sup>4</sup>

### 2. Insecticide-Treated mosquito Nets (ITNs)

ITNs are used to effect vector control i.e. such methods aim to decrease malaria incidence by reducing the levels of transmission by mosquitoes. ITNs help keep mosquitoes away from people and are extremely effective in controlling spread of the disease. Simple bed nets do not

provide a perfect barrier and are therefore, often treated with an insecticide designed to kill the mosquito before it can find a way past the net. Between 2000 and 2008, the use of ITNs has prevented an estimated 250,000 infants in sub-Saharan Africa from contracting the disease.<sup>9</sup> Most nets are impregnated with pyrethroids, a class of insecticides with low toxicity. Commonly used pyrethroids are permethrin or deltamethrin. It is highly recommended to re-impregnate ITNs with a suitable insecticide every 6 months. WHO recommends Long-lasting Insecticidal Nets (LLINs) for all people at risk of malaria.<sup>4</sup>

### 3. Indoor Residual Spraying (IRS)

Insecticide-based mediations have led to ~78% of the reduction in the malaria burden in sub-Saharan Africa since 2000.<sup>19</sup> IRS is also a vector control treatment. It is carried out by spraying insecticides on the walls inside a house.<sup>9</sup> It is a powerful way to rapidly reduce malaria transmission. Usually, after feeding on human blood, mosquitoes tend to rest on nearby surfaces in order to digest their meal. These surfaces are often walls inside human establishments. WHO recommends insecticides, like DDT and the pyrethroids, cyfluthrin and deltamethrin, usually be sprayed on the walls indoors to target such resting mosquitoes.<sup>4</sup> Other classes of insecticides used are carbamates and organophosphates. Pyrethroids and the organochlorine DDT share the same target site, the voltage-gated sodium channel, while carbamates and organophosphates are acetylcholinesterase inhibitors.

### 4. Other methods of malaria prevention

Decreasing the availability of stagnant water by installing and maintaining good drainage systems, can significantly reduce mosquito breeding.<sup>9</sup> Introduction of mosquito larvae eating fish into ponds and stagnant waters is also gaining momentum. Use of electronic mosquito-repellent devices and mosquito-repellent creams contribute substantially. Community participation and health education strategies promoting awareness and the importance of control measures have been successfully used to curb the incidence of malaria.

## G. RESISTANCE

Resistance to antimalarial drugs is a growing and recurring problem. The development of resistance to antimalarial drugs poses one of the greatest threats to malaria control and results in increased malaria morbidity and mortality.<sup>14</sup> Resistance to currently available antimalarial drugs has been confirmed for two parasite species, *P. falciparum* and *P. vivax*. De novo emergence of such resistance requires the spontaneous arising of mutations or gene duplications conferring reduced drug susceptibility. For the resistant parasite, gene alteration should not affect its own functioning to a large extent. Drug-resistant mutations can arise in the parasitic sexual stage in the mosquito (where diploidy and meiosis occur), in the pre-erythrocytic liver stages or in the asexual erythrocytic stage.

*P. falciparum* resistance to previous generations of medicines, such as chloroquine and sulphadoxine-pyrimethamine, became widespread in the 1950s and 1960s, undermining malaria control efforts and reversing gains in child survival. Chloroquine-resistant *P. vivax* was first identified somewhere near Papua, New Guinea. Though identified in other regions of the world, *P. vivax* malaria parasites, particularly from Oceania, demonstrate greater resistance to chloroquine than *P. vivax* isolates from other regions of the world.<sup>8</sup> Resistant forms of both species have been shown to develop an efflux pump mechanism to discharge the drug out from its cell. In recent years, parasite resistance to artemisinin has been detected in 5 countries of the Greater Mekong subregion: Cambodia, Laos, Myanmar, Thailand and Vietnam. Additional pockets of resistance have emerged independently in new geographic areas of the subregion.<sup>13-</sup>

<sup>14</sup> Concomitant emergence of partner drug resistance is now causing high ACT treatment failure rates in several areas. Single point mutations in the gene coding for the Kelch propeller domain of the K13 protein strongly correlate with artemisinin resistance.

History shows that antimalarial drug resistance in *Plasmodium falciparum* tends to emerge in low-transmission settings, in particular Southeast Asia and South America, before expanding to high-transmission settings in sub-Saharan Africa.<sup>13</sup> Southeast Asia has been the cradle, in the

last few decades, for the emergence of *P. falciparum* resistance to chloroquine, sulphadoxine-pyrimethamine, mefloquine and more recently to artemisinins.

Recently, evolved female *Anopheles* mosquitoes have demonstrated resistance to pyrethroids, organochlorines, carbamates and organophosphates used for IRS.<sup>19</sup> Insecticide resistance in malaria vectors could presage a catastrophic rebound in disease incidence and mortality. This is posing a major challenge in the fight to control the spread of malaria as much of the success in controlling the disease is by vector control.

## H. GLOBAL IMPACT OF MALARIA

In 2017, almost half of the world's population was at risk of malaria.<sup>20</sup> There were an estimated 219 million cases of malaria in 90 countries, an increase of 2 million cases over the previous year. The global tally of malaria deaths reached 435,000, about the same number reported in 2016. The WHO African Region bears a major share of the global malaria burden. In 2017, this region accounted for 92% of malaria cases and 93% of malaria deaths. Five countries accounted for nearly half of all malaria cases worldwide: Nigeria (25%), the Democratic Republic of Congo (11%), Mozambique (5%), India (4%) and Uganda (4%). Children under the age of 5 are the most susceptible to infection, illness and death. More than 70% of all malaria deaths occur in this age group, such that one child succumbs to death as a result of malaria infection every two minutes.

In 2017, *P. falciparum* accounted for 99.7% of all malaria cases in the WHO Africa Region. The same parasite was accountable for the majority of cases in the WHO regions of the Western Pacific (71.9%), the Eastern Mediterranean (69%) and South-East Asia (62.8%). *P. vivax* is the predominant parasite in the WHO Region of the Americas, representing 74.1% of malaria cases there. The total funding for malaria control in 2017 was estimated to be \$3.1 billion. All these statistics indicate that malaria is a major disease infecting and killing humans. In an effort to



eradicate the disease from the face of the earth, it is extremely imperative to develop new antimalarial drugs that target novel biological pathways.

## II. PLASMODIUM c-GMP DEPENDENT PROTEIN KINASE (PKG)

### A. PLASMODIUM PKG: BACKGROUND

The emergence and spread of artemisinin-resistant *P. falciparum* in Southeast Asia is a critical indication of the need to discover new targets for the global eradication of malaria. The first obligate step of the malarial parasite in the mammalian cycle is the infection of hepatocytes by sporozoites. The increase in parasite numbers at this stage enables the parasite to establish a reservoir in the human host.<sup>21</sup> The discovery of the vaccine RTS,S/AS02A has brought to light a very crucial observation - Diminishing sporozoite infection of the liver helps reduce the incidence and severity of the disease.<sup>22</sup> Additionally, blocking the invasion of hepatocytes would inhibit *P. vivax* hypnozoite formation, the major cause of disease relapse. In principle, it implies that drugs targeting the sporozoites and hepatic stages of the parasite ought to be the most pivotal component in the antimalarial effort. Therefore, it is essential to focus resources in this area of antimalarial research.

Sporozoites bear some similarities to other parasitic stages like ookinetes and merozoites, but they display certain unique characteristics.<sup>23</sup> Sporozoites exhibit enhanced motility over a large distance as they travel from the site of inoculation in the dermis to the hepatocytes. They traverse through several cells by encroaching their plasma membranes. Once they encounter suitable hepatocytes, they alter their mode of cell entry to one which involves the formation of a parasitophorous vacuole that serves as the site for further development. *Plasmodium* ookinetes, like sporozoites are motile and drift through the mosquito midgut epithelium but, their invasion does not involve the formation of a parasitophorous vacuole. *Plasmodium* merozoites, on the other hand, invade erythrocytes and do form parasitophorous vacuoles, but they are immotile and do not breach through cells.

It was hypothesized that molecular signals might be involved that allow sporozoites to know where they are and decide whether to continue to migrate or prepare for cell invasion.<sup>24</sup> It was suggested that on proteolytic cleavage of the major surface protein, the circumsporozoite (CS)

protein, the sporozoite could recognize different cell types. CS protein is processed by a parasitic cysteine protease belonging to the papain family and cleavage is specifically associated with invasion and not cell traversal. Coppi, et al., demonstrated that sporozoite invasion of hepatocytes is mediated through a cascade of signalling events triggered by the communication between the CS protein on the sporozoite surface and the highly negatively-charged heparan sulphate proteoglycans on the hepatocyte.<sup>25</sup> Sporozoites of the rodent malaria parasite *Plasmodium berghei* detect the sulphation level of heparan sulphate proteoglycans (HSPGs) to maneuver within the mammalian host. Contact with cells expressing low-sulphated HSPGs leads to migration of sporozoites through these cells, such as those in the dermis and endothelium. In contrast, contact with highly sulphated HSPGs of hepatocytes inhibits migration and activates sporozoites for invasion. These signalling interactions between the CS protein and hepatocytes has certain implications. It regulates various processes in the sporozoite such as cleavage of the CS protein, secretion of essential proteins needed for cellular invasion,  $\text{Ca}^{2+}$  mediated signalling and refining of surface adhesin molecules.

Studies have indicated that *Plasmodium* parasites rely on the controlled release of  $\text{Ca}^{2+}$  from intracellular stores to activate stage-specific  $\text{Ca}^{2+}$  dependent protein kinases (CDPKs).<sup>26</sup> Reverse genetics and pharmacological studies have identified 3'-5'-cyclic guanosine monophosphate (cGMP) as an important second messenger. The only known downstream target of cGMP in malaria parasites is a cGMP-dependent protein kinase (PKG). PKG was discovered in *Eimeria* and *Toxoplasma* as the target for potent anticoccidial inhibitors. These inhibitors achieve selectivity over vertebrate PKG by exploiting the small gatekeeper residue typically found in the PKG of Apicomplexa, including malaria parasites.<sup>27</sup> Baker, et al., used PKG inhibitors, in conjunction with transgenic strains of *Plasmodium* expressing inhibitor-insensitive mutant PKG enzyme, to demonstrate that PKG is vital for gametogenesis.<sup>28</sup> They also verified that intracellular  $\text{Ca}^{2+}$  is needed for differentiation and acts downstream to PKG. Subsequently, the role of PKG in the asexual blood-stage of the parasite's lifecycle was elucidated by the same group. It was observed that *P. falciparum* PKG (PfPKG) has a central

role in *P. falciparum* schizogony.<sup>29</sup> In addition to these studies, utilizing the motility of *P. berghei* ookinetes, it was discovered that PKG is directly responsible for the elevated levels of cytosolic  $\text{Ca}^{2+}$  required for gliding motility.<sup>26</sup> Analysis of cellular phospholipid levels demonstrated that in motile ookinetes, PKG regulates phosphoinositide biosynthesis. Accordingly, egress of *P. falciparum* merozoites from erythrocytes is associated with PKG directed phosphoinositide metabolism. This collection of experiments suggests that PKG could serve a primary role in the invasion of hepatocytes by sporozoites.

## B. EXPRESSION OF PKG IN P. BERGHEI SPOROZOITES AND HEPATIC FORMS

While the presence of PKG and its functions were established in gametocytes, erythrocytic merozoites and ookinetes,<sup>26, 28-29</sup> its expression in sporozoites and liver stages of the parasite had to be confirmed. Using immunofluorescence assays (IFA), the expression of human influenza haemagglutinin (HA) tagged *P. berghei* PKG was examined.<sup>23</sup> HA (Human Influenza haemagglutinin) is a surface glycoprotein of the human influenza virus that is commonly used by biologists as an epitope tag. An anti-HA antibody was used for immunostaining to aid in the visualization of HA-tagged *PbPKG*. Anti-Exp1, an antibody that detects the Exp1 protein localized in the membrane of the parasitophorous vacuole, was employed to enable its visualization. Merged images included DAPI (4', 6-diamidino-2-phenylindole) as a nuclear marker. It was observed that all the sporozoites and liver stages were found to express HA-tagged PKG in the cytoplasm as shown in **Figure 4A**. This implies that PKG performs critical functions that enable these parasitic stages to grow and sustain themselves in the mammalian host.

The next experiment carried out was to determine the presence of PKG in conditional gene knockout *P. berghei* sporozoites and liver stages.<sup>23</sup> Salivary gland sporozoites developed by ablation of the *PbPKG* open reading frame in developing midgut sporozoites (*PbPKG* cKO) were analysed for the expression of *PbPKG*. Polyclonal antisera generated against a carboxy terminal peptide of *PbPKG* (amino acids 988-1001) were used to confirm *PbPKG* in sporozoites

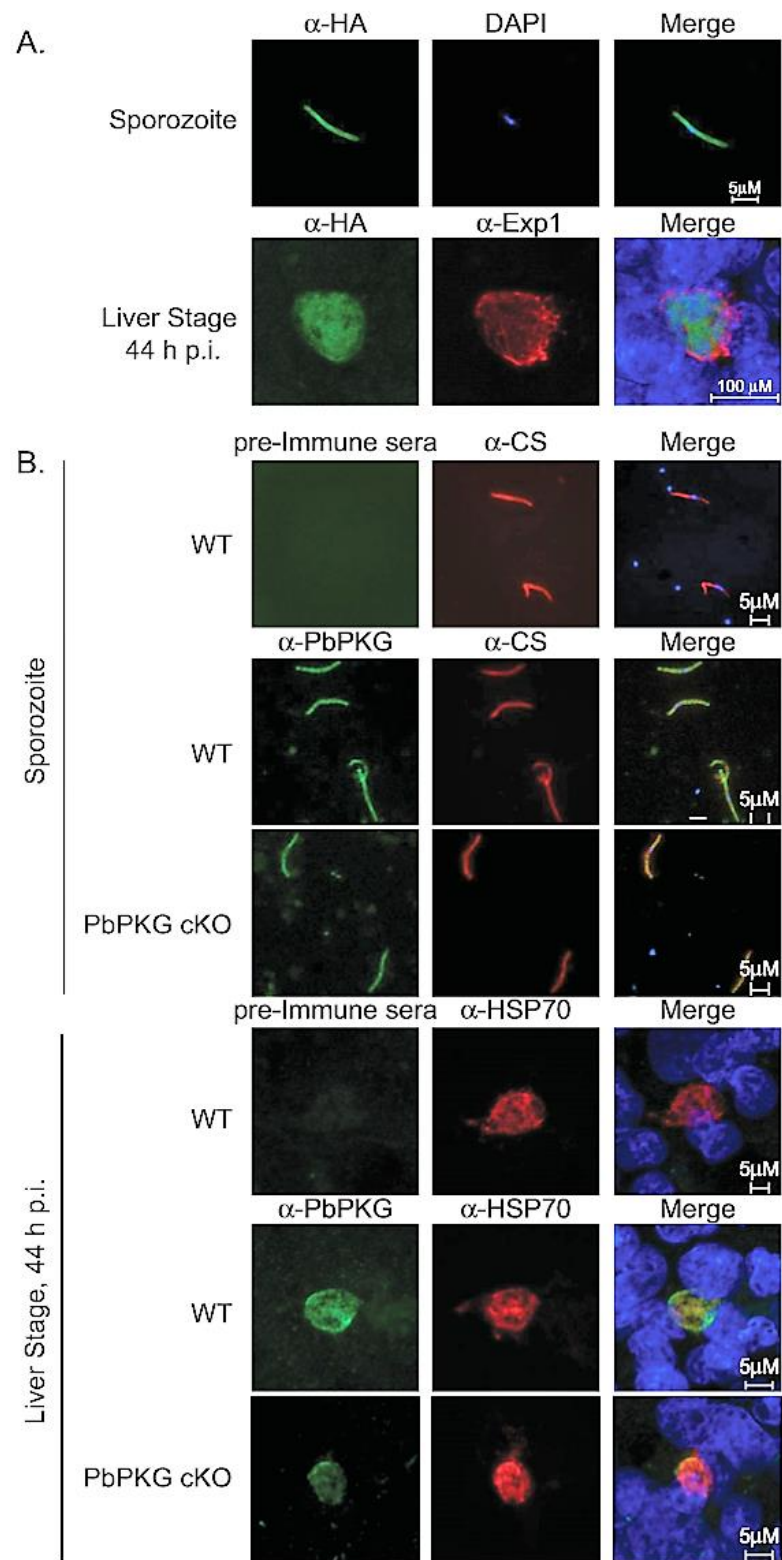


**Figure 4.** Expression of *PbPKG* in sporozoites and hepatic stages of *P. berghei* <sup>23</sup>

**A.** HA-tagged PKG detected in sporozoites and liver stages

**B.** PKG detected in *PbPKG* cKO and wildtype sporozoites

and liver stages from wildtype and *PbPKG* cKO parasites. The sporozoites were co-stained with an antibody against the CS protein endemic to sporozoites, while liver stages were co-stained with an antibody against Heat Shock Protein 70 (HSP70). PKG was instantly spotted in *PbPKG* cKO sporozoites by IFA. On the other hand, PKG protein expression in *PbPKG* cKO liver stages was significantly lower (**Figure 4B**). This observation suggests that *PbPKG* cKO sporozoites retain sufficient PKG from their preceding lifecycle stage, the oocysts. Using stable isotope labelling of ookinetes, it was established that 87% of *PbPKG* protein in ookinetes is acquired from the preceding gamete stages, suggesting that the turnover of plasmodial PKG is extremely sluggish.<sup>30</sup> In contrast, the liver stages displayed insignificant amounts of *PbPKG* as they could inherit only a fraction of the carryover PKG retained by the *PbPKG* cKO sporozoites.

### C. VALIDATION OF PLASMODIUM PKG AS A NOVEL ANTIMALARIAL TARGET

#### 1. Examination of PKG function using TSP

Since the presence of PKG in sporozoites and the hepatic stages was confirmed, it was necessary to examine if PKG could be a potential target for the treatment of malaria. Based on literature,<sup>31</sup> 4-[2-(4-fluorophenyl)-5-(1-methylpiperidine-4-yl)-1H-pyrrol-3-yl]pyridine or trisubstituted pyrrole (TSP) was employed to inhibit *PbPKG*. TSP was previously shown to inhibit the *in vitro* development of several Apicomplexan parasites such as *Eimeria tenella* and related species.<sup>31</sup>

It was noted in an *in vitro* study that TSP effectively blocked the infection of hepatocytes by *Plasmodium* sporozoites in a dose dependent manner.<sup>32</sup> *P. berghei* sporozoites were allowed to infect the human hepatoma cell line, HepG2, in the presence of different concentrations of TSP and the inhibitor was removed 12 hours post infection (p.i.). Sporozoite infectivity was measured by evaluating the number of intracellular hepatic stages that developed 40 hours p.i. TSP was observed to effectively inhibit the metamorphosis of sporozoites into hepatic stages in a dose-dependent manner as shown in **Figure 5A**. When employed at a concentration of

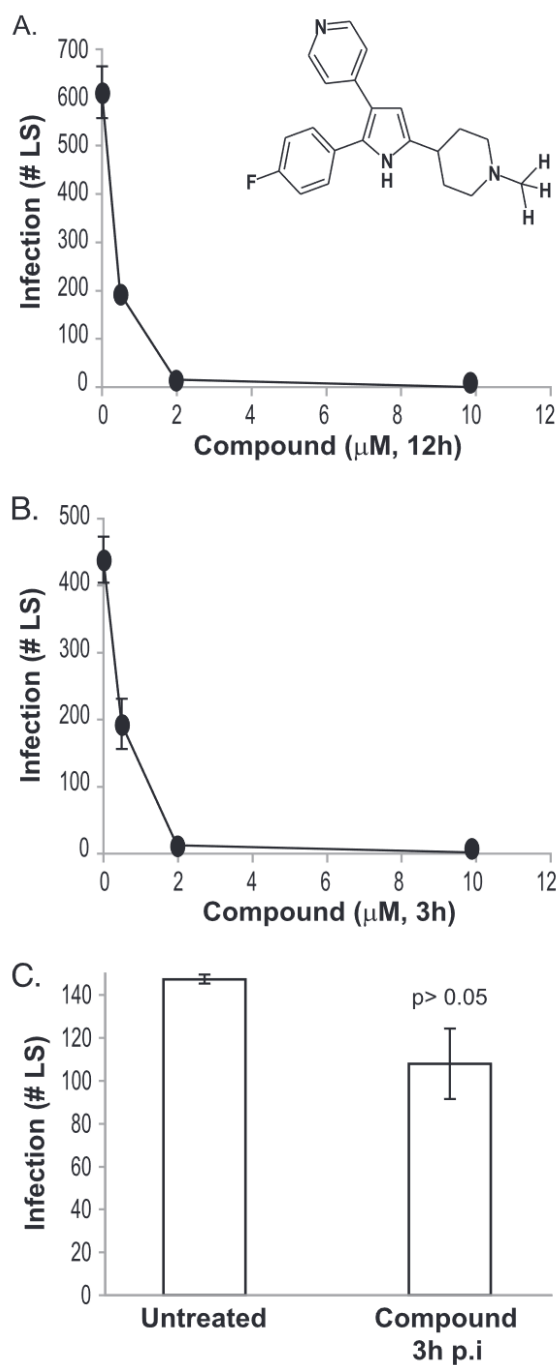


**Figure 5.** Impact of TSP on liver stage parasitaemia <sup>32</sup>

- A.** Dose-dependent reduction in the numbers of *P. berghei* liver stages (40 hours p.i.) when present for the first 12 hours of infection
- B.** Dose-dependent reduction in the numbers of *P. berghei* liver stages (40 hours p.i.) when present for the first 3 hours of infection
- C.** Insignificant reduction in the numbers of *P. berghei* liver stages (40 hours p.i.) when treated with 10  $\mu$ M TSP 3 hours p.i.

2  $\mu$ M, the number of liver stage parasites fell so drastically that they could not be detected. The observed reduction in the number of liver stage parasites could have been a result of the inhibition of several processes involved in infection - sporozoite motility, host cell invasion, or intravacuolar development of the parasite. The onset of activity for TSP was computed in order to determine which process it inhibited. Cells were infected with sporozoites in the presence of 2  $\mu$ M TSP and subsequently, the compound containing medium was removed 3 hours post infection. TSP was noted to inhibit liver stage numbers to similar extents when present for 3 hours (**Figure 5B**) as compared to cells that were exposed to the inhibitor for 12 hours. Since sporozoite invasion of host hepatocytes is generally accomplished within 2 to 3 hours, these results suggest that TSP inhibits sporozoite motility and/or invasion of host cells rather than the intravacuolar development of the parasite. This was confirmed when 10  $\mu$ M TSP, added to the cells 3 hours p.i., did not affect the number of liver stage parasites present 40 hours p.i. (**Figure 5C**).<sup>32</sup> This result provides a clear indication that PKG's critical functions are manifested during the early steps of sporozoite infection.

## 2. Target verification of TSP

To confirm the pharmacological target of TSP and rule out possibilities of off-target effects, a transgenic *P. berghei* line expressing a 3xHA-tagged, TSP-resistant allele of *PbPKG* was created.<sup>23</sup> The modified *PbPKG* allele bares a substitution of the 'gatekeeper' Thr<sub>619</sub> residue with Gln (PKG T<sub>619</sub>Q-HA) that prevented TSP from accessing the enzyme's binding pocket. As a result, PKG T<sub>619</sub>Q-HA is an artificially engineered strain that is resistant to TSP while exhibiting normal catalytic performance. A TSP-sensitive line expressing 3xHA-tagged wildtype *PbPKG* (PKG-HA) was used as control. *P. berghei* sporozoites were allowed to infect HepG2 cells in the presence of TSP. Compound exposure was maintained for 14 hours p.i. following which, the number of infected cells was quantified 44 hours p.i. Infection of HepG2 cells by PKG T<sub>619</sub>Q-HA sporozoites was about 19-fold less sensitive to TSP as compared to infection by PKG-HA sporozoites (**Figure 6A**).



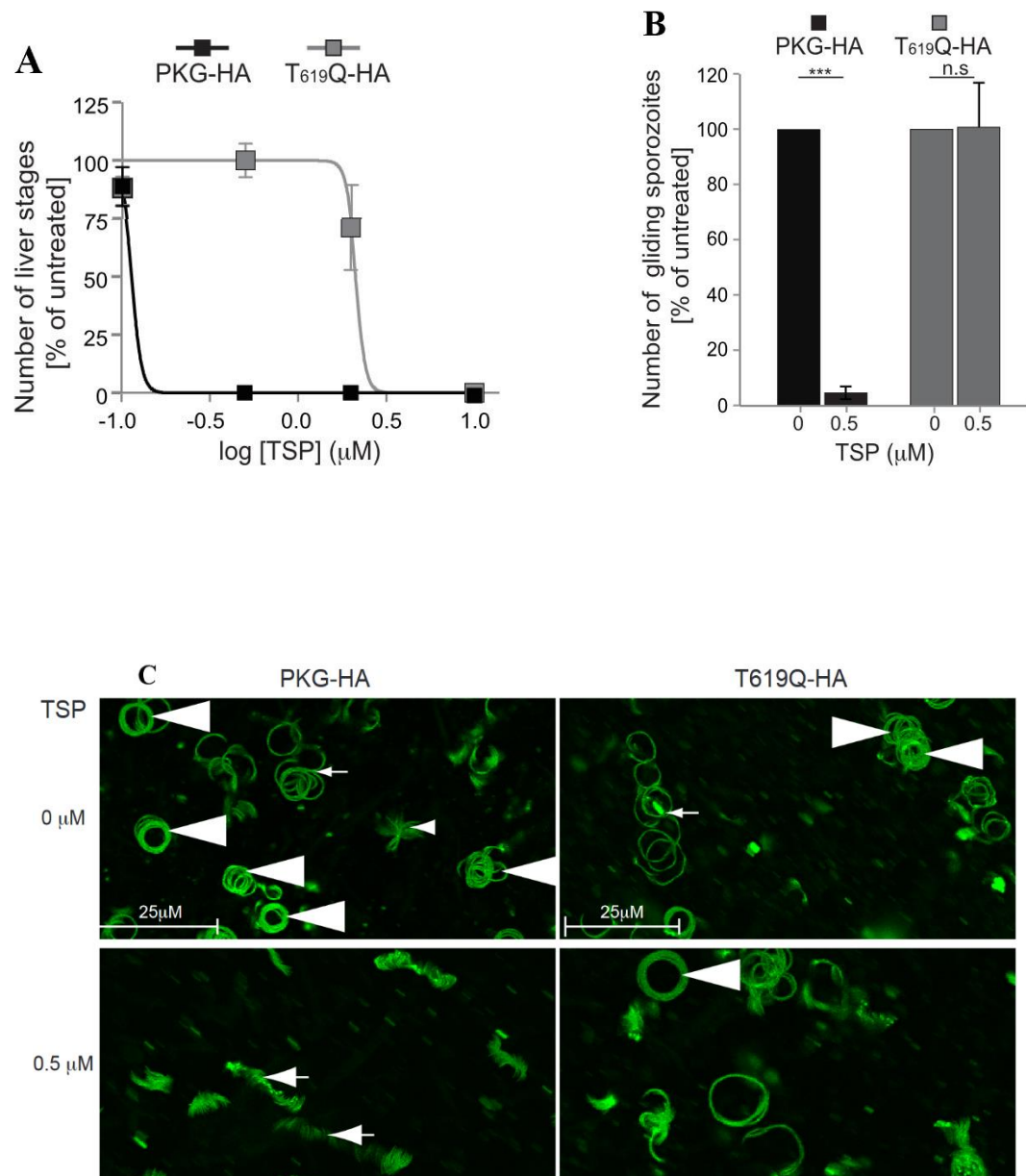


**Figure 6.** Target verification of TSP by employing a transgenic TSP-resistant enzyme, PKG T<sub>619</sub>Q-HA, using PKG-HA as control <sup>23</sup>

- A.** Insensitivity of PKG T<sub>619</sub>Q-HA as compared to PKG-HA demonstrated by detecting the number of liver stages when treated with increasing concentration of TSP
- B.** Marked reduction in the number of gliding PKG-HA sporozoites. Inability of TSP to reduce the number of gliding PKG T<sub>619</sub>Q-HA sporozoites
- C.** Visualization of the reduction of gliding PKG-HA v/s PKG T<sub>619</sub>Q-HA sporozoites

TSP was calculated to have an  $IC_{50}$  of about  $2.12\mu M$  against PKG T<sub>619</sub>Q-HA sporozoites and about  $0.11\mu M$  against PKG-HA sporozoites. The insensitivity of PKG T<sub>619</sub>Q-HA sporozoites to TSP as shown in **Figure 6** clearly validates that TSP blocks sporozoite infection of the hepatocytes by inhibiting its biological target, PKG, and therefore, sporozoite infection of hepatocytes requires PKG.

#### D. FUNCTIONS OF PLASMODIUM PKG IN SPOROZOITES AND LIVER STAGES

##### 1. Sporozoite Motility

Incursion of hepatocytes by sporozoites can be categorized into three distinct steps – attachment to the substrate (in this case, traversing cells), motility to reach the hepatocytes and passage into the hepatocytes.<sup>23</sup> *Plasmodium* sporozoites were found to rely on the formation and rupture of adhesion points with their substrate for cell motility.<sup>33</sup> Sporozoites move rapidly by a phenomenon known as stick-and-slip motility. This process is comprised of two phases - a slow stick phase where the sporozoite adheres to the substrate with one or both ends, and a rapid slip phase where the sporozoite slides rapidly onto the substrate over a central adhesion point.

PKG's role in sporozoite motility was tested by filming PKG-HA and PKG T<sub>619</sub>Q-HA sporozoites for 120 seconds at 1 Hz.<sup>23</sup> Sporozoite movement patterns *in vitro* are categorized as :

- a. Gliding sporozoites that move in circular paths for the total observation duration of 120 seconds
- b. Adherent sporozoites that adhere to the substrate with minor displacement
- c. Waving sporozoites which have one end attached to the substrate and the other end flapping freely
- d. Complex sporozoites which display a combination of the above-mentioned patterns

Reported observations clearly indicate that treatment with  $0.5\mu M$  TSP significantly decreased the number of PKG-HA gliding sporozoites and the number of circles completed by them during the observation period (**Figures 6B** and **6C**). In the absence of TSP, the gliding

sporozoites made  $15.7 \pm 1.7$  circles/sporozoite on average in 180 seconds. Whereas, in the presence of TSP, gliding sporozoites completed  $12.7 \pm 1.5$  circles/sporozoite on average in 180 seconds.<sup>23</sup> These values quantify the inhibitory effects of TSP on the motility of sporozoites.

To rule out the possibility that the HA tag might cause functional changes to PKG, the motility of *P. berghei* Green Fluorescence Protein – Luciferase expressing (*PbGFP-Luc*) sporozoites was examined. These sporozoites possess an unmodified PKG locus.<sup>23</sup> The motility of *PbGFP-Luc* sporozoites was also found to be actively inhibited by TSP, although they were less sensitive to lower doses of TSP compared to PKG-HA sporozoites. This difference may be due to distinct genetic backgrounds or it could indicate indirect effects of the HA-tag. TSP decreased the percentage of gliding *PbGFP-Luc* sporozoites and also the number of circles they made from  $13.7 \pm 4.7$  circles/sporozoite for vehicle-treated to  $7.0 \pm 1.7$  for 2.0  $\mu$ M inhibitor-treated sporozoites in 180 seconds.<sup>23</sup>

## 2. Secretion of micronemal proteins

Sporozoites make use of specialized proteins to navigate their way around the human body. These proteins are secreted by specialized secretory organelles called micronemes via exocytosis. Micronemes are located on the apical portion of the sporozoite's body. Past investigations with *T. gondii* tachyzoites and *P. falciparum* merozoites have demonstrated that PKG is essential for the secretion of micronemal proteins.<sup>34-35</sup> To examine *PbPKG*'s function in regulating the secretion of micronemal proteins in sporozoites, the expression of Thrombospondin-related anonymous protein (TRAP), an important surface adhesin, was quantified.<sup>23</sup> TRAP is a recognized micronemal protein whose secretion onto the sporozoite surface and subsequent cleavage is essential for motility. In general, sporozoites incubated at 37°C display increased secretion of TRAP at the surface. The TRAP expression of sporozoites incubated at 4°C was used as control. Using this principle, the surface expression of TRAP in *PbGFP-Luc* sporozoites was quantified using immunofluorescence intensities and expression of the CS protein was used as an internal reference control. It was observed that there was no increase in TRAP expression (**Figure 7A**) when sporozoites were incubated at 37°C in the

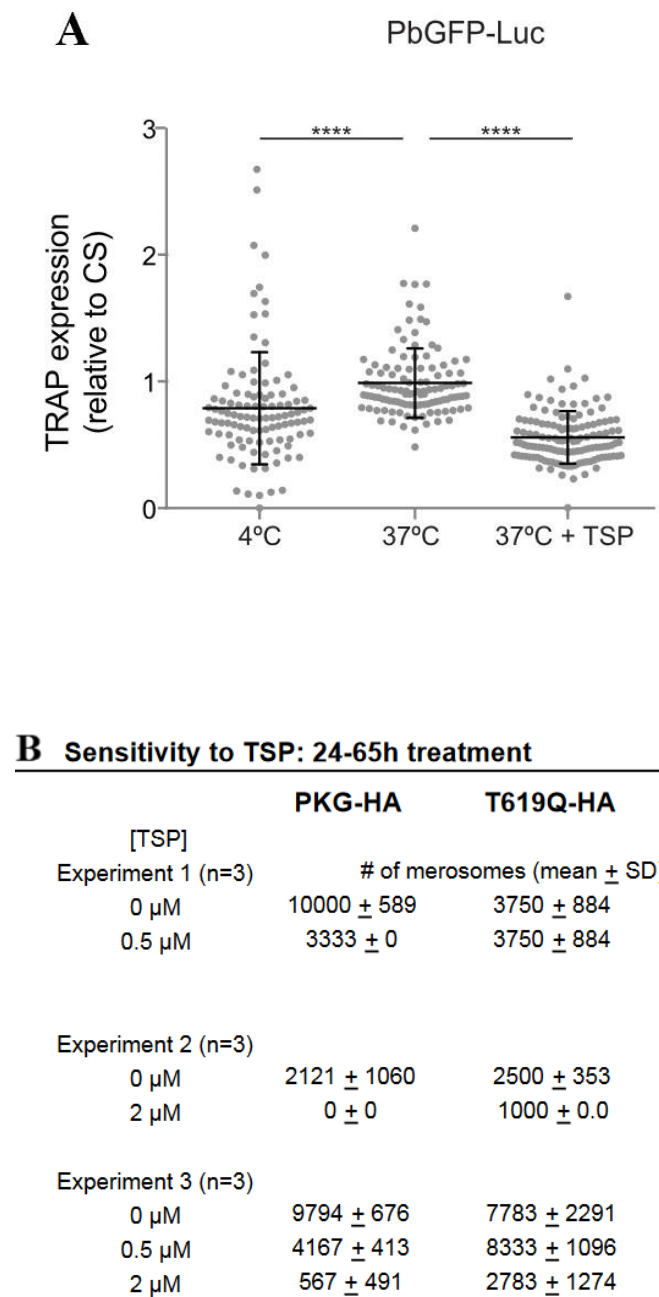


**Figure 7.** PKG regulates the secretion of micronemal proteins and formation and/or release of merosomes<sup>23</sup>

- A.** No increase in TRAP expression observed when *PbGFP-Luc* sporozoites were incubated at 37°C in the presence of 2  $\mu$ M TSP
- B.** Significant dose-dependent reduction in the number of PKG-HA merosomes released when treated with TSP. PKG T619Q-HA parasites appear to unaffected by TSP

presence of 2  $\mu$ M TSP. This can be attributed to TSP, which seemingly suppresses the increase in TRAP expression at the sporozoite surface by inhibiting parasitic PKG.<sup>23</sup>

### 3. Formation and release of merozoites

Merozoites were recently identified to exit hepatocytes in the form of packets surrounded by host tissue. These short-lived life forms are known as merozoites. The effect of TSP on the formation and release of merozoites was tested on PKG-HA and PKG T<sub>619</sub>Q-HA parasites.<sup>23</sup> It was observed that TSP decreased the number of merozoites (**Figure 7B**) found in the media at 65 hours p.i. when added to HepG2 cells infected with PKG-HA sporozoites in a dose-dependent manner. On the other hand, PKG T<sub>619</sub>Q-HA merozoite formation and/or release was found to be far less sensitive to TSP as compared to PKG-HA parasites.

### 4. Summary

From the set of experiments performed using chemical inhibition by TSP, the following conclusions could be drawn:

- a. Sporozoite motility is a key factor of hepatocytic invasion
- b. PKG plays a prime role in mediating *Plasmodium* sporozoite motility
- c. PKG regulates exocytosis of micronemal proteins like TRAP in sporozoites
- d. PKG's regulation of sporozoite motility occurs through regulation of TRAP secretion
- e. PKG plays an essential role in merozoite formation and/or release from hepatocytes

### E. Current research on *Plasmodium* PKG inhibitors

Substantial research on *Plasmodium* PKG inhibitors is being conducted in different parts of the world. After validating PKG as an extremely viable target in the treatment of malaria, researchers are now focusing on developing appropriately potent and selective chemotypes to chemically inhibit the pathogen's enzyme. The focus on PKG as an antimalarial target is applicable across the different life stages of the parasite, and not only confined to sporozoites.

PKG of the erythrocytic stage of *P. falciparum* is currently being examined as a potential antimalarial target as described in Dr David Baker's programme.

#### 1. Imidazopyridine chemotype

The Merck imidazopyridine compound **1** was the starting point for this programme.<sup>36</sup> This compound was generated through a partnership between MRC Technology and the London School of Hygiene and Tropical Medicine. Compound **1** was extensively studied for its PKG inhibiting activity against *Eimeria* in chickens and *Toxoplasma* in mice.<sup>37</sup> Starting with compound **1**, after several series of design and synthesis, compounds **2-10** were generated as shown in **Figure 8A**. The ability of these compounds to block *P. falciparum* asexual erythrocytic growth *in vitro* was determined using a growth inhibition assay.<sup>36</sup> Compound **10** was seen to possess an IC<sub>50</sub> of 160 pM against recombinant PfPKG and an EC<sub>50</sub> value of 2 nM against erythrocytic *P. falciparum*. Compounds **1**, **4** and **10** were tested for *in vivo* efficacy in BALB/c mice infected with *P. berghei*. The compounds were administered twice daily at a dose of 25 mg/kg by oral gavage. Blood stage parasitaemia, measured after 4 days treatment, revealed a decrease between 52.0 and 60.4% compared to untreated controls. When tested in the synchronous *P. chabaudi* model instead of the asynchronous *P. berghei*, the results were slightly different. A single daily oral dose (50 mg/kg) of either **1** or **4**, given to groups of mice just prior to the predicted onset of schizogony, led to a 67.9 and 56.5% reduction in blood stage parasitaemia, respectively. This series of compounds was also successful in blocking the transmission of *P. falciparum* to mosquitoes due to its effect on gametocytes. To gain insights into the interactions between *Plasmodium* PKG and the new class of inhibitors, the group successfully obtained diffracting crystal structures from *P. vivax* PKG with compounds **1** and **10** in its binding pocket (**Figure 8B**). The *P. vivax* and *P. falciparum* orthologues are 92% identical in amino acid sequences and therefore, the results could be easily extrapolated to *P. falciparum*.

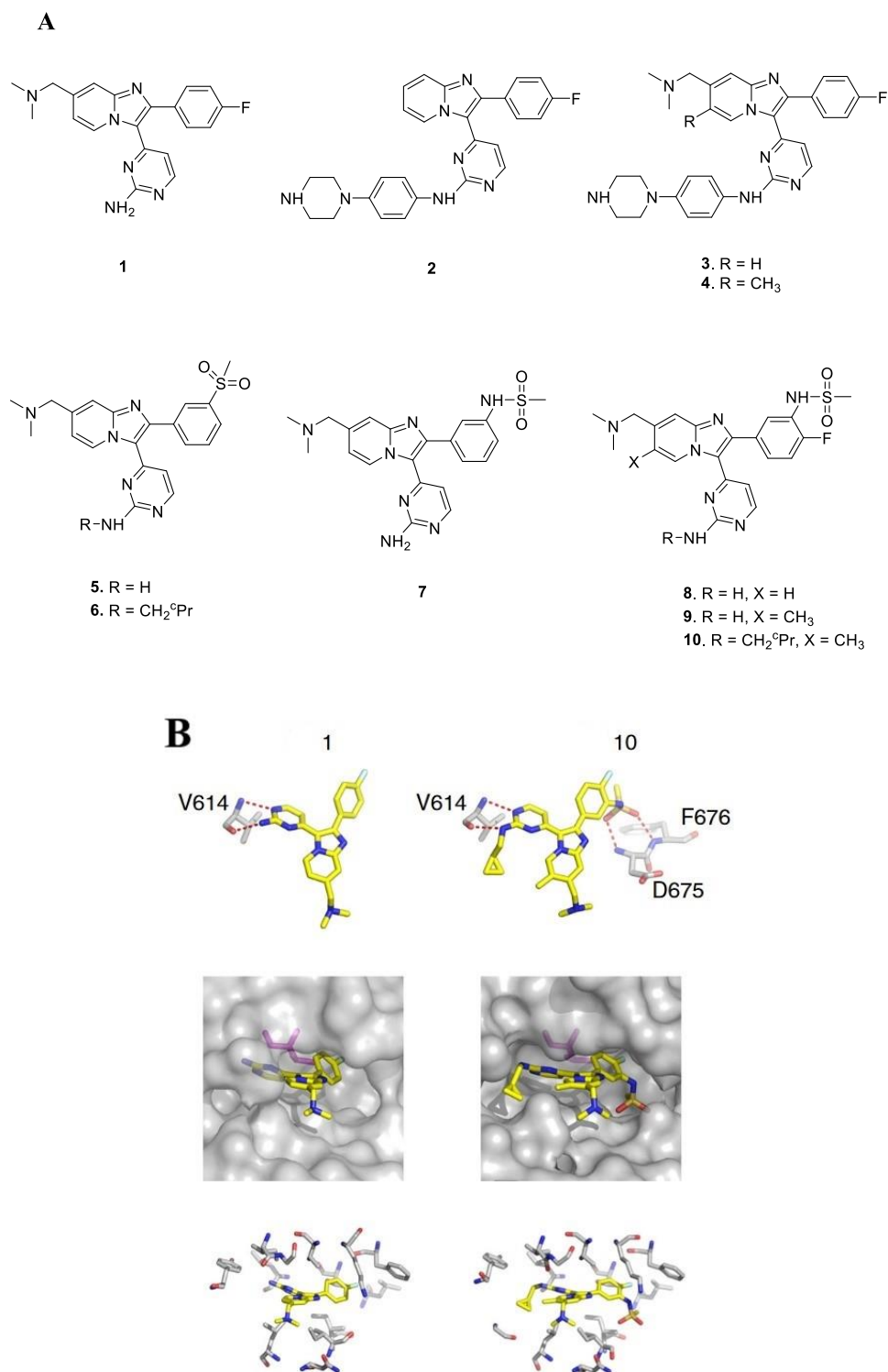


**Figure 8.** Imidazopyridine-based PKG inhibitors <sup>36</sup>

**A.** Structures of compounds **1-10**

**B.** Co-crystal structure of **1** and **10** in the binding pocket of *P. vivax* PKG.

Key interactions with amino acids in the binding pocket are indicated

#### Key Interactions (**Figure 8B**) :

- a. Hydrogen bonds between the aminopyrimidine and the backbone of V614 form the typical hinge interactions seen in ATP-mimicking kinase inhibitors for both structures
- b. The 4-fluorophenyl moiety of both compounds fills the hydrophobic pocket next to the gatekeeper T618 residue
- c. The sulphonamide in compound **10** forms hydrogen bonds with D675 and F676
- d. Both compounds are involved in hydrophobic interactions with a network of residues from both lobes and the hinge of the kinase domain

This programme generated optimism and exposed the potential of PKG inhibitors in the treatment of malaria.

#### 2. Trisubstituted thiazole chemotype

Continuing their programme of study, Baker et al., most recently decided to pursue new scaffolds against erythrocytic *Plasmodium* PKG. Based on literature search results of compounds having similar structures to **1**, they decided to pursue thiazole-based chemotypes.<sup>38</sup>

It was envisioned that the imidazopyridine core could be replaced by a thiazole core to maintain the interactions made by the appended groups. This claim was confirmed by homology modelling, which indicated a good fit for the new chemotype in the binding pocket of the parasitic enzyme. Essentially, the monocyclic pyrrole core of TSP was replaced with a thiazole core and the pyridine was substituted with 2-aminopyrimidine to generate a new series of compounds. The first compound generated from this series, compound **11** (**Figure 9A**), exhibited a similar IC<sub>50</sub> value as that of TSP and **1** but decreased slightly in terms of cellular potency when compared to TSP and **1**. This was seen as an encouraging result and it made sense to further optimize this chemotype. After considerable optimization, several key compounds were identified including compounds **12** and **13** (**Figure 9A**). The docking of compounds into an apo crystal structure of *Pf*PKG made it possible to view the key interactions in the ATP binding site of the enzyme (**Figures 9B and 9C**).



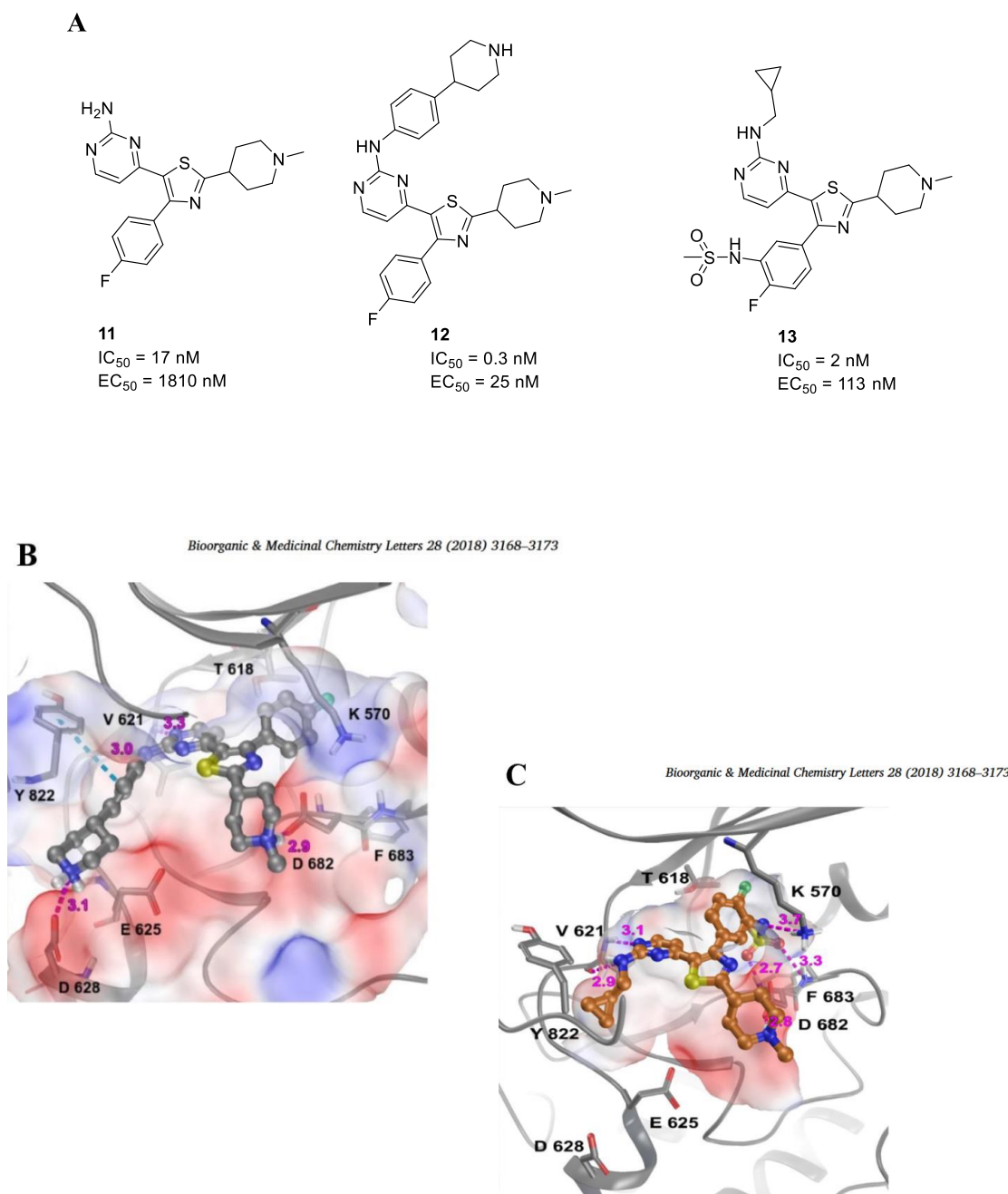


**Figure 9.** Thiazole-based PKG inhibitors <sup>38</sup>

**A.** Structures of Compounds **11**, **12** and **13**

**B.** Apo crystal structure of compound **12** docked in the binding pocket of *Pj*PKG

**C.** Apo crystal structure of compound **13** docked in the binding pocket of *Pj*PKG

Key Interactions (**Figures 9B and 9C**):

- a. The 4-fluorophenyl ring is seen to be buried deep in the hydrophobic pocket between K570 and the gatekeeper T618
- b. The piperidine attached to the thiazole core projects outward toward the solvent, engaging in charge interactions with D682
- c. The 2-aminopyrimidine forms hydrogen bonds with the backbone of V621 present at the hinge region
- d. The phenyl ring in compound **12** is involved in aromatic  $\pi$ -stacking interactions with Y822 and positions the terminal amine to form charge interactions with D628

In addition to the key interactions discussed above, compound **13** also engages in polar interactions. The cyclopropylmethyl group efficiently fills the hydrophobic pocket between V621 and Y822, while the sulphonamide forms hydrogen bonds with the DFG loop and picks up a charge interaction with K570. Compound **13** was also found to be selective for *Pf*PKG and lacked activity against the human kinases p38a MAPK and PKA, an issue that was seen with the previous chemotypes. This series is currently being further developed to improve antimalarial activity.

### III. PYRROLES

#### A. PROPERTIES AND OCCURENCE OF PYRROLES

Pyrrole is a 5-membered heterocyclic aromatic compound containing a single nitrogen in the ring nucleus. Pyrrole was first isolated in 1857 from bone oil by Anderson.<sup>39</sup> It is a colourless liquid with a boiling point of 129.8°C and melting point of -23.4°C at 1 atm. It gradually turns brown upon exposure to air and is slightly hygroscopic. Aromaticity is achieved by delocalization of the nitrogen lone pair of electrons into the ring. Hence, it displays negligible basicity and the protonated pyrrole has an estimated  $pK_a$  of -3.8. The pyrrole N-H is weakly acidic with a  $pK_a$  of 17.5. The ring nitrogen can be easily deprotonated using NaH or a similar base.



**Figure 10.** Dipole moment of Pyrrole and Furan

By comparing their resonance stabilization energies (pyrrole = 15.1 kJ mol<sup>-1</sup>, benzene = 25.0 kJ mol<sup>-1</sup>), it can be inferred that pyrrole is less aromatic than benzene. Pyrrole has a dipole moment of 1.58-2.1D depending on the solvent, which is much greater than that of other five-membered heterocycles such as furan and thiophene. An important characteristic observed here is that the positive pole of the dipole in pyrrole appears to be on the nitrogen atom with the dipole vector aligned towards the ring (**Figure 10**). This is in stark contrast to the dipole vector in furan which has its negative pole on the oxygen and is directed away from the ring (**Figure 10**).

Pyrrole compounds are widely abundant in nature and are of crucial importance for living organisms. Chlorophyll and haem (**Figure 11**), two of the most important pigments in the plant and animal kingdoms, are porphyrins that are composed of pyrrole units. The

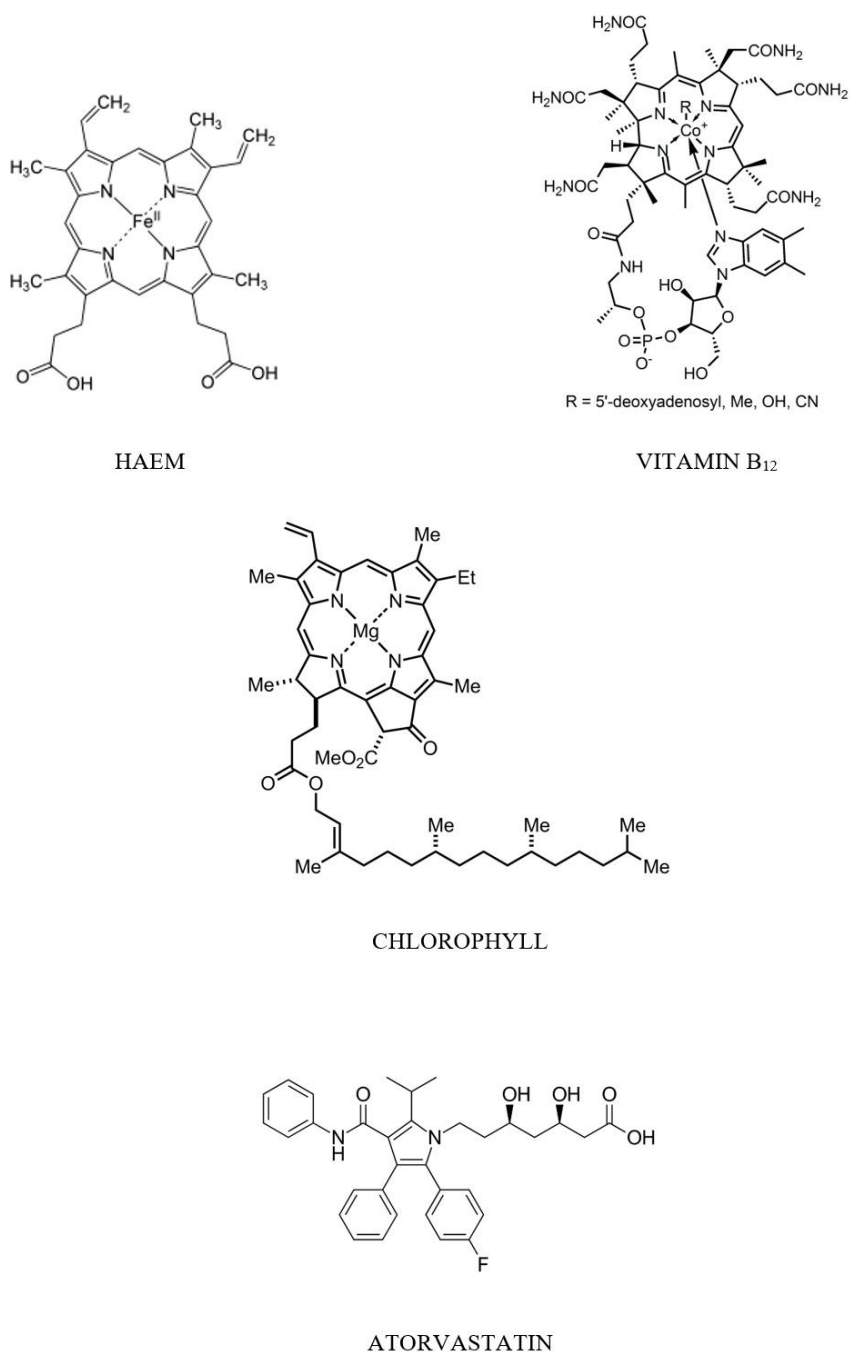


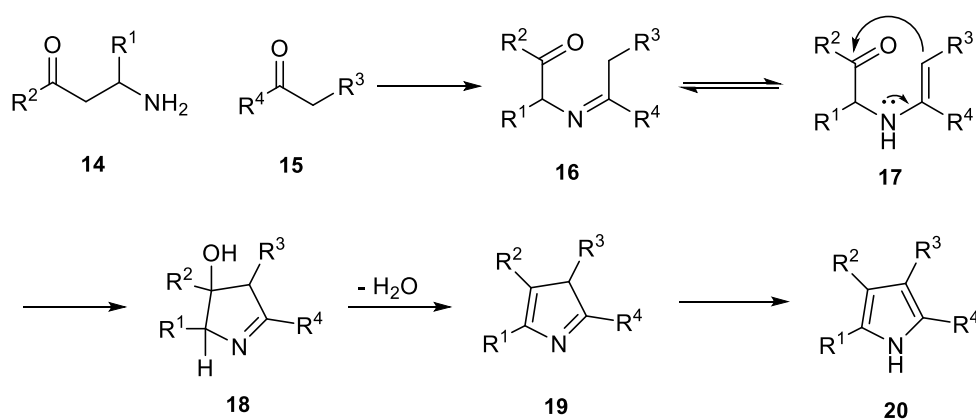
**Figure 11.** Pyrrole-based natural products and drugs

trisubstituted pyrrole porphobilinogen is a key intermediate in the biosynthesis of porphyrins and many other pyrrole-based natural products like vitamin B<sub>12</sub>, bile pigments and the haem component of cytochrome p450 enzymes. The pyrrole ring is commonly found in a number of drugs such as aloracetam (nootropic), atorvastatin (hypolipidemic statin), elopiprazole (anti-

psychotic), loriprazole (anxiolytic), nargenicin (antibiotic and anti-neoplastic), tolmetin (NSAID) and ketorolac (NSAID).

## B. SYNTHESIS OF PYRROLES

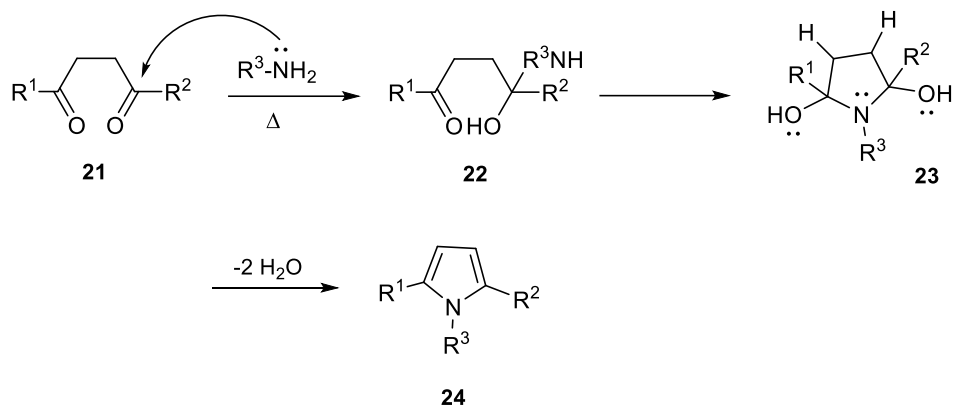
### 1. Knorr Synthesis



**Scheme 1.** Knorr Synthesis of Pyrroles

This Knorr synthesis of pyrroles, discovered by the German chemist Ludwig Knorr in the 1880s, is initiated by the condensation of an  $\alpha$ -aminoketone **14** with a compound containing an EWG  $\alpha$  to a carbonyl ( $R^3 = \text{EWG}$ ) **15** to generate an imine intermediate **16**. The imine tautomerizes to the enamine **17** which undergoes cyclization followed by dehydration to form the 3H-pyrrole **19**. This compound readily undergoes tautomerization to generate the more stable 1H-pyrrole **20**.

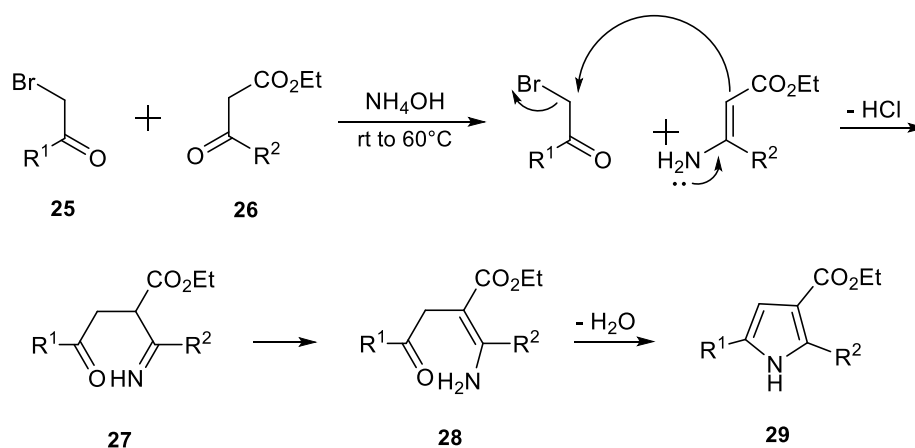
## 2. Paal-Knorr Synthesis



**Scheme 2.** Paal-Knorr Synthesis of Pyrroles

This synthesis was initially reported independently by both Carl Paal and Ludwig Knorr in 1884 for the synthesis of furans. The method was later adapted to synthesize pyrroles by condensation of a 1,4-dicarbonyl compound with a primary amine. The sequence begins with the nucleophilic attack of the amine on one of the carbonyls of **21** as seen in **Scheme 2**. This is followed by a second nucleophilic attack of the amine on the other carbonyl to generate the dihydroxy pyrrolidine intermediate **23** which undergoes dehydration to give the pyrrole **24**.

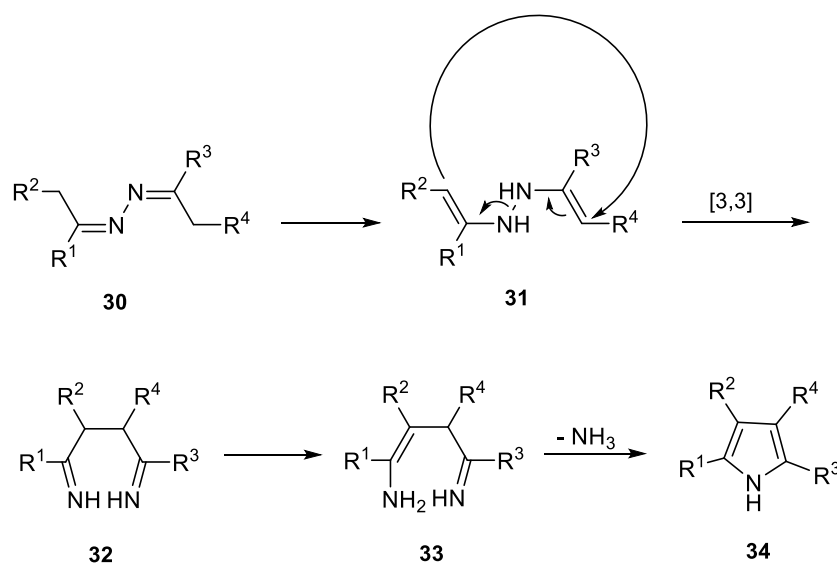
## 3. Hantzsch Synthesis



**Scheme 3.** Hantzsch Synthesis of Pyrroles

The Hantzsch synthesis of pyrroles utilizes an  $\alpha$ -bromocarbonyl compound **25** and a  $\beta$ -ketoester **26** along with a mild base such as  $\text{NH}_4\text{OH}$ . The enamine produced by the reaction of the  $\beta$ -ketoester with  $\text{NH}_4\text{OH}$  displaces the bromide to form the 1,4-imine carbonyl intermediate **27**. Upon tautomerization to the enamine **28**, nucleophilic attack of the amine onto the carbonyl bearing  $\text{R}^1$  followed by subsequent dehydration, produces the pyrrole ring **29**.

#### 4. Piloty Synthesis<sup>39</sup>



**Scheme 4.** Piloty Synthesis of Pyrroles

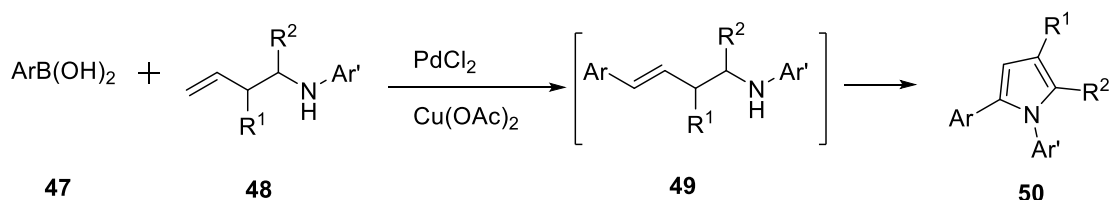
The starting point for this synthesis is an azine **30** which is synthesized by the condensation of 2 equivalents of a carbonyl compound with 2 equivalents of hydrazine. The azine undergoes tautomerization to produce the dienamine intermediate **31**. Subsequently, a [3,3] sigmatropic rearrangement leads to the 1,4-diimine **32**. Tautomerization to the enamine **33** and subsequent condensation with the release of ammonia produces the pyrrole **34**.

## 5. Ruthenium-Catalyzed Synthesis <sup>40</sup>



The proposed mechanisms for the ruthenium-catalyzed synthesis of pyrroles are shown in **Scheme 6**. The first step is the generation of the enamine **39** or imine **40** from the condensation of the ketone **35** with the primary amine **36**. Next, the diol **37** undergoes metal-induced double or mono dehydrogenation to produce the corresponding 1,2-dicarbonyl or  $\alpha$ -hydroxycarbonyl compounds respectively. Depending on the position of the next condensation reaction and the double or mono dehydrogenated diol involved, 4 intermediates (**41**, **43**, **45** and **46**) may be formed. Intermediates **41** and **43** are produced by the condensation of the 1,2-dicarbonyl with **39** and **40** respectively. **41** and **43** undergo hydrogenation to give **42** and **44** respectively. A second condensation generates the pyrrole **38**. Intermediates **45** and **46** are produced by the condensation of the  $\alpha$ -hydroxycarbonyl with **39** and **40** respectively. Subsequent tautomerization to **42** and **44** followed by a second condensation generates the pyrrole **38**. This technique can be used to generate a variety of substituted pyrroles in high yields and with relative ease in a single-step reaction.

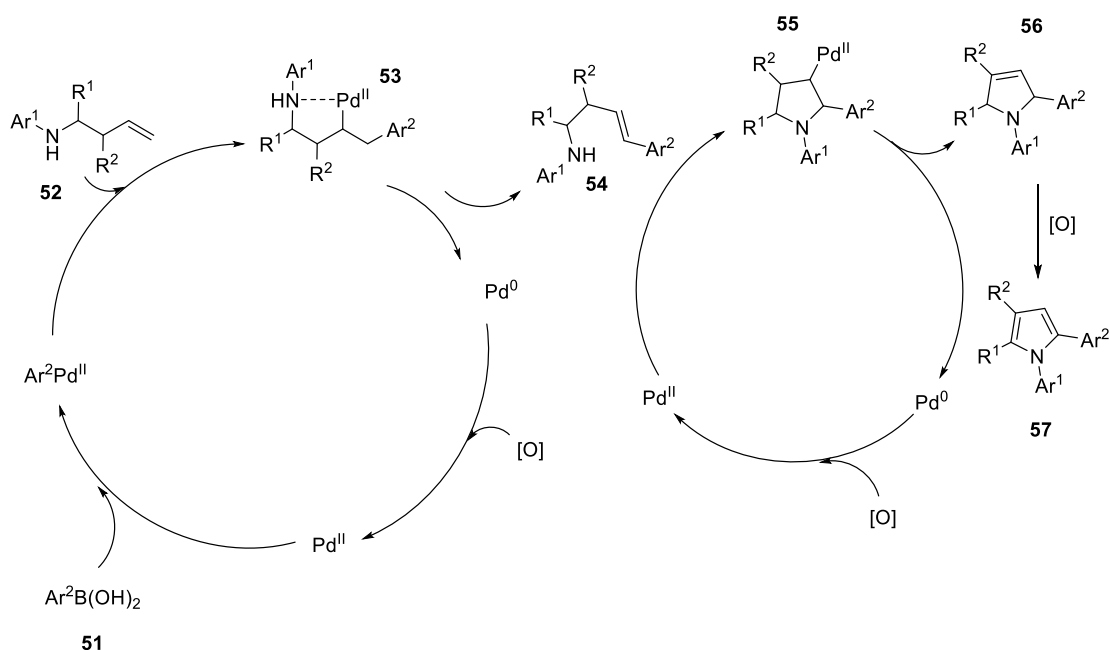
#### 6. Palladium-Catalyzed Synthesis <sup>41</sup>



**Scheme 7.** Palladium-catalyzed Oxidative Heck/Oxidative Amination cascade for the Synthesis of Pyrroles

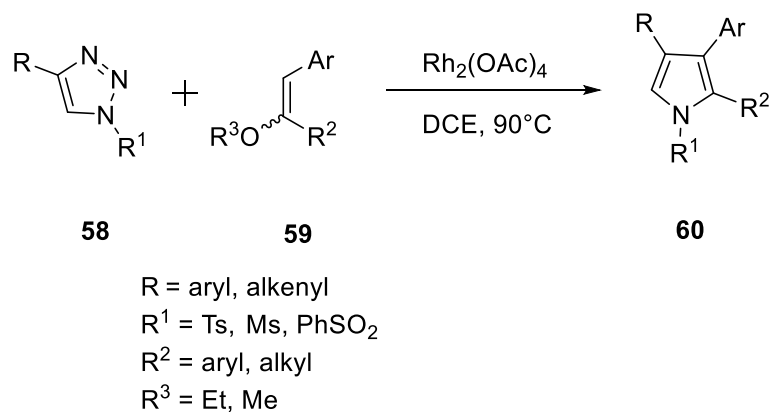
This palladium-catalyzed one pot synthesis couples aryl boronic acid **47** with an  $\gamma,\delta$ -unsaturated amine **48** by an oxidative Heck pathway to give intermediate **49**. Subsequent Pd-catalyzed intramolecular oxidative amination forms the pyrrole **50** as shown in **Scheme 7**. The catalyst employed is a palladium salt such as  $\text{PdCl}_2$  or  $\text{Pd}(\text{OAc})_2$  along with  $\text{Cu}(\text{OAc})_2$  as an oxidant and triethylamine as a base. The yields reported are typically in the range of 60-85%. According to the proposed mechanism (**Scheme 8**), the aryl boronic acid **47** first undergoes

transmetalation with the Pd catalyst to generate arylpalladium (II). This species inserts into the olefin by migratory insertion after which,  $\beta$ -hydride elimination forms the  $\gamma,\delta$ -unsaturated amine **54**. Subsequently, Pd-catalyzed intramolecular aminopalladation gives the pyrrolidine palladium intermediate **55**. A second  $\beta$ -hydride elimination followed by oxidative dehydrogenation produces the desired pyrrole **57**.



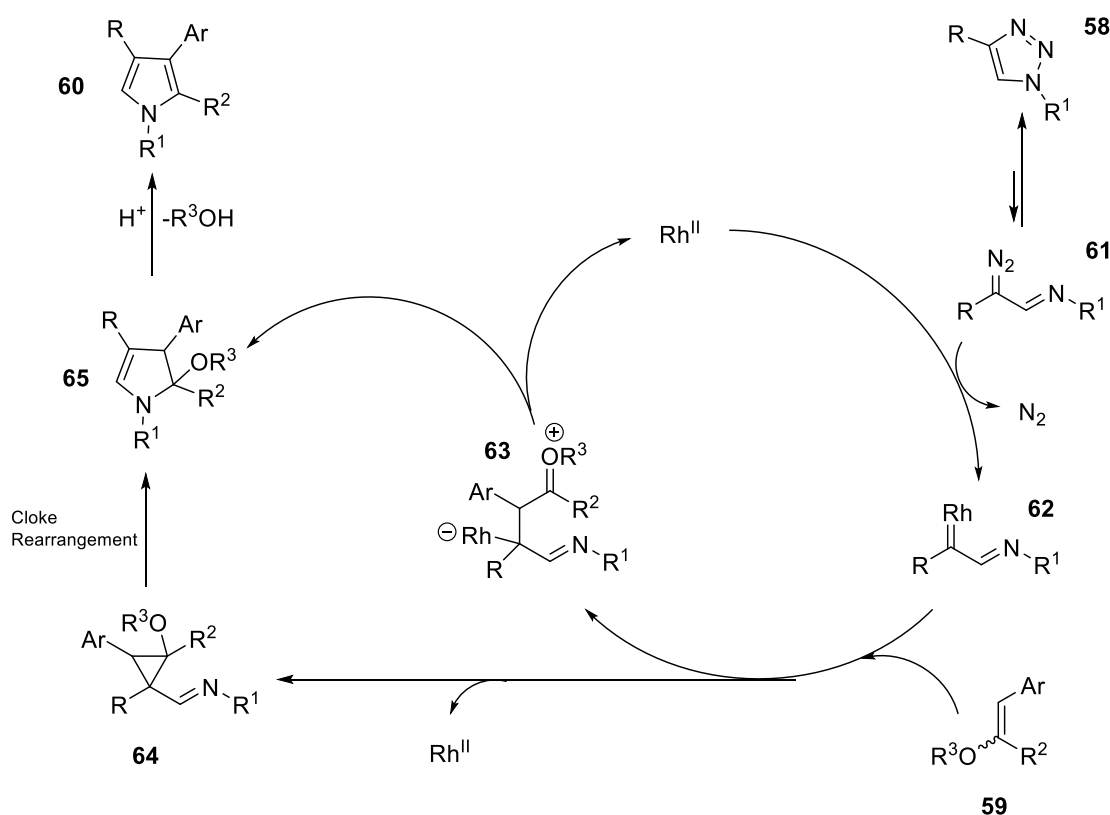
**Scheme 8.** Proposed Mechanism for the Palladium-Catalyzed Synthesis of Pyrroles <sup>41</sup>

## 7. Rhodium-Catalyzed Transannulations <sup>42</sup>



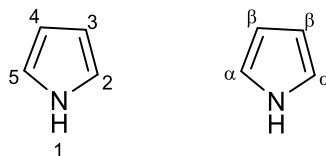
**Scheme 9.** Synthesis of Pyrroles by Rhodium-Catalyzed Transannulations of 1,2,3-Triazoles

Transannulation of an N-sulphonyl-1,2,3-triazole **58** with a vinyl ether **59** by a rhodium-catalyzed mechanism can be used to synthesize various types of polysubstituted pyrroles **60** in yields of 50-85% (**Scheme 9**).  $\text{Rh}_2(\text{OAc})_4$  is the only reported catalyst for such transannulations. Apart from the catalyst, no other reagent is needed for this reaction. A plausible mechanism for this reaction is illustrated in **Scheme 10**. The triazole is thought to rearrange to an  $\alpha$ -diazimine **61** which inserts  $\text{Rh}(\text{II})$  with the expulsion of nitrogen to give the rhodium carbenoid intermediate **62**. This intermediate may react with the vinyl ether **59** via two plausible mechanisms. One mechanism involves a rhodium carbenoid behaving as a nucleophile reacting with the vinyl ether to form the zwitter ionic rhodium intermediate **63** that upon cyclization gives the pyrroline **65**. The second mechanism follows the formation of a cyclopropane intermediate **64** which then undergoes a subsequent Cloke rearrangement to generate the same pyrroline intermediate **65**. Acid-mediated elimination of the alcohol to achieve aromatization forms the desired pyrrole product **60**.

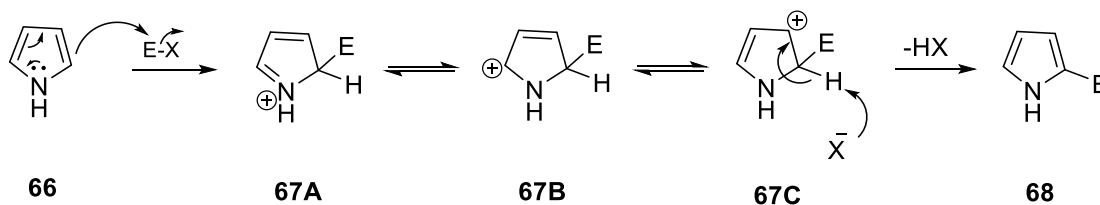


**Scheme 10.** Proposed Mechanism for the Rhodium-Catalyzed Synthesis of Pyrroles <sup>42</sup>

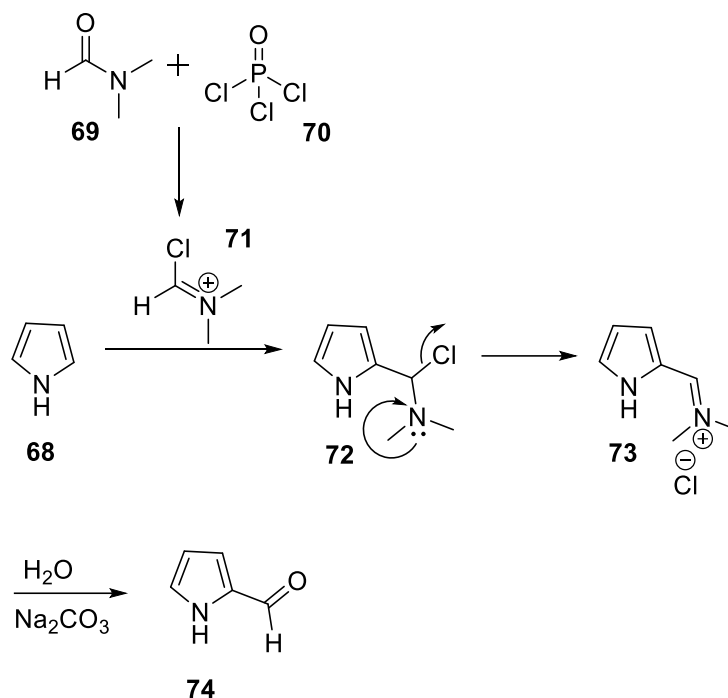
## C. REACTIVITY OF PYRROLES

**Figure 12.** Structure and numbering of 1*H*-Pyrrole

Pyrroles are  $\pi$ -excessive heterocyclic systems making them extremely susceptible to electrophilic aromatic substitution (EAS) reactions. Pyrrole is much more reactive than benzene towards EAS. Between the  $\alpha$  (2 and 5) and  $\beta$  (3 and 4) positions as shown in **Figure 12**, the  $\alpha$ -position is more reactive, and electrophilic attack at this position is favoured over the  $\beta$ -position. The reason behind this increased reactivity is that upon electrophilic addition, the  $\alpha$ -position produces a cation that is more extensively resonance stabilized. Electrophiles are directed to the  $\beta$ -position if both the  $\alpha$ -positions are substituted. The pyrrole nitrogen can be protected using various protecting groups. Sterically bulky protecting groups such as TIPS can direct electrophiles to the  $\beta$ -position.<sup>39</sup> Strongly electron-withdrawing groups, like tosyl, also have the ability to direct electrophiles to the  $\beta$ -position. Halogenation, nitration and sulphonation of pyrrole are all accomplished with relatively mild conditions. A general mechanism for electrophilic substitution of pyrroles is shown in **Scheme 11**. Two such examples of this substitution are illustrated in **Schemes 12** and **13**.

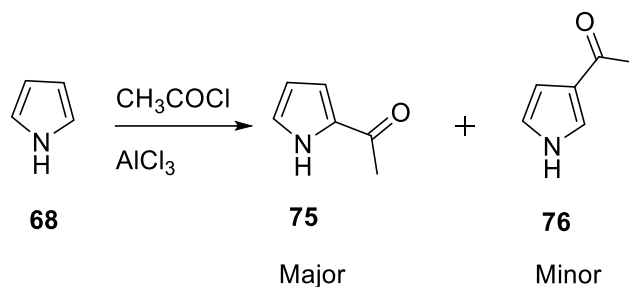
**Scheme 11.** Electrophilic Aromatic Substitutions of Pyrroles

## 1. Vilsmeier-Haack Formylation

**Scheme 12.** Vilsmeier-Haack Formylation of Pyrroles

The Vilsmeier-Haack formylation of pyrroles is a mild and fairly selective reaction that provides good yields of the formylated product. DMF **69** is catalytically regenerated as part of the last step of this reaction. When the 1-position is blocked by a substituent (in most cases a protecting group), electrophilic attack at the 3-position predominates. Other N,N-disubstituted amides have reportedly been used to produce acylated pyrroles. Several examples of cyclic amides, such as pyrrolidin-2-one and pyrrolidine-3-one, have been used to produce dipyrroles or their precursors.<sup>43-44</sup>

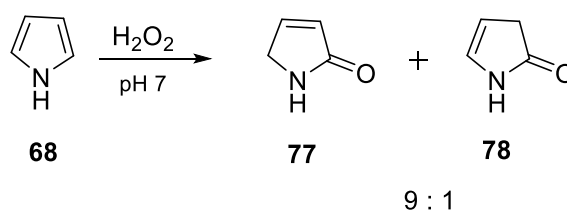
## 2. Friedel-Crafts Acylation



### Scheme 13. Friedel-Crafts Acylation of Pyrroles

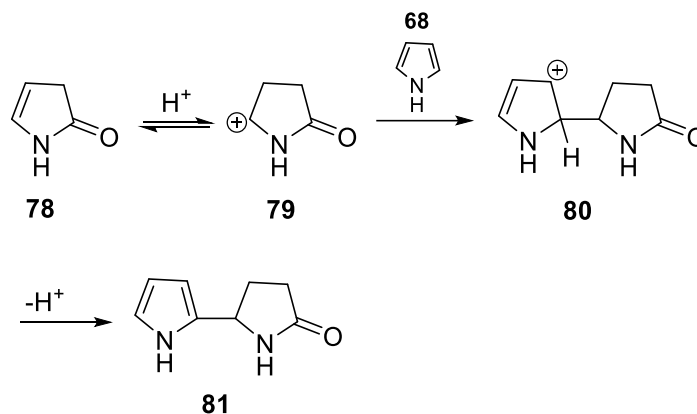
Pyrroles can be easily acylated by the Friedel-Crafts reaction using a Lewis acid catalyst at 60°C. In the absence of a Lewis acid, pyrroles can be acylated upon heating in acetic anhydride at 200°C. Using reactive acylating reagents like trichloroacetyl chloride, acylation can be accomplished at room temperature.

Pyrroles can be protonated with strong acids and the protonated form has a  $pK_a$  of -3.8. These compounds lose their aromatic character and behave as iminium salts. Protonation commonly occurs at the  $\beta$ -position due to enhanced resonance stabilization. Protonated pyrroles are activated towards nucleophilic aromatic substitutions, in stark contrast to pyrroles which are very poor substrates for nucleophiles.<sup>39</sup>



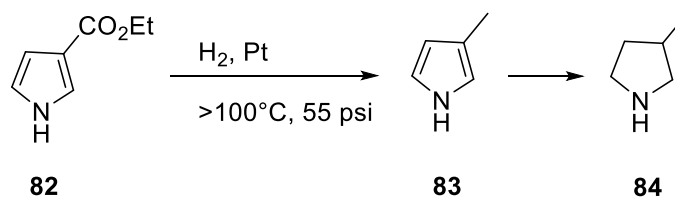
### Scheme 14. H<sub>2</sub>O<sub>2</sub> oxidation of Pyrroles at neutral pH

Pyrroles can be oxidized by hydrogen peroxide to yield pyrrolinones.<sup>39</sup> The products from such oxidations are pH dependent. Oxidation at neutral pH produces a mixture of 3-pyrrolin-2-one **77** and its isomer **78** in a ratio of about 9:1 (**Scheme 14**).



**Scheme 15.** H<sub>2</sub>O<sub>2</sub> oxidation of Pyrroles at acidic pH

Hydrogen peroxide oxidation in acidic solvents such as acetic acid as seen in **Scheme 15** produces oxidised polymers of pyrrole **81**. The polymers may be dimeric, trimeric or tetrameric. These polymerized products were initially referred to as pyrrole black.



**Scheme 16.** Hydrogenation of Pyrroles to Pyrrolidines

Pyrrole and its derivatives can undergo catalytic hydrogenation at high temperature and pressure using Pt, Pd, Rh, Ru or Raney-Ni to form pyrrolidines as shown in **Scheme 16**. The pyrrole nucleus is unreactive with LiAlH<sub>4</sub>, NaBH<sub>4</sub> and diborane and does not get reduced to pyrrolidine in the presence of these reducing agents. These reagents, therefore, are employed for the reduction of substituents on the pyrrole ring while leaving the aromaticity intact.

#### IV. TRISUBSTITUTED PYRROLE (TSP) AND ITS ANALOGUES

##### A. DISCOVERY OF TSP

Trisubstituted pyrroles were first identified in a kinase inhibitor program undertaken at Merck Research Laboratories in 1998.<sup>45</sup> The Inflammation Research group at Merck was screening compounds to inhibit the mammalian enzyme p38 kinase, which has been implicated in inflammatory processes. The series of compounds generated from this program was inspired from the SmithKline compound SB 203580.

Hybridization of structures of COX inhibitors like flumizole, triflumizole and levamisole led to the synthesis of SKF 86002 by SmithKline in their search for new NSAIDs (Non-Steroidal Anti-Inflammatory Drugs) (**Figure 13**). NSAIDs are a class of drugs that are used as antipyretic, analgesic, antithrombotic and anti-inflammatory agents. As the name suggests, these drugs do not bear the steroidal nucleus, yet produce eicosanoid depressive effects. SKF 86002 was seen to inhibit the biosynthesis of cytokines and this class of compounds was thereby termed CSAIDs (cytokine-suppressive anti-inflammatory drugs). The biological target for this new compound was determined to be the mitogen-activated kinase p38 (p38 MAP kinase). Structural modifications on the diaryl bicyclic imidazole SKF 86002, led to the discovery of the trisubstituted imidazole SB 203580 (**Figure 13**).<sup>46</sup> This compound, being a monocyclic imidazole, could tautomerize to its regioisomer fairly easily. During the optimization process of SKF 86002 to SB 203580, it was noted that the imidazole scaffold was not essential for anti-inflammatory activity.

The Inflammation Research group at Merck intended to investigate stable heterocyclic regioisomers instead of tautomeric imidazoles as present in SB 203580.<sup>45</sup> Subsequently, pyrrole, furan and pyrazolone based chemotypes were synthesized and tested for their p38 inhibitory activities. During this search, a potent pyrrole-based compound, L-167307 (**Figure 13**), was identified. Additionally, the compound known today as TSP was one of the pyrrole-based analogues generated from the same program.



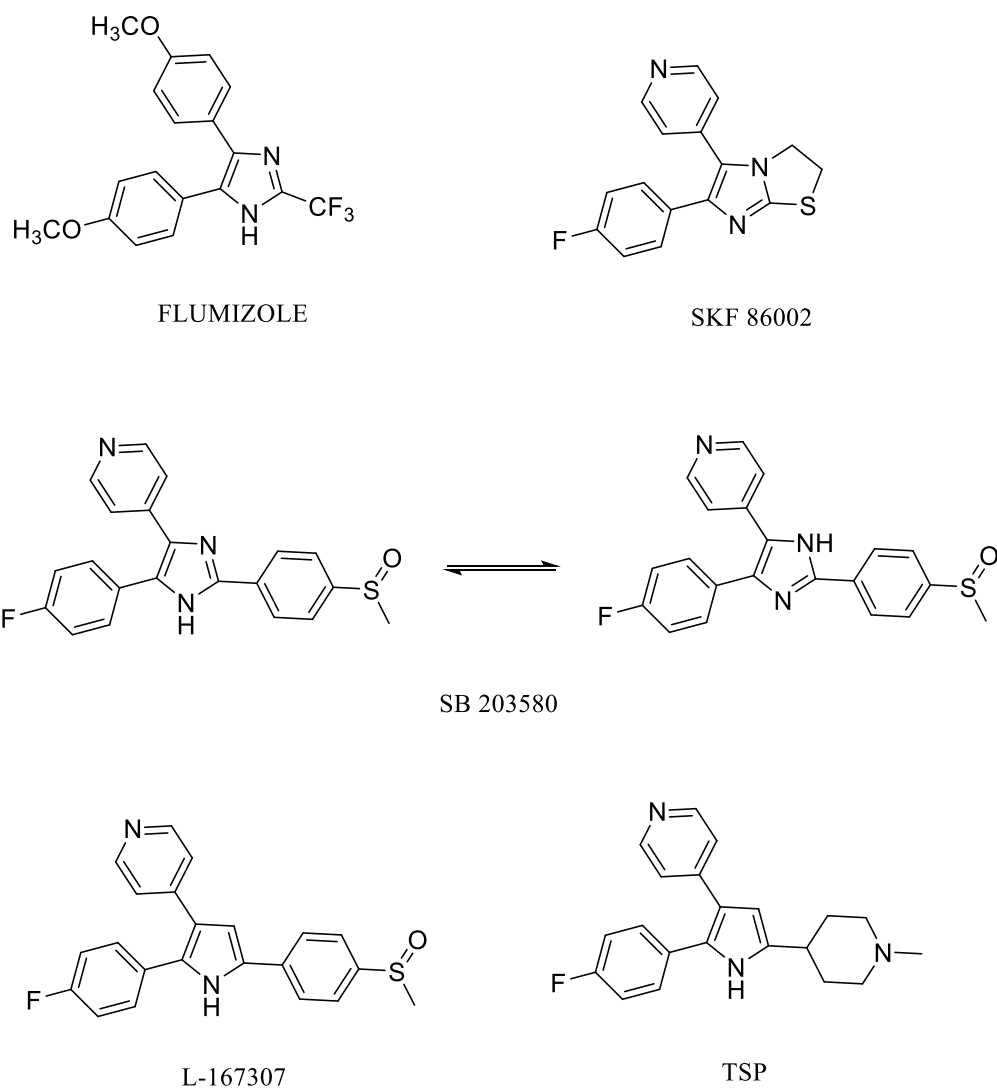


**Figure 13.** Optimization of kinase inhibitors leading to the discovery of TSP

In the following years, the Human and Animal Infectious Disease Research group at Merck performed a High Throughput Screening (HTS) search for compounds to treat coccidiosis.<sup>31</sup> Coccidiosis is a widespread protozoan infection that affects domesticated animals like dogs, cattle and poultry. The causative organisms were identified as different species of protozoa belonging to the genus *Eimeria*. The poultry industry incurs huge losses owing to the rampant spread of coccidiosis infections in young chicks. Polyether ionophores were previously used as anti-coccidiosis agents. But sometime around the 1980s, parasites resistant to these drugs started to surface and spread rapidly. This instilled the need to design and develop new anti-

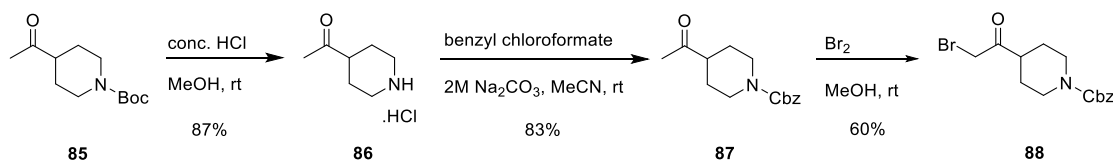
coccidiosis agents. One such HTS search in the early 2000s generated TSP as a hit. TSP exhibited inhibitory effects on the growth of Apicomplexan parasites like *E. tenella*, *T. gondii*, *N. caninum* and *B. jellisoni*.<sup>31</sup> In the context of coccidiosis, TSP was orally active against *E. tenella* and *E. acervulina* in parasite infested chickens. To deduce the biological target of TSP, a tritiated version of the compound was employed as a ligand. Biochemical purification of the protein, to which the tritiated analogue was bound, revealed the target to be the parasitic cGMP-dependent Protein Kinase (PKG).<sup>31</sup>

Based on this data, a wide array of TSP analogues with different substituents were designed and synthesized.<sup>47-50</sup> All the compounds were tested *in vitro* against *E. tenella* PKG (*Et*-PKG) and *in vivo* in two sets of White Leghorn chickens infected separately with *E. tenella* and *E. acervulina*. The pyrrole nucleus of TSP was substituted with other heterocycles like imidazole, furan, thiophene, thiazole and pyridazine.<sup>47</sup> The six-membered pyridazine was far less active than the five-membered heterocycles. Among the five membered rings, the pyrrole, oxazole and furan-based analogues were seen to be active *in vivo* against both species of the parasite. The pyrrole-based compound (TSP) was determined to be the most potent.

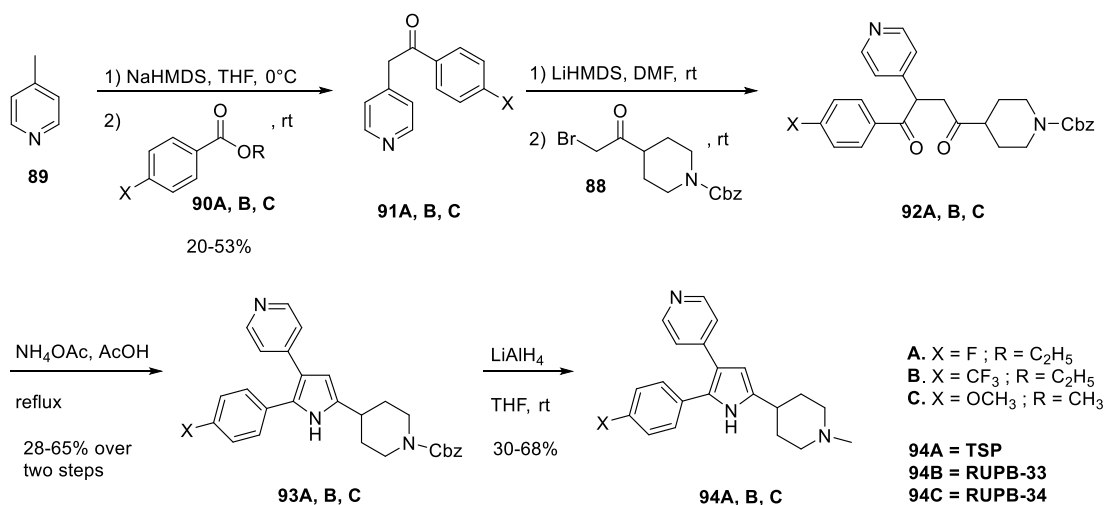
The group at Merck also designed a novel core that contained an imidazopyridine to target *Eimeria* PKG.<sup>51</sup> A large collection of imidazopyridine compounds were synthesized and tested in the same manner as the previously made TSP analogues.<sup>51-52</sup> Several compounds were found to be more potent than TSP and related compounds. The *Plasmodium* PKG inhibitor **1** was one of the compounds generated in this study.

The biology of Apicomplexan parasites like *Eimeria* and *Toxoplasma* was extrapolated to *Plasmodium*, also an Apicomplexan. This provided the rationale for testing TSP as a potential antimalarial drug that could inhibit *Plasmodium* PKG.<sup>32</sup> TSP was seen to potently prevent sporozoites from invading the hepatocytes and could possibly offer a feasible option for malaria prophylaxis.

## B. CHEMISTRY OF PLASMODIUM PKG INHIBITORS

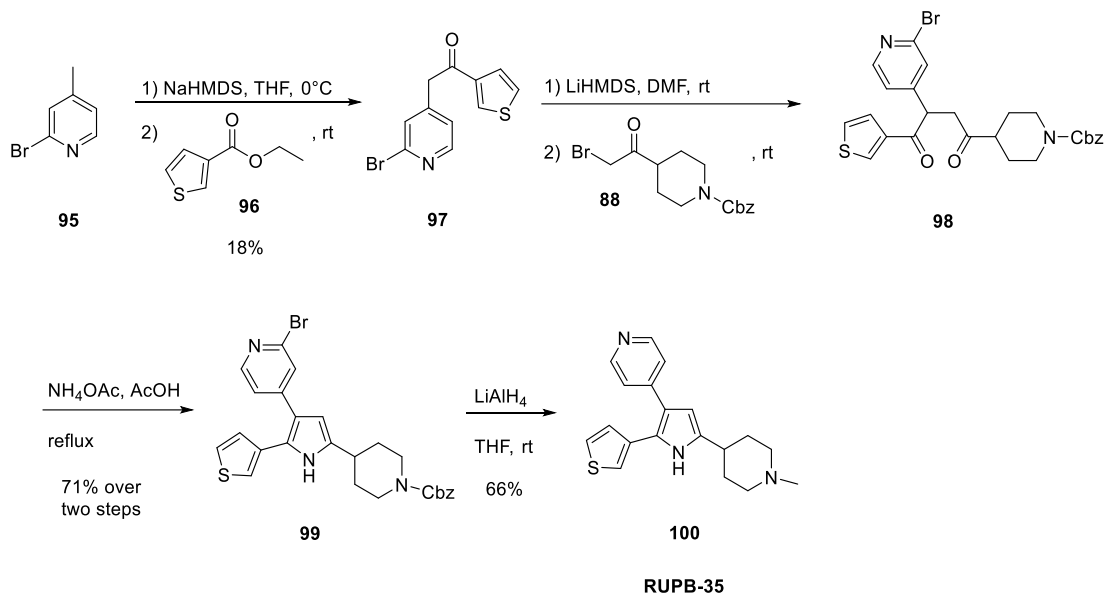
**Scheme 17.** Synthesis of  $\alpha$ -bromoketone **88**

The N-Boc piperidine methyl ketone **85** was deprotected using strongly acidic conditions to give the unprotected hydrochloride salt of **86** in 87% yield. Using 2M Na<sub>2</sub>CO<sub>3</sub> and benzyl chloroformate, the piperidine nitrogen of **86** was protected as a Cbz carbamate to give **87** in 83% yield. Subsequent electrophilic bromination of **87** provided the key  $\alpha$ -bromoketone intermediate **88** in 60% yield.

**Scheme 18.** Synthesis of analogues **94A**, **94B** and **94C**

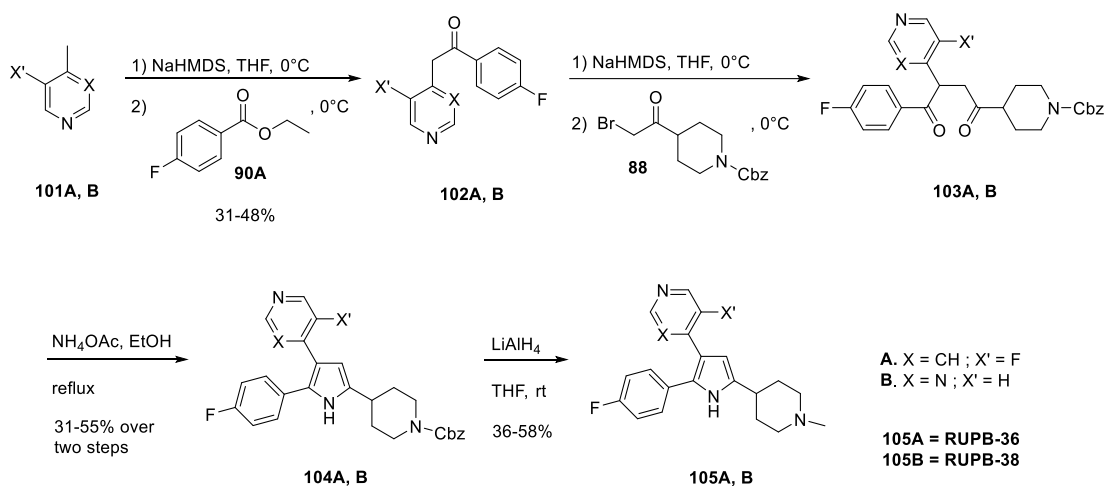
4-Methylpyridine **89** was deprotonated with NaHMDS and the enolate reacted with the benzoate esters **90A**, **B**, **C** to give corresponding diaryl ketones **91A**, **B**, **C** in 20-53% overall yields. Deprotonation of the diaryl ketones with LiHMDS and subsequent reaction with the  $\alpha$ -bromoketone **88** generated 1,4-diketones **92A**, **B**, **C**. Intramolecular cyclization of the 1,4-diketones with NH<sub>4</sub>OAc in AcOH gave the cyclized pyrrole intermediates **93A**, **B**, **C** in

28-65% yields over two steps. LAH reduction of the Cbz protected intermediates generated the N-methyl compounds **94A, B, C** in 30-68% overall yields (**Scheme 18**).



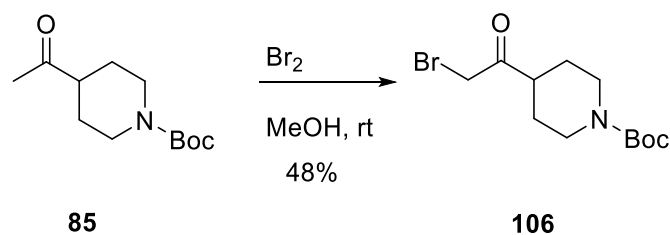
#### Scheme 19. Synthesis of analogue **100**

Following the same approach as seen in **Scheme 18**, the final compound **100** was synthesized. The diaryl ketone **97** was synthesized in an 18% yielding reaction using **95**, NaHMDS and the thiophene ester **96**. Deprotonation of **97** and reaction with the electrophile **88** generated the 1,4-diketone **98**. Subsequent cyclization with  $\text{NH}_4\text{OAc}$  gave the pyrrole **99** in 71% yield over two steps. Treatment of **99** with LAH reduced the N-Cbz piperidine to the N-methyl piperidine and debrominated the pyridine to give the final compound **100** in 66% yield.



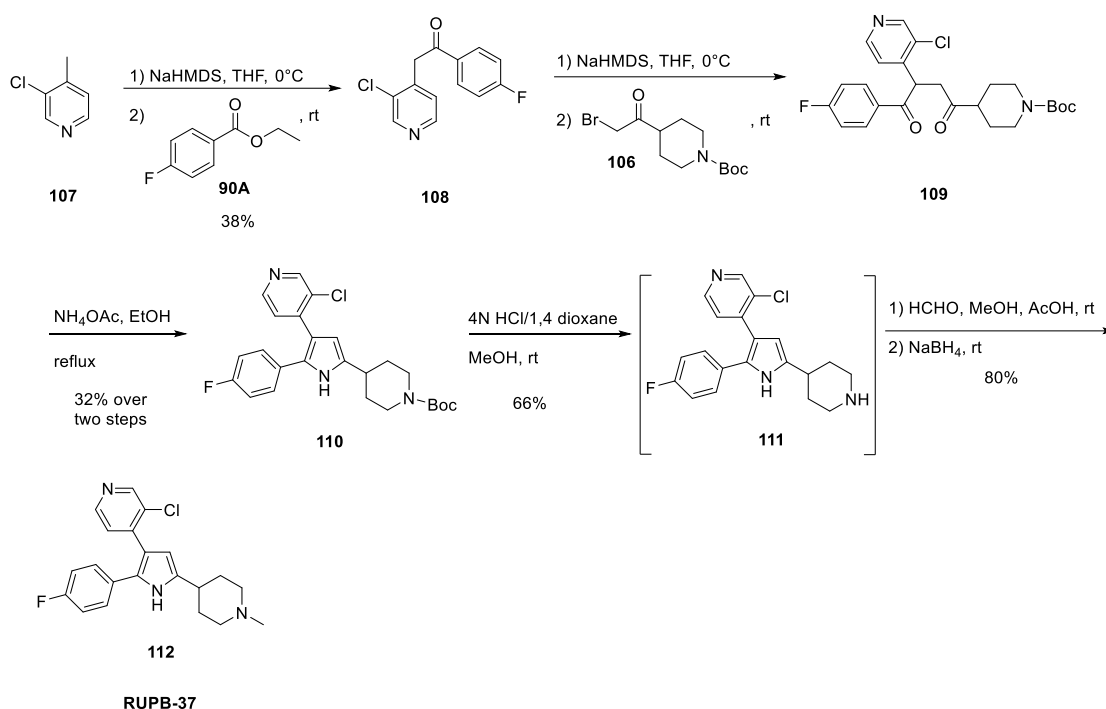
**Scheme 20.** Synthesis of analogues **105A** and **105B**

Following the same approach as described in **Scheme 18**, the final compounds **105A, B** were synthesized as shown in **Scheme 15**. The diaryl ketones **102A, B** were made using **101A, B** and **90A** in 31% and 48% yields respectively. The diaryl ketones **102A, B** were deprotonated with NaHMDS and addition of the electrophile **88** generated the 1,4-diketones **103A, B**. Cyclization of **103A, B** with  $\text{NH}_4\text{OAc}$  in ethanol gave the pyrrole intermediates **104A, B** in 31-55% yields over two steps. Treatment of **104A, B** with LAH, gave the final compounds **105A, B** in 58% and 36% yields respectively.



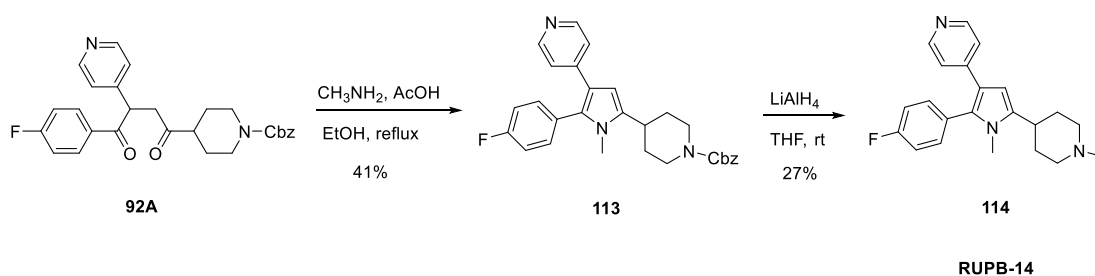
**Scheme 21.** Synthesis of  $\alpha$ -bromoketone **106**

The Boc-protected piperidine methyl ketone **85** was brominated using  $\text{Br}_2$  in methanol to give the crucial  $\alpha$ -bromoketone intermediate **106** in 48% yield.



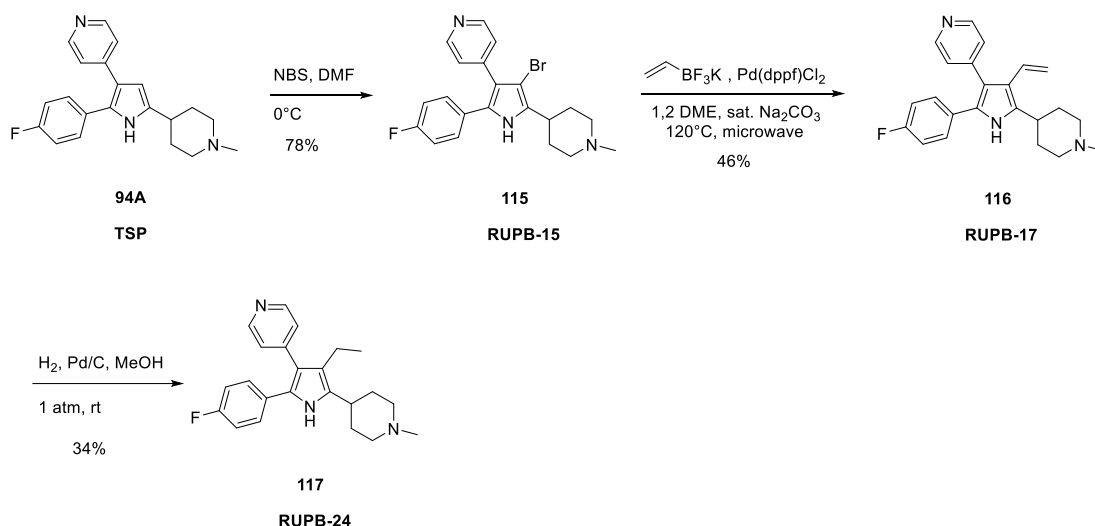
**Scheme 22.** Synthesis of analogue **112**

Following a similar approach as stated in **Scheme 18**, the final compound **112** was synthesized. **107** was deprotonated using NaHMDS and the anion generated was reacted with **90A** to give the diaryl ketone **108** in 38% yield. Treatment of **108** with NaHMDS in THF generated the corresponding anion which reacted with **106** to give the 1,4-diketone **109**. Intramolecular cyclization of **109** with  $\text{NH}_4\text{OAc}$  in ethanol gave the cyclized pyrrole intermediate **110**. Deprotection of the boc protected intermediate **110** with 4N HCl in 1,4-dioxane produced **111** in 66% yield. Finally, reductive amination of **111** using formaldehyde and  $\text{NaBH}_4$  in acidic conditions generated the final compound **112** in 80% yield.



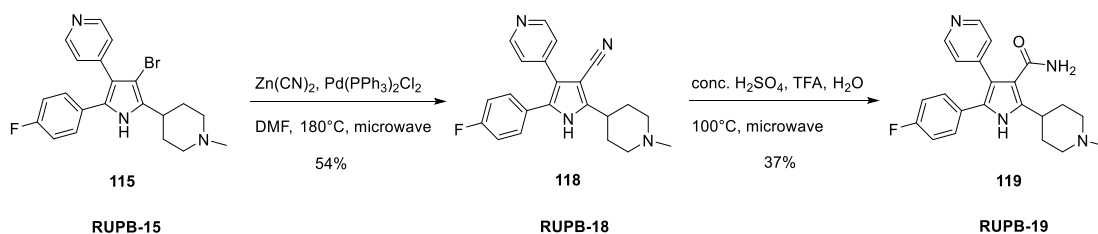
**Scheme 23.** Synthesis of analogue **114**

The 1,4-diketone **92A** was subjected to intramolecular cyclization with methylamine in ethanol and acetic acid as solvents to give the N-Cbz pyrrole **113** in 41% yield. The Cbz protected intermediate **113** was reduced to the N-methylpiperidine analogue **114** using LAH in THF in 27% yield (**Scheme 23**).



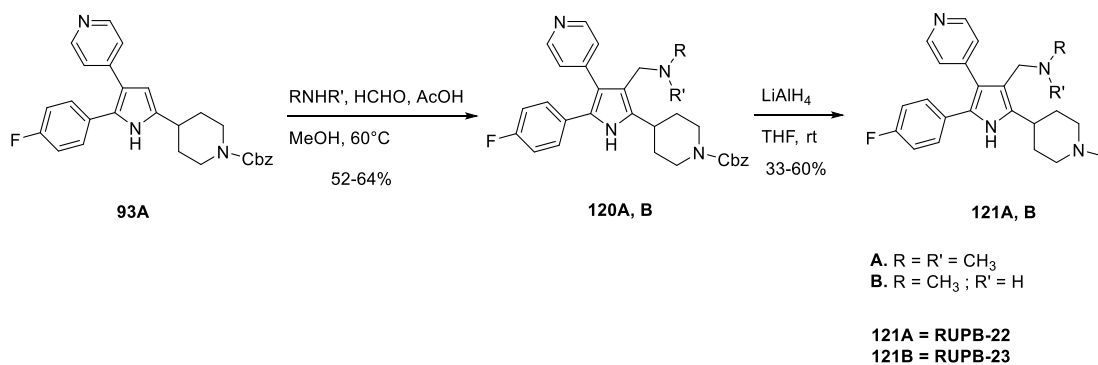
#### Scheme 24. Synthesis of analogues **115**, **116** and **117**

Compound **94A** was brominated with NBS to give analogue **115** in 78% yield. Standard Suzuki conditions were employed to couple **115** with trifluorovinyl borate, using Pd(dppf)Cl<sub>2</sub> as the catalyst, to give the vinyl pyrrole analogue **116** in 46% yield. **116** was subjected to Pd/C hydrogenation at 1 atm to generate the analogue **117** in 34% yield.



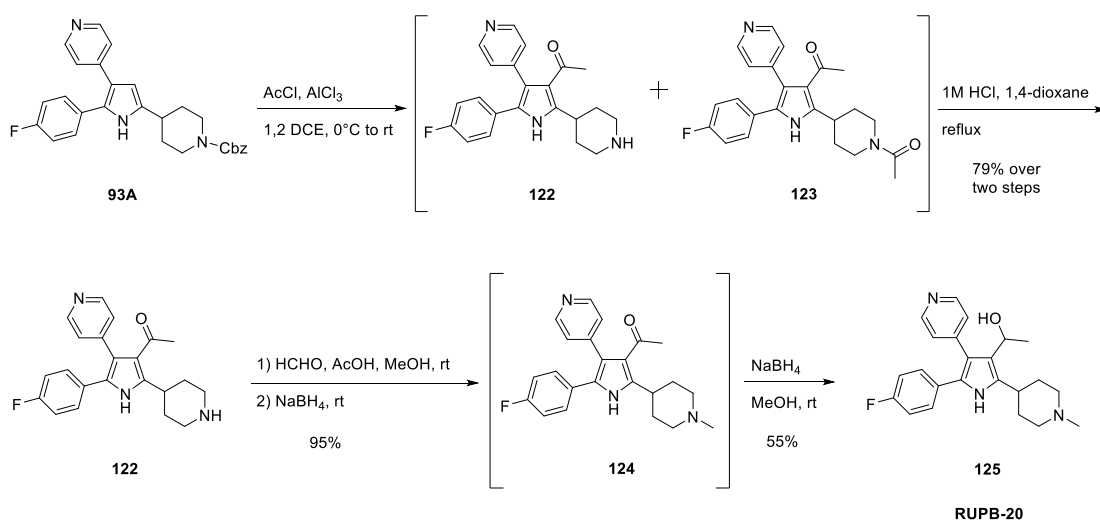
#### Scheme 25. Synthesis of analogues **118** and **119**

Compound **115** was coupled with  $\text{Zn(CN)}_2$ , using  $\text{Pd(PPh}_3)_2\text{Cl}_2$  as catalyst, to give the cyano pyrrole analogue **118** in 54% yield. **119** was synthesized in 37% yield by subjecting **118** to acid-catalyzed hydrolysis (**Scheme 25**).



**Scheme 26.** Synthesis of analogues **121A** and **121B**

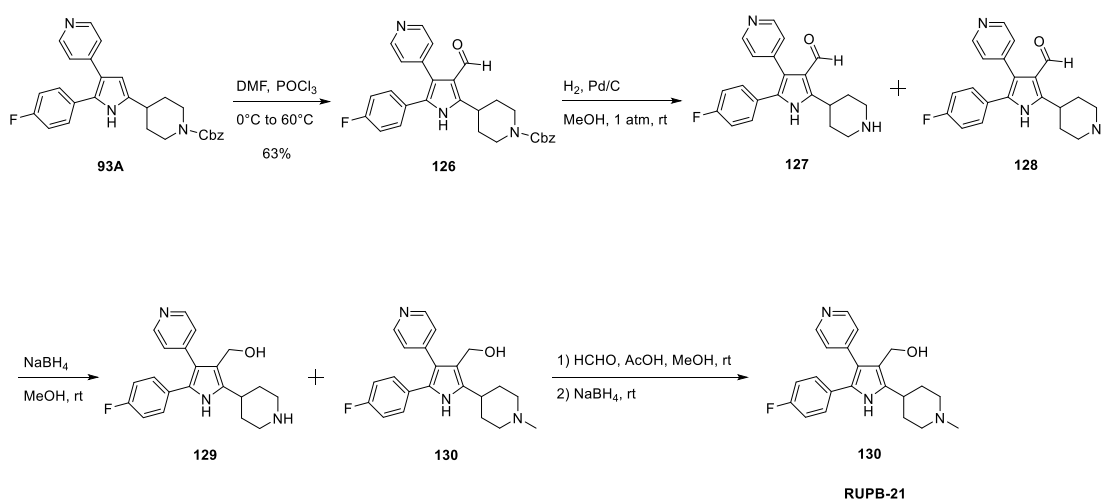
Intermediate **93A** was subjected to Mannich conditions using dimethylamine and methylamine to give corresponding intermediates **120A** and **120B** in yields of 64% and 52% respectively. **120A, B** were reduced by LAH in THF to give the final compounds **121A, B** in yields of 60% and 33% respectively.



**Scheme 27.** Synthesis of analogue **125**

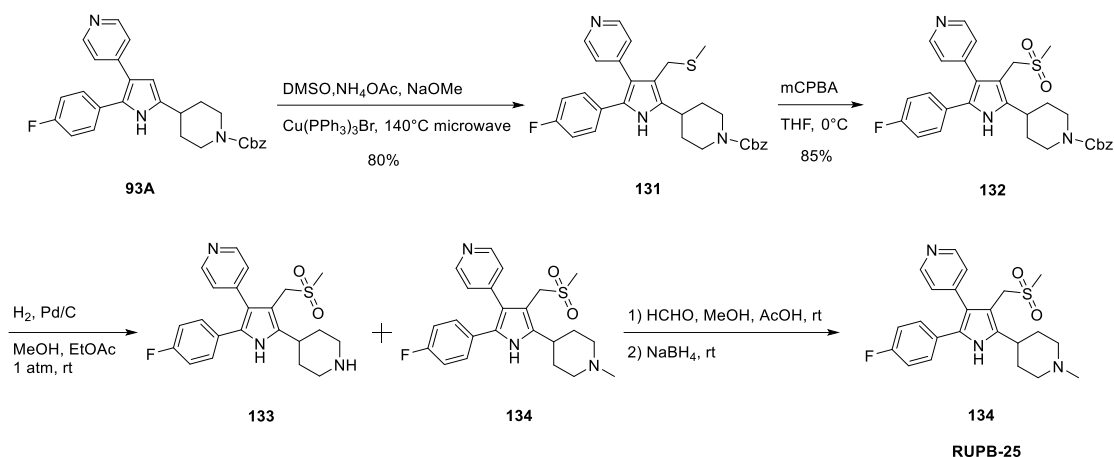


Intermediate **93A** was acylated under standard Friedel-Crafts conditions using acetyl chloride as the acylating agent and aluminium chloride as the Lewis acid to generate the desired product compound **122** and the side product **123**. Both products were devoid of the Cbz group. Treatment with 1N HCl in 1,4 dioxane converted the mixture of **122** and **123** to the desired product **122** in a yield of 79% over 2 steps. Reductive amination with formaldehyde and NaBH<sub>4</sub> under acidic conditions converted **122** to the N-methylpiperidine acetyl pyrrole intermediate **124** in a yield of 95% without reducing the acetyl moiety. Reduction of the acetyl group in **124** to the secondary alcohol using NaBH<sub>4</sub> gave the final compound **125** in a 55% yield (**Scheme 27**).



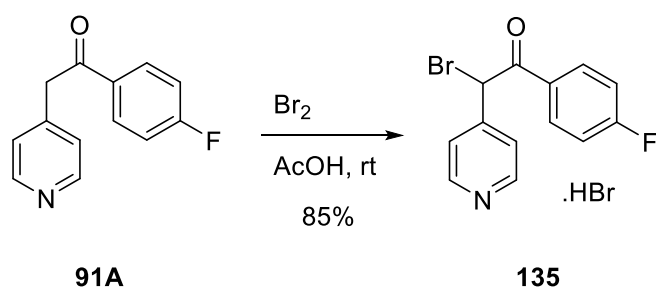
**Scheme 28.** Synthesis of analogue **130**

Compound **93A** was converted to the pyrrole aldehyde **126** in a yield of 63% by employing the Vilsmeier-Haack formylation using DMF and POCl<sub>3</sub>. Pd/C hydrogenation of **126** at 1 atm to deprotect the amine generated a mixture of products **127** and **128**. NaBH<sub>4</sub> reduction of the aldehyde in **127** and **128** gave a mixture of the primary alcohol products **129** and **130**. Finally, reductive amination using formaldehyde and NaBH<sub>4</sub> under acidic conditions converted **129** from the mixture to the final compound **130**.



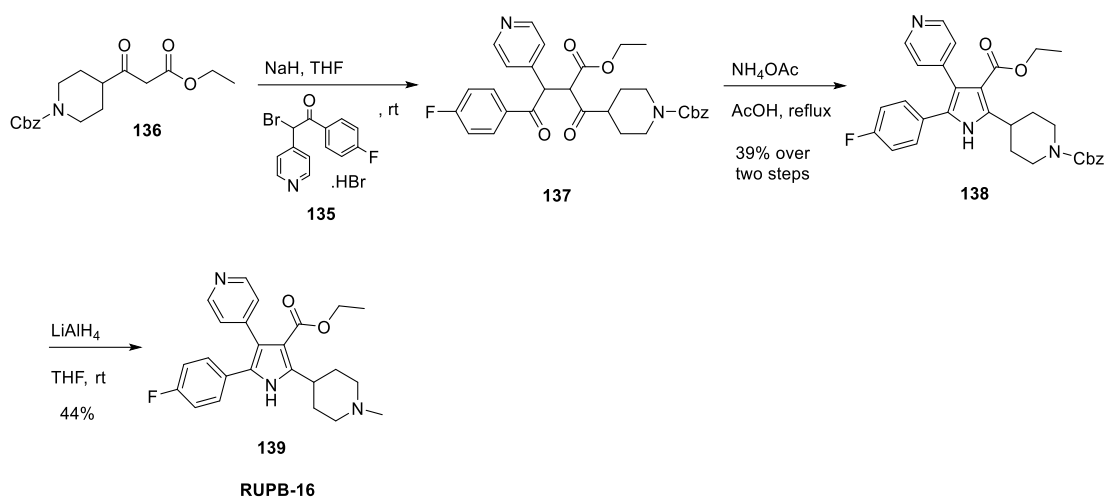
### Scheme 29. Synthesis of analogue 134

Intermediate **93A** was coupled with DMSO using  $\text{Cu(PPh}_3)_3\text{Br}$  as catalyst and sodium methoxide as base to give the thioether pyrrole intermediate **131** in 80% yield. Intermediate **131** was oxidized with mCPBA to the sulphone pyrrole intermediate **132** in yield of 85%. Pd/C hydrogenation of **132** gave a mixture of the N-H and N-Me products **133** and **134** respectively. Reductive amination using formaldehyde and  $\text{NaBH}_4$  under acidic conditions transformed the N-H intermediate **133** to the N-Me final compound **134**.



### Scheme 30. Synthesis of bromo diaryl ketone 135

The diaryl ketone intermediate **91A** was treated with  $\text{Br}_2$  in AcOH to generate the hydrobromide salt of **135** in a high yield of 85%.



**Scheme 31.** Synthesis of analogue **139**

The  $\beta$ -ketoester **136** was deprotonated with NaH to generate the corresponding carbanion while the hydrobromide salt of **135** was converted to its free base by NaH. The anion generated reacted with the bromo diaryl ketone to give the 1,4-diketone **137**. Intramolecular cyclization of **137** initiated by  $\text{NH}_4\text{OAc}$  gave the cyclized pyrrole ester intermediate **138** in 39% yield over two steps. Finally, LAH reduction of the Cbz group to the N-methyl produced the final compound **139** in 44% yield without reducing the ester moiety.

Standard Suzuki conditions were employed to couple the fluoro bromoindole **140** with pyridine-4-boronic acid using Pd(dppf)Cl<sub>2</sub> as catalyst to give **141** in a high yield of 89%. The indole nitrogen of **141** was tosylated to produce intermediate **142** in 97% yield. **142** was lithiated at the 2-position with LDA and TMEDA and subsequently reacted with the bromide to generate the 2-bromoindole **143** in 47% yield. The Suzuki product **144** was synthesized in 76% yield by coupling **143** with tetrahydropyridine dioxaborolane using Pd(dppf)Cl<sub>2</sub> as catalyst. The tosyl group of **144** was taken off by treatment with 1N NaOH under microwave conditions to generate the unprotected indole **145** in 54% yield. Pd/C hydrogenation at atmospheric pressure reduced the tetrahydropyridine of **145** to the piperidine of **146** in 72% yield. The piperidine nitrogen of **146** was deprotected using 4N HCl/1,4-dioxane to give intermediate **147** in 86% yield. Finally, standard reductive amination conditions using formaldehyde and NaBH<sub>4</sub> were employed to give the final compound **148** in 50% yield.

## V. PLASMODIUM FALCIPARUM PKG INHIBITORS

### A. RESULTS AND DISCUSSION

TSP and all the analogues generated in this program were tested for their *in vitro* activity against human and *P. falciparum* PKG. The compounds were assayed at a concentration of 10  $\mu$ M against human and *P. falciparum* PKG and 1  $\mu$ M against *P. falciparum* PKG. The percentage of enzymatic inhibition at a single concentration and the IC<sub>50</sub> values were determined (**Table 1**).

**TSP (94A)** is reported to be an extremely potent (IC<sub>50</sub> = 18 nM) and reasonably selective compound in inhibiting the parasitic enzyme over the human enzyme (59% inhibition of human PKG at 10  $\mu$ M). Analogues were prepared to map the binding pocket of the enzyme to further improve potency and selectivity.

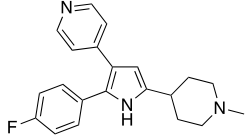
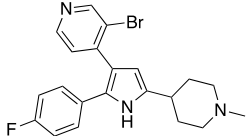
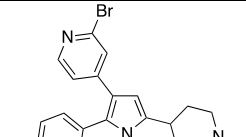
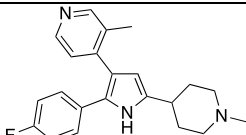
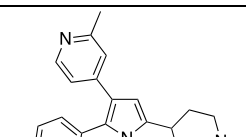
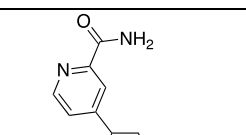
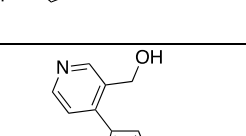
#### 1. Modifications of the 4-fluorophenyl moiety

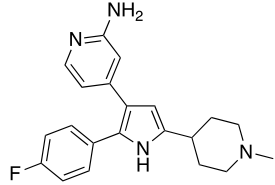
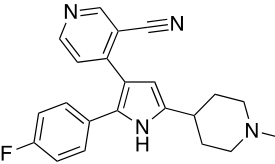
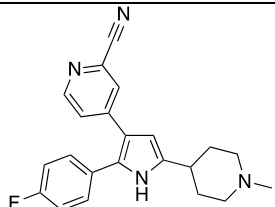
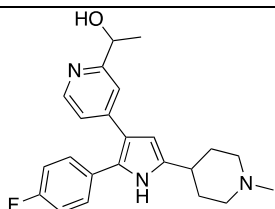
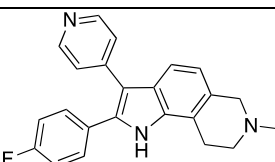
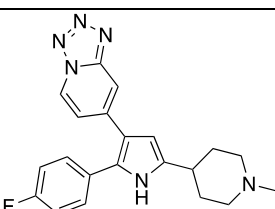
Replacement of the fluorine of the 4-fluorophenyl moiety generated analogues **RUPB-33 (94B)** and **RUPB-34 (94C)**. Substitution with the electron withdrawing CF<sub>3</sub> group as in **RUPB-33** (IC<sub>50</sub> = 115 nM) lead to an almost 5-fold decrease in activity even though selectivity for *Pf*PKG was improved with respect to **TSP**. On the other hand, substituting the fluorine with an electron donating methoxy group as in **RUPB-34** (IC<sub>50</sub> = 63 nM) decreased activity by a factor of 2.5 while maintaining similar selectivity as **TSP** for both enzymes. The SAR tells us that electronic features are less important here. In keeping with this notion, replacing the 4-fluorophenyl ring with a thiophene as in **RUPB-35 (100)** (IC<sub>50</sub> = 130 nM) lead to a 7-fold decrease in activity while maintaining potency similar to the p-CF<sub>3</sub> analogue **RUPB-33**.

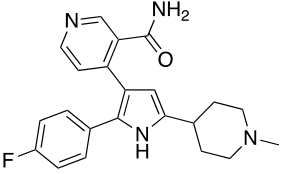
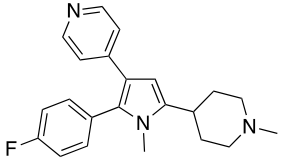
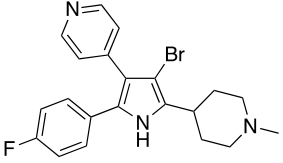
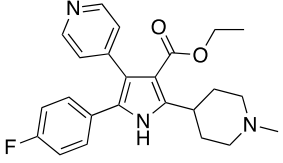
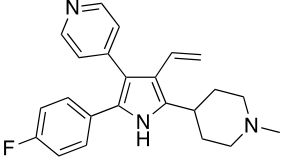
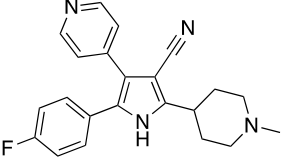
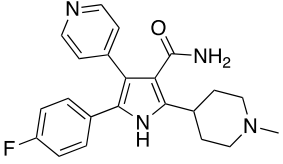
#### 2. Modifications of the pyridine ring

Various functional groups were introduced at the 2- and 3-positions of the pyridine ring. Introduction of a bromide at the 3-position gave **RUPB-1** (IC<sub>50</sub> = 20 nM) which is equipotent to **TSP** in terms of activity. Introduction of a bromide at the 2-position as in **RUPB-2** (IC<sub>50</sub> = 101 nM) decreased activity by a factor of 5 when compared to **RUPB-1**. Based on the activity

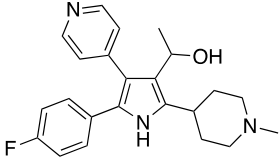
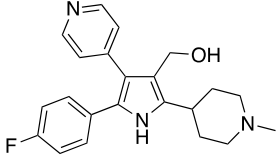
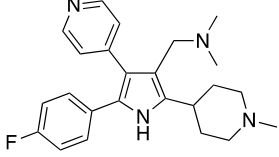
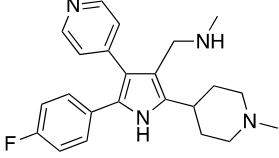
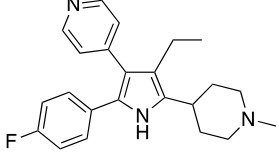
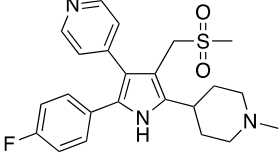
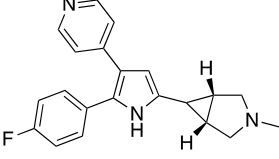
**Table 1.** Biological activity of *Plasmodium falciparum* PKG Inhibitors

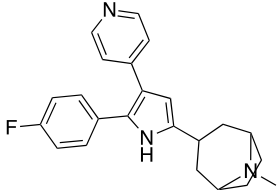
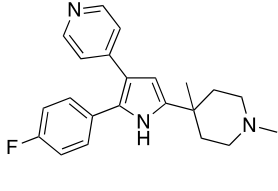
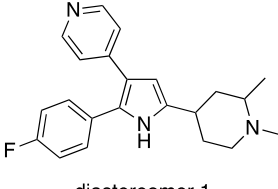
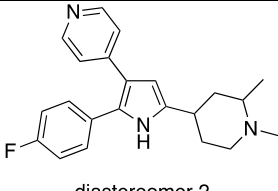
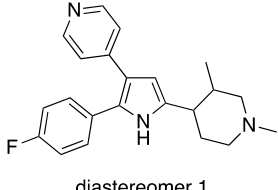
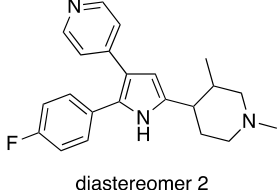
Compound	Structure	Molecular Weight	Human PKG inhibition (10 $\mu$ M)	<i>Pf</i> PKG inhibition (1 $\mu$ M)	IC <sub>50</sub> Mean (nM)	Chemist
<b>TSP 94A</b>		335.43	59	103	18	RF <sup>a</sup>
<b>RUPB-1</b>		414.32	39	96	20	JG <sup>b</sup>
<b>RUPB-2</b>		414.32	60	96	101	JG
<b>RUPB-3</b>		349.45	45	99	195	JG
<b>RUPB-4</b>		349.45	30	91	238	JG
<b>RUPB-5</b>		378.45	28	83	627	JG
<b>RUPB-6</b>		365.45	-1	89	771	JG

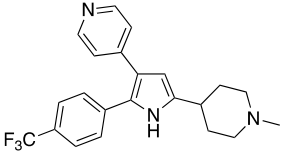
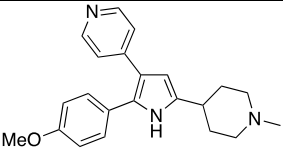
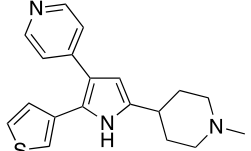
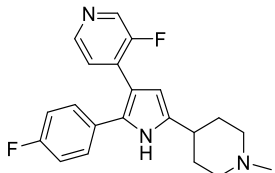
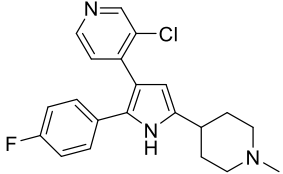
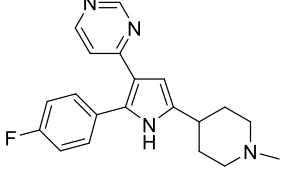
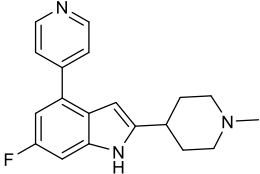
Compound	Structure	Molecular Weight	Human PKG inhibition (10 $\mu$ M)	<i>Pj</i> PKG inhibition (1 $\mu$ M)	IC <sub>50</sub> Mean (nM)	Chemist
<b>RUPB-7</b>		350.44	48	95	133	JG
<b>RUPB-8</b>		360.44	12	100	18	JG
<b>RUPB-9</b>		360.44	16	98	27	JG
<b>RUPB-10</b>		379.48	-4	49	>1 $\mu$ M	JG
<b>RUPB-11</b>		357.43	35	95	24	JG
<b>RUPB-12</b>		376.44	-35	27	>1 $\mu$ M	JG

Compound	Structure	Molecular Weight	Human PKG inhibition (10 $\mu$ M)	<i>Pj</i> PKG inhibition (1 $\mu$ M)	IC <sub>50</sub> Mean (nM)	Chemist
<b>RUPB-13</b>		378.45	-2	29	>1 $\mu$ M	JG
<b>RUPB-14</b> <b>114</b>		349.48	-	-	79	RF
<b>RUPB-15</b> <b>115</b>		414.32	52	100	149	RF
<b>RUPB-16</b> <b>139</b>		407.49	18	32	>1 $\mu$ M	RF
<b>RUPB-17</b> <b>116</b>		361.46	34	96	712	RF
<b>RUPB-18</b> <b>118</b>		360.44	57	97	24	RF
<b>RUPB-19</b> <b>119</b>		378.45	-8	67	>1 $\mu$ M	RF



Compound	Structure	Molecular Weight	Human PKG inhibition (10 $\mu$ M)	<i>Pj</i> PKG inhibition (1 $\mu$ M)	IC <sub>50</sub> Mean (nM)	Chemist
<b>RUPB-20</b> <b>125</b>		379.48	3	72	>1 $\mu$ M	RF
<b>RUPB-21</b> <b>130</b>		365.45	12	97	255	RF
<b>RUPB-22</b> <b>121A</b>		392.52	-3	49	>1 $\mu$ M	RF
<b>RUPB-23</b> <b>121B</b>		378.50	0	91	1030	RF
<b>RUPB-24</b> <b>117</b>		363.48	43	100	450	RF
<b>RUPB-25</b> <b>134</b>		427.54	17	98	73	RF
<b>RUPB-26</b>		333.41	7	94	258	JG

Compound	Structure	Molecular Weight	Human PKG inhibition (10 $\mu$ M)	<i>Pj</i> PKG inhibition (1 $\mu$ M)	IC <sub>50</sub> Mean (nM)	Chemist
<b>RUPB-27</b>		361.46	32	98	80	JG
<b>RUPB-28</b>		349.45	29	100	81	JG
<b>RUPB-29</b>	 diastereomer 1	349.45	26	95	107	JG
<b>RUPB-30</b>	 diastereomer 2	349.45	5	98	80	JG
<b>RUPB-31</b>	 diastereomer 1	349.45	82	99	13	JG
<b>RUPB-32</b>	 diastereomer 2	349.45	66	103	23	JG

Compound	Structure	Molecular Weight	Human PKG inhibition (10 $\mu$ M)	<i>Pj</i> PKG inhibition (1 $\mu$ M)	IC <sub>50</sub> Mean (nM)	Chemist
<b>RUPB-33</b> <b>94B</b>		385.43	9	102	115	RF
<b>RUPB-34</b> <b>94C</b>		347.46	38	103	63	RF
<b>RUPB-35</b> <b>100</b>		323.46	66	103	130	RF
<b>RUPB-36</b> <b>105A</b>		353.42	-	-	19	RF
<b>RUPB-37</b> <b>112</b>		369.87	-	-	34	RF
<b>RUPB-38</b> <b>105B</b>		336.41	-	-	28	RF
<b>RUPB-39</b> <b>148</b>		309.39	-	-	2525	RF

RF<sup>a</sup> (Raheel Fondekar); JG<sup>b</sup> (John Gilleran)

profile of **RUPB-1**, **RUPB-36** (**105A**) and **RUPB-37** (**112**) were designed to investigate the electronic and steric effects of other substituents at the 3-position of the pyridine ring. Replacing the bromide in **RUPB-1** with fluoride gave **RUPB-36** ( $IC_{50} = 19$  nM) which is just as equipotent as **TSP** and **RUPB-1**. Replacing the bromide of **RUPB-1** with chloride gave **RUPB-37** ( $IC_{50} = 34$  nM) which is 1.5 times less active than bromide **RUPB-1**.

Incorporation of a methyl group at the 2- and 3- positions of the pyridine reduced activity as seen with compounds **RUPB-3** ( $IC_{50} = 195$  nM) and **RUPB-4** ( $IC_{50} = 238$  nM) respectively. Having an amide at the 2-position as in **RUPB-5** ( $IC_{50} = 627$  nM) lead to a 35-fold decrease in activity, whereas the 3-pyridyl amide **RUPB-13** was found to be inactive.

Introduction of a hydroxymethyl group at the 3-position as in **RUPB-6** ( $IC_{50} = 771$  nM) lead to a 43-fold fall in activity with respect to **TSP**. The 2-aminopyridine analogue **RUPB-7** ( $IC_{50} = 133$  nM) is almost 7 times less potent than **TSP**. The 2-cyano pyridine **RUPB-9** ( $IC_{50} = 27$  nM) is exactly 1.5 times less active than **TSP** whereas the 3-cyano pyridine **RUPB-8** ( $IC_{50} = 18$  nM) is equipotent to **TSP** and displayed much better selectivity. Incorporation of a secondary alcohol at the 2-position of the pyridine ring as seen in **RUPB-10** and a tetrazole fused to the pyridine ring as seen in **RUPB-12** resulted in complete loss of activity. All the substitutions on the pyridine ring indicate that EDGs are detrimental to activity whereas sterically smaller EWGs especially at the 3-position are extremely well tolerated.

The pyridine ring of **TSP** was substituted with a pyrimidine ring to generate **RUPB-38** (**105B**) ( $IC_{50} = 28$  nM). This change incorporated a nitrogen heterocycle which lacks the dipole moment and is not nearly as basic as pyridine. However, the pyrimidine nitrogens could still accept a hydrogen bond. **RUPB-38** is slightly less active at 28 nM.

### 3. Modifications at the 4-position of the pyrrole nucleus

A wide variety of functional group substituents were introduced at the unsubstituted 4-position of the pyrrole nucleus of **TSP**. Bromination of **TSP** at the 4-position gave rise to **RUPB-15** (**115**) ( $IC_{50} = 149$  nM) which is almost 8 times less potent than **TSP**. Introduction of a vinyl group at this position, as seen in **RUPB-17** (**116**) ( $IC_{50} = 712$  nM) lead to a 40-fold decrease in

potency with respect to **TSP**. Reduction of the vinyl moiety of **RUPB-17** to an ethyl chain produced **RUPB-24** (**117**) ( $IC_{50} = 450$  nM) which is 1.5 times more active than **RUPB-17** but still much less potent than **TSP**. Introduction of ester and amide moieties at this position gave inactive compounds as seen in the case of **RUPB-16** (**139**) and **RUPB-19** (**119**). **RUPB-20** (**125**) and **RUPB-21** (**130**) are benzylic alcohol analogues of **TSP** and lack the activity profile of **TSP**. While the primary alcohol analogue **RUPB-21** ( $IC_{50} = 255$  nM) is moderately active, the secondary alcohol **RUPB-20** did not display efficient inhibition at 1  $\mu$ M against the parasitic enzyme. Installation of benzylic amines at the 4-position of the pyrrole nucleus generated **RUPB-22** (**121A**) and **RUPB-23** (**121B**) ( $IC_{50} = 1030$  nM), both of which exhibited extremely poor activity profiles. This data suggests that EDGs at the 4-position of the pyrrole nucleus as seen in compounds **RUPB-20-23** are not well tolerated and severely detrimental to activity. Introduction of a nitrile at the unsubstituted 3-position of the pyrrole core of **TSP** generated **RUPB-18** (**118**). This compound is almost as potent as **TSP** with an  $IC_{50}$  of 24 nM while the selectivity is marginally hampered. The benzylic sulphone **RUPB-25** (**134**) ( $IC_{50} = 73$  nM) is 4 times less potent but displays a better selectivity profile than **TSP**. Substitution at the 4-position of the pyrrole core was met with failure except for the small electron withdrawing group, the nitrile of **RUPB-18**.

#### 4. Modifications on the piperidine ring

The azabicyclic analogues **RUPB-26** ( $IC_{50} = 258$  nM) and **RUPB-27** ( $IC_{50} = 80$  nM) are not as effective as **TSP** in inhibiting the parasitic enzyme. Introduction of a methyl at the 4-position of the piperidine ring generated **RUPB-28** ( $IC_{50} = 81$  nM) which is noted to be 4.5 times less active than **TSP**. Incorporation of a methyl at the 3-position of the piperidine ring produced diastereomeric compounds **RUPB-31** and **RUPB-32**. **RUPB-32** ( $IC_{50} = 23$  nM) is almost equipotent to **TSP** whereas **RUPB-31** ( $IC_{50} = 13$  nM) is 1.4 times more potent than **TSP**. The 2-methyl piperidine diastereomers **RUPB-29** ( $IC_{50} = 107$  nM) and **RUPB-30** ( $IC_{50} = 80$  nM) are not as active as **TSP** in inhibition of the parasitic enzyme.

## 5. Miscellaneous modifications

Introduction of a methyl group on the pyrrole nitrogen of **TSP** produced **RUPB-14 (114)** which is modestly active. This provides an opportunity for more N-substituted analogues on the pyrrole ring to be examined. We also decided to investigate new heterocyclic chemotypes. **RUPB-11**, which is an indolo-piperidine, is observed to be extremely potent with an  $IC_{50}$  of 24 nM. **RUPB-39 (148)** was designed in such a way so as to replace the pyrrole nucleus with an indole. A key aspect in the design of this analogue is that all the functional groups or substituents occupy more or less the same spatial arrangement as they did for **TSP** in order to maintain all the key interactions. However, **RUPB-39** ( $IC_{50} = 2525$  nM) is extremely inactive as the  $IC_{50}$  dropped by a factor of 140 with respect to **TSP**.

## B. EXPERIMENTALS

### 1-(piperidin-4-yl)ethan-1-one hydrochloride (**86**)

tert-Butyl 4-acetylpiperidine-1-carboxylate **85** (6.92 g, 30.444 mmol, 1 eq) was dissolved in 30 mL MeOH. Concentrated HCl (5 mL) was added and the reaction was stirred at room temperature. After 1.5 hours, the reaction was determined complete by TLC and concentrated to 5 mL under reduced pressure. A white solid precipitated out after addition of 50 mL acetone. The suspension was filtered and dried to give 1-(piperidin-4-yl)ethan-1-one hydrochloride **86** (4.31 g, 87% yield) as a crystalline white solid.

### Benzyl 4-acetylpiperidine-1-carboxylate (**87**)

To a solution of 1-(piperidin-4-yl)ethan-1-one hydrochloride **86** (4.31 g, 26.429 mmol, 1 eq) in 70 mL MeCN, 2M Na<sub>2</sub>CO<sub>3</sub> (55 mL) was added. The reaction was stirred at room temperature for 15 minutes. Benzyl chloroformate (3.76 mL, density = 1.2 g/mL, 26.429 mmol, 1 eq) was added dropwise and the reaction was allowed to stir overnight at room temperature. The reaction was determined complete by TLC analysis and was concentrated under reduced pressure. The residue was partitioned between EtOAc and water. The organic phase was separated, and the aqueous phase was extracted with EtOAc (3 x). The combined organic phase was washed with brine (1 x), dried over sodium sulphate and concentrated under reduced pressure. Purification by silica gel chromatography (10% → 20% → 30% → 50% EtOAc/Hexanes) afforded benzyl 4-acetylpiperidine-1-carboxylate **87** (5.75 g, 83% yield, 95% purity by LC-MS) as a clear-white solid.

<sup>1</sup>H NMR (400 MHz, DMSO-*d*<sub>6</sub>) δ 7.43 – 7.23 (m, 5H), 5.04 (s, 2H), 3.95 (dddd, *J* = 13.3, 4.5, 3.2, 1.3 Hz, 2H), 2.85 (s, 2H), 2.54 (tt, *J* = 11.3, 3.7 Hz, 1H), 2.09 (s, 3H), 1.85 – 1.72 (m, 2H), 1.37 – 1.19 (m, 2H). (M+H)<sup>+</sup> 261.80

### Benzyl 4-(2-bromoacetyl)piperidine-1-carboxylate (**88**)

Benzyl 4-acetylpiperidine-1-carboxylate **87** (5.75 g, 22.003 mmol, 1 eq) was dissolved in 80 mL MeOH. Bromine (1.13 mL, density = 3.1 g/mL, 22.003 mmol, 1 eq) was separately dissolved in 10 mL MeOH. The methanolic solution of bromine was added to the methanolic

solution of **87** portion-wise over a period of 15 minutes and the reaction was allowed to stir at room temperature. After 2.5 hours, the reaction was determined complete by TLC and LC-MS analysis and the reaction was concentrated under reduced pressure. The residue was partitioned between EtOAc and water and the organic phase was separated. The aqueous phase was extracted with EtOAc (3 x) and the combined organic phase was washed with brine (1 x), dried over sodium sulphate and concentrated. Purification by silica gel chromatography (10% → 15% → 20% → 25% EtOAc/Hexanes) afforded benzyl 4-(2-bromoacetyl)piperidine-1-carboxylate **88** (5.46 g, 60% yield, 93% purity by LC-MS) as a light-yellow viscous liquid.

<sup>1</sup>H NMR (500 MHz, DMSO-*d*<sub>6</sub>) δ 7.43 – 7.23 (m, 5H), 5.05 (s, 2H), 4.49 (s, 2H), 3.98 (dt, *J* = 13.4, 3.1 Hz, 2H), 2.81 (tt, *J* = 11.4, 3.7 Hz, 3H), 1.83 (d, *J* = 10.4 Hz, 2H), 1.43 – 1.27 (m, 2H). (M+H)<sup>+</sup> 339.60; 341.60

#### **1-(4-fluorophenyl)-2-(pyridin-4-yl)ethan-1-one (91A)**

4-methylpyridine **89** (3.98 g, 42.74 mmol, 1 eq) was dissolved in 10 mL anhydrous THF and cooled to 0°C under nitrogen. NaHMDS 1M solution in THF (64.1 mL, 64.1 mmol, 1.5 eq) was added to the THF solution of **89** by means of a syringe in a portion-wise manner over 10 minutes. The reaction was stirred for 1 hour maintaining the temperature at 0°C. Ethyl 4-fluorobenzoate **90A** (5.04 g, 44.01 mmol, 1.1 eq) was dissolved in 8 mL THF and added to the anion generated by means of a syringe and the reaction was allowed to warm to room temperature. After 3.5 hours, the reaction was determined complete by LC-MS analysis, quenched by addition of 3 mL water and concentrated under reduced pressure. The residue was partitioned between EtOAc and water and the organic phase was separated. The aqueous phase was extracted with EtOAc (3 x) and the combined organic phase was washed with brine, dried over sodium sulphate and concentrated. Purification by silica gel chromatography (25% → 37% → 50% → 75% EtOAc/Hexanes) afforded 1-(4-fluorophenyl)-2-(pyridin-4-yl)ethan-1-one **91A** (4.91 g, 53% yield, 98% purity by LC-MS) as a pale-yellow crystalline solid.

<sup>1</sup>H NMR (400 MHz, DMSO-*d*<sub>6</sub>) δ 8.52 – 8.45 (m, 2H), 8.16 – 8.08 (m, 2H), 7.41 – 7.32 (m, 2H), 7.30 – 7.24 (m, 2H), 4.47 (s, 2H). (M+H)<sup>+</sup> 215.55



**Benzyl 4-(4-(4-fluorophenyl)-4-oxo-3-(pyridin-4-yl)butanoyl)piperidine-1-carboxylate (92A)**

To a solution of 1-(4-fluorophenyl)-2-(pyridin-4-yl)ethan-1-one **91A** (1.86 g, 8.64 mmol, 1 eq) in 20 mL anhydrous DMF, LiHMDS 1M solution in THF (10.4 mL, 10.4 mmol, 1.2 eq) was added under nitrogen. The reaction was stirred at room temperature for 1 hour. Benzyl 4-(2-bromoacetyl)piperidine-1-carboxylate **88** (4.18 g, 12.29 mmol, 1.4 eq) was dissolved in 12 mL anhydrous DMF and added to the preformed enolate by means of a syringe. The reaction was stirred at room temperature and was determined complete in 45 minutes by LC-MS analysis. The reaction was concentrated under reduced pressure to remove most of the DMF. The concentrate was partitioned between water and EtOAc and the organic phase was separated. The aqueous phase was extracted with EtOAc (3 x). The combined organic phase was washed with brine (1 x), dried over sodium sulphate and concentrated. Excess DMF was eliminated by forming an azeotropic mixture with toluene to give benzyl 4-(4-(4-fluorophenyl)-4-oxo-3-(pyridin-4-yl)butanoyl)piperidine-1-carboxylate **92A** (6.0 g, 34% purity by LC-MS) as a dark maroon viscous liquid which was taken onto the next step without further purification. (M+H)<sup>+</sup> 474.75

**Benzyl 4-(5-(4-fluorophenyl)-4-(pyridin-4-yl)-1H-pyrrol-2-yl)piperidine-1-carboxylate (93A)**

Crude benzyl 4-(4-(4-fluorophenyl)-4-oxo-3-(pyridin-4-yl)butanoyl)piperidine-1-carboxylate **92A** (6.0 g) was dissolved in 30 mL glacial AcOH. Ammonium acetate (5g, excess) was added and the reaction was heated to reflux. After 1.5 hours, the reaction was deemed complete by LC-MS analysis and concentrated under reduced pressure to remove most of the AcOH. The concentrate was partitioned between water and EtOAc and the organic phase was separated. The aqueous phase was extracted with EtOAc (3 x). The combined organic phase was washed with brine (1 x), dried over sodium sulphate and concentrated. Excess AcOH was eliminated by forming an azeotropic mixture with toluene. Purification by silica gel chromatography (25% → 37% → 50% EtOAc/Hexanes) afforded benzyl 4-(5-(4-fluorophenyl)-4-(pyridin-4-yl)-1H-

pyrrol-2-yl)piperidine-1-carboxylate **93A** (2.64 g, 38% yield over two steps, 84% purity by LC-MS) as a yellow solid.

$^1\text{H}$  NMR (400 MHz, DMSO- $d_6$ )  $\delta$  11.12 (d,  $J$  = 2.8 Hz, 1H), 8.39 – 8.26 (m, 2H), 7.39 – 7.29 (m, 7H), 7.23 – 7.16 (m, 2H), 7.15 – 7.11 (m, 2H), 6.14 (dd,  $J$  = 2.6, 0.6 Hz, 1H), 5.07 (s, 2H), 4.15 – 4.03 (m, 2H), 2.91 (s, 2H), 2.76 (tt,  $J$  = 11.9, 3.6 Hz, 1H), 1.92 (d,  $J$  = 12.0 Hz, 2H), 1.54 (qd,  $J$  = 12.6, 4.2 Hz, 2H). (M+H) $^+$  455.90

#### **4-(2-(4-fluorophenyl)-5-(1-methylpiperidin-4-yl)-1H-pyrrol-3-yl)pyridine (94A) [TSP]**

To a solution of benzyl 4-(5-(4-fluorophenyl)-4-(pyridin-4-yl)-1H-pyrrol-2-yl)piperidine-1-carboxylate **93A** (60 mg, 0.132 mmol, 1 eq) in 5 mL anhydrous THF, Lithium aluminium hydride 2M solution in THF (0.26 mL, 0.526 mmol, 4 eq) was added by means of a syringe. The reaction was stirred at room temperature and was determined complete in 20 minutes by LC-MS analysis. The reaction was quenched using the Feiser & Feiser quench (0.02 mL water, 0.02 mL 15% NaOH and 0.06 mL water in a sequential manner) and stirred for an additional 30 minutes. The reaction was filtered over celite and the filtrate was concentrated. Purification by silica gel chromatography (2%  $\rightarrow$  4%  $\rightarrow$  6%  $\rightarrow$  8% MeOH/ $\text{CHCl}_3$  with 0.25%  $\text{NH}_3$ ) afforded 4-(2-(4-fluorophenyl)-5-(1-methylpiperidin-4-yl)-1H-pyrrol-3-yl)pyridine **94A** [TSP] (30 mg, 68% yield, 100% purity by LC-MS) as an off-white solid.

$^1\text{H}$  NMR (400 MHz, DMSO- $d_6$ )  $\delta$  11.08 (d,  $J$  = 2.4 Hz, 1H), 8.38 – 8.25 (m, 2H), 7.37 – 7.29 (m, 2H), 7.24 – 7.15 (m, 2H), 7.15 – 7.11 (m, 2H), 6.11 (dd,  $J$  = 2.7, 0.8 Hz, 1H), 2.81 (dt,  $J$  = 12.0, 3.2 Hz, 2H), 2.47 – 2.41 (m, 1H), 2.16 (s, 3H), 1.98 – 1.84 (m, 4H), 1.63 (qd,  $J$  = 12.4, 3.7 Hz, 2H).

$^{13}\text{C}$  NMR (126 MHz, Methanol- $d_4$ )  $\delta$  162.16 (d,  $J$  = 245.6 Hz), 148.15, 146.39, 137.61, 130.11 (d,  $J$  = 8.1 Hz), 129.66 (d,  $J$  = 3.4 Hz), 128.62, 122.25, 117.49, 115.10 (d,  $J$  = 21.9 Hz), 104.44, 55.26, 45.00, 34.01, 31.51. HRMS calculated for  $\text{C}_{21}\text{H}_{22}\text{FN}_3$  (M+H) $^+$  336.1876, found 336.1889.

### **2-(pyridine-4-yl)-1-(4-(trifluoromethyl)phenyl)ethan-1-one (91B)**

Following the procedure as described for the synthesis of **91A**, using 4-methylpyridine **89** (196 mg, 2.1 mmol, 1 eq), NaHMDS 1M solution in THF (3.15 mL, 3.15 mmol, 1.5 eq) and ethyl 4-trifluoromethyl benzoate **90B** (504 mg, 2.31 mmol, 1.1 eq), the title compound **91B** was synthesized. Purification using silica gel chromatography (10% → 25% → 50% EtOAc/Hexanes) afforded 2-(pyridine-4-yl)-1-(4-(trifluoromethyl)phenyl)ethan-1-one **91B** (225 mg, 40% yield, 88% purity by LC-MS).

<sup>1</sup>H NMR (400 MHz, DMSO-*d*<sub>6</sub>) δ 8.53 – 8.46 (m, 2H), 8.26 – 8.18 (m, 2H), 7.97 – 7.89 (m, 2H), 7.32 – 7.25 (m, 2H), 4.55 (s, 2H). (M+H)<sup>+</sup> 265.80

### **Benzyl 4-(4-oxo-3-(pyridine-4-yl)-4-(4-(trifluoromethyl)phenyl)butanoyl)piperidine-1-carboxylate (92B)**

Following the procedure as described for the synthesis of **92A**, using 2-(pyridine-4-yl)-1-(4-(trifluoromethyl)phenyl)ethan-1-one **91B** (213 mg, 0.803 mmol, 1 eq), LiHMDS 1M solution in THF (1 mL, 1 mmol, 1.25 mmol) and benzyl 4-(2-bromoacetyl)piperidine-1-carboxylate **88** (382 mg, 1.124 mmol, 1.4 eq), the title compound benzyl 4-(4-oxo-3-(pyridine-4-yl)-4-(4-(trifluoromethyl)phenyl)butanoyl)piperidine-1-carboxylate **92B** (690 mg, 25% purity by LC-MS) was synthesized which was taken onto the next step without silica gel purification. (M+H)<sup>+</sup> 525.05

### **Benzyl 4-(4-(pyridine-4-yl)-5-(4-(trifluoromethyl)phenyl)-1H-pyrrol-2-yl)piperidine-1-carboxylate (93B)**

Following the procedure as described for the synthesis of **93A**, using crude benzyl 4-(4-oxo-3-(pyridine-4-yl)-4-(4-(trifluoromethyl)phenyl)butanoyl)piperidine-1-carboxylate **92B** (690 mg) and NH<sub>4</sub>OAc (2 g, excess), the title compound **93B** was synthesized. Purification by silica gel chromatography (10% → 25% → 50% EtOAc/Hexanes) afforded benzyl 4-(4-(pyridine-4-yl)-5-(4-(trifluoromethyl)phenyl)-1H-pyrrol-2-yl)piperidine-1-carboxylate **93B** (115 mg, 28% yield over two steps, 75% purity by LC-MS).

$^1\text{H}$  NMR (400 MHz,  $\text{DMSO-}d_6$ )  $\delta$  11.30 (d,  $J = 2.7$  Hz, 1H), 8.41 – 8.36 (m, 2H), 7.53 – 7.47 (m, 2H), 7.40 – 7.26 (m, 7H), 7.21 – 7.15 (m, 2H), 6.18 – 6.15 (m, 1H), 5.08 (s, 2H), 4.09 (d,  $J = 13.2$  Hz, 2H), 2.94 (s, 2H), 2.80 (tt,  $J = 11.7, 3.6$  Hz, 1H), 1.99 – 1.90 (m, 2H), 1.56 (qd,  $J = 12.6, 4.2$  Hz, 2H).  $(\text{M}+\text{H})^+$  506.0

**4-(5-(1-methylpiperidin-4-yl)-2-(4-(trifluoromethyl)phenyl)-1H-pyrrol-3-yl)pyridine (94B) [RUPB-33]**

Following the procedure as described for the synthesis of **94A** [TSP], using benzyl 4-(4-(pyridine-4-yl)-5-(4-(trifluoromethyl)phenyl)-1H-pyrrol-2-yl)piperidine-1-carboxylate **93B** (102 mg, 0.202 mmol, 1 eq) and LAH 2M solution in THF (0.4 mL, 0.8 mmol, 4 eq), the title compound **94B** was synthesized. The crude product was dissolved in 1N HCl and partitioned between EtOAc and water. The aqueous phase was separated, and the organic phase was extracted with water (2 x). The combined acidic aqueous phase was basified to pH 9 with 1N NaOH and EtOAc was added. The organic phase was separated, and the neutralised aqueous phase was extracted with EtOAc (3 x). The combined organic phase was dried over sodium sulphate and concentrated. Purification by silica gel chromatography (2%  $\rightarrow$  5%  $\rightarrow$  8%  $\rightarrow$  10% MeOH/ $\text{CHCl}_3$  with 0.25%  $\text{NH}_3$ ) afforded 4-(5-(1-methylpiperidin-4-yl)-2-(4-(trifluoromethyl)phenyl)-1H-pyrrol-3-yl)pyridine **94B** [RUPB-33] (30 mg, 38% yield, >99% purity by LC-MS) as a pale-yellow solid.

$^1\text{H}$  NMR (500 MHz,  $\text{DMSO-}d_6$ )  $\delta$  11.32 (d,  $J = 2.6$  Hz, 1H), 8.41 – 8.36 (m, 2H), 7.68 (d,  $J = 8.3$  Hz, 2H), 7.54 – 7.48 (m, 2H), 7.22 – 7.15 (m, 2H), 6.14 (d,  $J = 2.4$  Hz, 1H), 2.82 (dt,  $J = 12.0, 3.1$  Hz, 2H), 2.16 (s, 3H), 1.99 – 1.85 (m, 4H), 1.72 – 1.55 (m, 3H).

$^{13}\text{C}$  NMR (126 MHz, Methanol- $d_4$ )  $\delta$  148.38, 146.24, 138.85, 136.99, 128.20 (t,  $J = 32.4, 31.5$  Hz), 127.48, 125.41, 125.16 (q,  $J = 3.9$  Hz), 123.25, 122.80, 119.19, 105.53, 55.23, 45.00, 34.05, 31.50. HRMS calculated for  $\text{C}_{22}\text{H}_{22}\text{F}_3\text{N}_3$   $(\text{M}+\text{H})^+$  386.1844, found 386.1861.

### **1-(4-methoxyphenyl)-2-(pyridin-4-yl)ethan-1-one (91C)**

Following the procedure as described for the synthesis of **91A**, using 4-methylpyridine **89** (464 mg, 4.98 mmol, 1 eq), NaHMDS 1M solution in THF (7.4 mL, 7.4 mmol, 1.5 eq) and methyl 4-methoxybenzoate **90C** (1.08 g, 6.5 mmol, 1.3 eq), the title compound **91C** was synthesized. Purification by silica gel chromatography (10% → 25% → 50% EtOAc/Hexanes) afforded 1-(4-methoxyphenyl)-2-(pyridin-4-yl)ethan-1-one **91C** (229 mg, 20% yield, 98% purity by LC-MS).

<sup>1</sup>H NMR (400 MHz, DMSO-*d*<sub>6</sub>) δ 8.54 – 8.42 (m, 2H), 8.09 – 7.95 (m, 2H), 7.33 – 7.21 (m, 2H), 7.12 – 6.99 (m, 2H), 4.39 (s, 2H), 3.83 (s, 3H). (M+H)<sup>+</sup> 227.75

### **Benzyl 4-(4-(4-methoxyphenyl)-4-oxo-3-(pyridin-4-yl)butanoyl)piperidine-1-carboxylate (92C)**

Following the procedure as described for the synthesis of **92A**, using 1-(4-methoxyphenyl)-2-(pyridin-4-yl)ethan-1-one **91C** (215 mg, 0.947 mmol, 1 eq), LiHMDS 1M solution in THF (1.15 mL, 1.15 mmol, 1.2 eq) and benzyl 4-(2-bromoacetyl)piperidine-1-carboxylate **88** (415 mg, 1.231 mmol, 1.3 eq), the title compound benzyl 4-(4-(4-methoxyphenyl)-4-oxo-3-(pyridin-4-yl)butanoyl)piperidine-1-carboxylate **92C** (580 mg, 65% yield over two steps, 77% purity by LC-MS) was synthesized which was taken onto the next step without silica gel purification. (M+H)<sup>+</sup> 486.95

### **Benzyl 4-(5-(4-methoxyphenyl)-4-(pyridin-4-yl)-1H-pyrrol-2-yl)piperidine-1-carboxylate (93C)**

Following the procedure as described for the synthesis of **93A**, using crude benzyl 4-(5-(4-methoxyphenyl)-4-(pyridin-4-yl)-1H-pyrrol-2-yl)piperidine-1-carboxylate **92C** (580 mg) and NH<sub>4</sub>OAc (2 g, excess), the title compound **93C** was synthesized. Purification by silica gel chromatography (10% → 25% → 50% EtOAc/Hexanes) afforded benzyl 4-(5-(4-methoxyphenyl)-4-(pyridin-4-yl)-1H-pyrrol-2-yl)piperidine-1-carboxylate **93C** (288 mg, 89% purity by LC-MS).

$^1\text{H}$  NMR (400 MHz,  $\text{DMSO-}d_6$ )  $\delta$  11.00 (d,  $J = 2.7$  Hz, 1H), 8.30 (d,  $J = 4.9$  Hz, 2H), 7.40 – 7.27 (m, 5H), 7.27 – 7.21 (m, 2H), 7.17 – 7.11 (m, 2H), 6.97 – 6.89 (m, 2H), 6.12 (d,  $J = 2.6$  Hz, 1H), 5.07 (s, 2H), 4.14 – 4.01 (m, 2H), 3.75 (s, 3H), 3.03 – 2.69 (m, 3H), 1.91 (dd,  $J = 10.8$ , 8.2 Hz, 2H), 1.54 (qd,  $J = 12.5$ , 4.2 Hz, 2H).  $(\text{M}+\text{H})^+$  468.15

#### **4-(2-(4-methoxyphenyl)-5-(1-methylpiperidin-4-yl)-1H-pyrrol-3-yl)pyridine (94C)**

##### **[RUPB-34]**

Following the procedure as described for the synthesis of **94A** [TSP], using benzyl 4-(5-(4-methoxyphenyl)-4-(8-lyridine-4-yl)-1H-pyrrol-2-yl)piperidine-1-carboxylate **93C** (160 mg, 0.343 mmol, 1 eq) and LAH 2M solution in THF (0.68 mL, 1.37 mmol, 4 eq), the title compound **94C** was synthesized. The crude product was dissolved in 1N HCl and partitioned between EtOAc and water. The aqueous phase was separated, and the organic phase was extracted with water (2 x). The combined acidic aqueous phase was basified to pH 9 with 1N NaOH and EtOAc was added. The organic phase was separated, and the neutralised aqueous phase was extracted with EtOAc (3 x). The combined organic phase was dried over sodium sulphate and concentrated. Purification by silica gel chromatography (2%  $\rightarrow$  4%  $\rightarrow$  6%  $\rightarrow$  8%  $\rightarrow$  10% MeOH/ $\text{CHCl}_3$  with 0.25%  $\text{NH}_3$ ) afforded 4-(2-(4-methoxyphenyl)-5-(1-methylpiperidin-4-yl)-1H-pyrrol-3-yl)pyridine **94C** [RUPB-34] (62 mg, 53% yield, 97% purity by LC-MS) as a yellow solid.

$^1\text{H}$  NMR (500 MHz,  $\text{DMSO-}d_6$ )  $\delta$  10.99 (d,  $J = 2.7$  Hz, 1H), 8.34 – 8.27 (m, 2H), 7.27 – 7.21 (m, 2H), 7.17 – 7.11 (m, 2H), 6.97 – 6.90 (m, 2H), 6.10 (dd,  $J = 2.7$ , 0.8 Hz, 1H), 3.76 (s, 3H), 2.92 – 2.83 (m, 2H), 2.52 (s, 1H), 2.22 (s, 3H), 2.03 (s, 2H), 1.97 – 1.88 (m, 2H), 1.71 – 1.58 (m, 2H).

$^{13}\text{C}$  NMR (126 MHz, Methanol- $d_4$ )  $\delta$  159.26, 148.00, 146.65, 136.77, 129.99, 129.52, 125.75, 122.01, 116.65, 113.74, 104.06, 55.14, 54.32 (d,  $J = 1.4$  Hz), 44.74, 33.77, 31.30.

HRMS calculated for  $\text{C}_{22}\text{H}_{25}\text{N}_3\text{O}$   $(\text{M}+\text{H})^+$  348.2076, found 348.2087.

### **2-(2-bromopyridin-4-yl)-1-(thiophen-3-yl)ethan-1-one (97)**

Following the procedure as described for the synthesis of 1-(4-fluorophenyl)-2-(pyridin-4-yl)ethan-1-one **91A**, using 2-bromo-4-methylpyridine **95** (1.032 g, 6 mmol, 1 eq), NaHMDS 1M solution in THF (6 mL, 6 mmol, 1 eq) and ethyl thiophene-3-carboxylate **96** (936 mg, 6 mmol, 1 eq), the title compound **97** was synthesized. Purification by silica gel chromatography (10% → 25% → 50% EtOAc/Hexanes) afforded 2-(2-bromopyridin-4-yl)-1-(thiophen-3-yl)ethan-1-one **97** (300 mg, 18% yield, 85% purity by LC-MS).

<sup>1</sup>H NMR (400 MHz, DMSO-*d*<sub>6</sub>) δ 8.64 (dd, *J* = 2.8, 1.3 Hz, 1H), 8.31 (dd, *J* = 5.0, 0.7 Hz, 1H), 7.65 (dd, *J* = 5.1, 2.8 Hz, 1H), 7.58 (dt, *J* = 1.3, 0.6 Hz, 1H), 7.52 (dd, *J* = 5.1, 1.3 Hz, 1H), 7.37 – 7.31 (m, 1H), 4.41 (d, *J* = 0.6 Hz, 2H). (M+H)<sup>+</sup> 281.65; 283.60

### **Benzyl 4-(3-(2-bromopyridin-4-yl)-4-oxo-4-(thiophen-3-yl)butanoyl)piperidine-1-carboxylate (98)**

Following the procedure as described for the synthesis of **92A**, using 2-(2-bromopyridin-4-yl)-1-(thiophen-3-yl)ethan-1-one **97** (228 mg, 0.812 mmol, 1 eq), LiHMDS 1M solution in THF (0.98 mL, 0.98 mmol, 1.2 eq) and benzyl 4-(2-bromoacetyl)piperidine-1-carboxylate **88** (360 mg, 1.056 mmol, 1.3 eq), the title compound benzyl 4-(3-(2-bromopyridin-4-yl)-4-oxo-4-(thiophen-3-yl)butanoyl)piperidine-1-carboxylate **98** (596 mg, 78% purity by LC-MS) was synthesized and taken onto the next step without silica gel purification. (M+H)<sup>+</sup> 540.85; 542.85

### **Benzyl 4-(4-(2-bromopyridin-4-yl)-5-(thiophen-3-yl)-1H-pyrrol-2-yl)piperidine-1-carboxylate (99)**

Following the procedure as described for the synthesis of **93A**, using crude benzyl 4-(3-(2-bromopyridin-4-yl)-4-oxo-4-(thiophen-2-yl)butanoyl)piperidine-1-carboxylate **98** (596 mg) and NH<sub>4</sub>OAc (2 g, excess), the title compound **99** was synthesized. Purification by silica gel chromatography (10% → 25% → 50% EtOAc/Hexanes) afforded benzyl 4-(4-(2-bromopyridin-4-yl)-5-(thiophen-3-yl)-1H-pyrrol-2-yl)piperidine-1-carboxylate **99** (300 mg, 71% yield over two steps, 89% purity by LC-MS).

$^1\text{H}$  NMR (400 MHz,  $\text{DMSO-}d_6$ )  $\delta$  11.23 – 11.09 (m, 1H), 8.12 (dd,  $J = 5.3, 0.6$  Hz, 1H), 7.60 (dd,  $J = 5.0, 2.9$  Hz, 1H), 7.49 (dd,  $J = 2.9, 1.3$  Hz, 1H), 7.42 – 7.25 (m, 6H), 7.21 (dd,  $J = 5.3, 1.6$  Hz, 1H), 7.05 (dd,  $J = 5.0, 1.3$  Hz, 1H), 6.22 (dd,  $J = 2.6, 0.7$  Hz, 1H), 5.07 (s, 2H), 4.14 – 4.01 (m, 2H), 3.02 – 2.68 (m, 3H), 1.98 – 1.83 (m, 2H), 1.53 (qd,  $J = 12.6, 4.2$  Hz, 2H).  $(\text{M}+\text{H})^+$  521.80; 523.80

#### **4-(5-(1-methylpiperidin-4-yl)-2-(thiophen-3-yl)-1H-pyrrol-3-yl)pyridine (100) [RUPB-35]**

Following the procedure as described for the synthesis of **94A** [TSP], using benzyl 4-(4-(2-bromopyridin-4-yl)-5-(thiophen-2-yl)-1H-pyrrol-2-yl)piperidine-1-carboxylate **99** (200 mg, 0.384 mmol, 1 eq) and LAH 2M solution in THF (1 mL, 2.0 mmol, 5.2 eq), the title compound **100** was synthesized. The crude product was dissolved in 1N HCl and partitioned between EtOAc and water. The aqueous phase was separated, and the organic phase was extracted with water (2 x). The combined acidic aqueous phase was basified to pH 9 with 1N NaOH and EtOAc was added. The organic phase was separated, and the neutralised aqueous phase was extracted with EtOAc (3 x). The combined organic phase was dried over sodium sulphate and concentrated. Purification by silica gel chromatography (2%  $\rightarrow$  4%  $\rightarrow$  6%  $\rightarrow$  8% MeOH/ $\text{CHCl}_3$  with 0.25%  $\text{NH}_3$ ) afforded 4-(5-(1-methylpiperidin-4-yl)-2-(thiophen-3-yl)-1H-pyrrol-3-yl)pyridine **100** [RUPB-35] (82 mg, 66% yield, 98% purity by LC-MS) as a yellow solid.

$^1\text{H}$  NMR (500 MHz,  $\text{DMSO-}d_6$ )  $\delta$  11.05 (d,  $J = 2.6$  Hz, 1H), 8.38 – 8.30 (m, 2H), 7.55 (dd,  $J = 5.0, 2.9$  Hz, 1H), 7.44 (dd,  $J = 3.0, 1.3$  Hz, 1H), 7.24 – 7.16 (m, 2H), 7.02 (dd,  $J = 5.0, 1.3$  Hz, 1H), 6.10 (dd,  $J = 2.7, 0.8$  Hz, 1H), 2.87 (d,  $J = 11.8$  Hz, 2H), 2.54 – 2.50 (m, 1H), 2.22 (s, 3H), 2.03 (t,  $J = 11.5$  Hz, 2H), 1.96 – 1.87 (m, 2H), 1.65 (qd,  $J = 12.7, 3.7$  Hz, 2H).  $^{13}\text{C}$  NMR (126 MHz, Methanol- $d_4$ )  $\delta$  147.28, 145.63, 136.03, 132.93, 126.53, 124.68, 124.30, 121.35, 120.84, 116.80, 103.35, 54.24, 43.79, 32.82, 30.35. HRMS calculated for  $\text{C}_{19}\text{H}_{21}\text{N}_3\text{S}$   $(\text{M}+\text{H})^+$  324.1534, found 324.1558.

#### **1-(4-fluorophenyl)-2-(3-fluoropyridin-4-yl)ethan-1-one (102A)**

3-fluoro-4-methylpyridine **101A** (220 mg, 1.98 mmol, 1 eq) was dissolved in 8 mL anhydrous THF and cooled to 0°C under nitrogen. NaHMDS 1M solution in THF (3 mL, 3.0 mmol, 1.5



eq) was added portion-wise over 2 minutes, and the reaction was stirred for 1 hour. Ethyl 4-fluorobenzoate **90A** (255 mg, 2.38 mmol, 1.2 eq) was dissolved in 4 mL THF and added to the preformed enolate by means of a syringe. The reaction was allowed to stir overnight in an ice bath and was deemed complete by LC-MS analysis. The reaction was quenched by the addition of 1 mL water and was concentrated under reduced pressure. The concentrate was partitioned between EtOAc and water and the organic phase was separated. The aqueous phase was extracted with EtOAc (3 x). The combined organic phase was washed with brine (1 x), dried over sodium sulphate and concentrated. Purification by silica gel chromatography (10% → 25% → 50% EtOAc/Hexanes) afforded 1-(4-fluorophenyl)-2-(3-fluoropyridin-4-yl)ethan-1-one **102A** (145 mg, 31% yield, 95% purity by LC-MS) as a pale yellow crystalline solid.

<sup>1</sup>H NMR (500 MHz, DMSO-*d*<sub>6</sub>) δ 8.52 (d, *J* = 1.5 Hz, 1H), 8.38 (dd, *J* = 4.8, 1.3 Hz, 1H), 8.18 – 8.11 (m, 2H), 7.44 – 7.36 (m, 3H), 4.60 (s, 2H). (M+H)<sup>+</sup> 234.0

**Benzyl 4-(4-(4-fluorophenyl)-3-(3-fluoropyridin-4-yl)-4-oxobutanoyl)piperidine-1-carboxylate (103A)**

1-(4-fluorophenyl)-2-(3-fluoropyridin-4-yl)ethan-1-one **102A** (145 mg, 0.622 mmol, 1 eq) was dissolved in 8 mL anhydrous THF and cooled to 0°C under nitrogen. NaHMDS 1M solution in THF (0.7 mL, 0.7 mmol, 1.1 eq) was added to the THF solution of **102A** in a drop wise manner by means of a syringe and the reaction was stirred at 0°C for 45 minutes. Benzyl 4-(2-bromoacetyl)piperidine-1-carboxylate **88** (235 mg, 0.684 mmol, 1.1 eq) was dissolved in 2 mL THF and added to the anion generated by means of a syringe. The reaction was further stirred for 45 minutes and was deemed complete by LC-MS evaluation. The reaction was quenched by the addition of 2 mL water and was concentrated under reduced pressure. The concentrate was partitioned between EtOAc and water, and the organic phase was separated. The aqueous phase was extracted with EtOAc (3 x). The combined organic phase was dried over sodium sulphate and concentrated to give benzyl 4-(4-(4-fluorophenyl)-3-(3-fluoropyridin-4-yl)-4-oxobutanoyl)piperidine-1-carboxylate **103A** (450 mg, 31% purity by LC-MS) as a deep maroon oil which was taken onto the next step without silica gel purification. (M+H)<sup>+</sup> 493.10

**Benzyl 4-(5-(4-fluorophenyl)-4-(3-fluoropyridin-4-yl)-1H-pyrrol-2-yl)piperidine-1-carboxylate (104A)**

Crude benzyl 4-(4-(4-fluorophenyl)-3-(3-fluoropyridin-4-yl)-4-oxobutanoyl)piperidine-1-carboxylate **103A** (450 mg) was dissolved in 20 mL EtOH. Ammonium acetate (2 g, excess) was added and the reaction was heated to reflux and stirred overnight. The reaction was determined as complete by LC-MS evaluation and concentrated under reduced pressure. The concentrate was partitioned between EtOAc and water and the organic phase was separated. The aqueous phase was extracted with EtOAc (2 x) and the combined organic phase was washed with brine (1 x), dried over sodium sulphate and concentrated. Purification by silica gel chromatography (10% → 25% → 50% EtOAc/Hexanes) gave the title compound benzyl 4-(5-(4-fluorophenyl)-4-(3-fluoropyridin-4-yl)-1H-pyrrol-2-yl)piperidine-1-carboxylate **104A** (88 mg, 31% yield over two steps, 89% purity by LC-MS) as a deep yellow solid.

<sup>1</sup>H NMR (500 MHz, DMSO-*d*<sub>6</sub>) δ 11.25 (d, *J* = 2.7 Hz, 1H), 8.45 – 8.37 (m, 1H), 8.24 (d, *J* = 5.0 Hz, 1H), 7.53 – 7.10 (m, 10H), 6.07 (t, *J* = 2.0 Hz, 1H), 5.13 – 5.02 (m, 2H), 4.09 (d, *J* = 13.5 Hz, 2H), 3.04 – 2.74 (m, 3H), 1.98 – 1.90 (m, 2H), 1.55 (qd, *J* = 12.5, 4.2 Hz, 2H).

(M+H)<sup>+</sup> 474.10

**3-fluoro-4-(2-(4-fluorophenyl)-5-(1-methylpiperidin-4-yl)-1H-pyrrol-3-yl)pyridine (105A) [RUPB-36]**

Benzyl 4-(5-(4-fluorophenyl)-4-(3-fluoropyridin-4-yl)-1H-pyrrol-2-yl)piperidine-1-carboxylate **104A** (80 mg, 0.169 mmol, 1 eq) was dissolved in 6 mL THF, and LAH 2M solution in THF (0.34 mL, 0.68 mmol, 4 eqs) was then added to the reaction in a drop-wise manner over 2 minutes. The reaction was stirred at room temperature for 2 hours and was determined complete by LC-MS evaluation. The Feiser & Feiser quench (0.02 mL water, 0.02 mL 15% NaOH and 0.06 mL water in a sequential manner) was employed, the reaction was filtered over celite and the filtrate was concentrated. Purification by silica gel chromatography (2% → 5% → 8% → 12% MeOH/CHCl<sub>3</sub> with NH<sub>3</sub>) afforded the title compound 3-fluoro-4-

(2-(4-fluorophenyl)-5-(1-methylpiperidin-4-yl)-1H-pyrrol-3-yl)pyridine **105A** [RUPB-36] (35 mg, 58% yield, 98% purity by LC-MS) as a yellow solid.

<sup>1</sup>H NMR (500 MHz, DMSO-*d*<sub>6</sub>) δ 11.31 – 11.24 (m, 1H), 8.41 (d, *J* = 2.4 Hz, 1H), 8.24 (dd, *J* = 5.0, 1.1 Hz, 1H), 7.33 – 7.23 (m, 2H), 7.23 – 7.12 (m, 3H), 6.07 (t, *J* = 2.2 Hz, 1H), 3.00 (s, 2H), 2.42 – 2.20 (m, 5H), 2.04 – 1.95 (m, 2H), 1.78 – 1.63 (m, 2H).

<sup>13</sup>C NMR (126 MHz, Methanol-*d*<sub>4</sub>) δ 162.07 (d, *J* = 245.5 Hz), 157.21 (d, *J* = 255.1 Hz), 144.34 (d, *J* = 5.2 Hz), 137.38 (d, *J* = 27.0 Hz), 136.35, 133.90 (d, *J* = 12.1 Hz), 129.87, 129.47 (d, *J* = 3.5 Hz), 129.17 (d, *J* = 8.4 Hz), 125.22, 115.04 (d, *J* = 21.9 Hz), 111.35, 106.14 (d, *J* = 4.1 Hz), 54.61, 43.78, 32.92, 30.44. HRMS calculated for C<sub>21</sub>H<sub>21</sub>F<sub>2</sub>N<sub>3</sub> (M+H)<sup>+</sup> 354.1781, found 354.1797.

#### 1-(4-fluorophenyl)-2-(pyrimidin-4-yl)ethan-1-one (**102B**)

Following the procedure as described for the synthesis of **102A**, using 4-methylpyrimidine **101B** (534 mg, 5.67 mmol, 1 eq), NaHMDS 1M solution in THF (8.5 mL, 8.50 mmol, 1.5 eq) and ethyl 4-fluorobenzoate **90A** (730 mg, 6.80 mmol, 1.2 eq), the title compound **102B** was synthesized. Purification by silica gel chromatography (10% → 25% → 50% EtOAc/Hexanes) afforded 1-(4-fluorophenyl)-2-(pyrimidin-4-yl)ethan-1-one **102B** (580 mg, 48% yield, 85% purity by LC-MS) as a pale yellow crystalline solid.

<sup>1</sup>H NMR (500 MHz, DMSO-*d*<sub>6</sub>) δ 9.08 (d, *J* = 1.4 Hz, 1H), 8.74 (d, *J* = 5.1 Hz, 1H), 8.16 – 8.07 (m, 2H), 7.42 – 7.33 (m, 2H), 7.10 (d, *J* = 5.7 Hz, 1H), 4.59 (s, 2H). (M+H)<sup>+</sup> 217.0

#### Benzyl 4-(4-(4-fluorophenyl)-4-oxo-3-(pyrimidin-4-yl)butanoyl)piperidine-1-carboxylate (**103B**)

Following the procedure as described for the synthesis of **103A**, using 1-(4-fluorophenyl)-2-(pyrimidin-4-yl)ethan-1-one **102B** (570 mg, 2.64 mmol, 1 eq), NaHMDS 1M solution in THF (3.16 mL, 3.16 mmol, 1.2 eq) and benzyl 4-(2-bromoacetyl)piperidine-1-carboxylate **88** (1.07 g, 3.16 mmol, 1.2 eq), the title compound benzyl 4-(4-(4-fluorophenyl)-4-oxo-3-(pyrimidin-4-yl)butanoyl)piperidine-1-carboxylate **103B** (1.02 g, 37% purity by LC-MS) was synthesized and was taken onto the next step without silica gel purification. (M+H)<sup>+</sup> 476.2

**Benzyl 4-(5-(4-fluorophenyl)-4-(pyrimidin-4-yl)-1H-pyrrol-2-yl)piperidine-1-carboxylate (104B)**

Following the procedure for the synthesis of **104A**, using crude benzyl 4-(4-(4-fluorophenyl)-4-oxo-3-(pyrimidin-4-yl)butanoyl)piperidine-1-carboxylate **103B** (1.02 g) and  $\text{NH}_4\text{OAc}$  (5 g, excess), the title compound **104B** was synthesized. Purification by silica gel chromatography (10%  $\rightarrow$  25%  $\rightarrow$  50% EtOAc/Hexanes) afforded benzyl 4-(5-(4-fluorophenyl)-4-(pyrimidin-4-yl)-1H-pyrrol-2-yl)piperidine-1-carboxylate **104B** (660 mg, 55% yield over two steps, >99% purity by LC-MS) as a deep yellow compound.

$^1\text{H}$  NMR (500 MHz,  $\text{DMSO}-d_6$ )  $\delta$  11.27 (d,  $J = 2.9$  Hz, 1H), 8.89 (d,  $J = 1.4$  Hz, 1H), 8.43 (d,  $J = 5.5$  Hz, 1H), 7.49 – 7.43 (m, 2H), 7.40 – 7.16 (m, 8H), 6.41 (dd,  $J = 2.7, 0.7$  Hz, 1H), 5.08 (s, 2H), 4.13 – 4.05 (m, 2H), 2.90 (s, 2H), 2.77 (tt,  $J = 11.7, 3.6$  Hz, 1H), 1.99 – 1.91 (m, 2H), 1.55 (qd,  $J = 12.4, 4.2$  Hz, 2H).  $(\text{M}+\text{H})^+$  457.1

**4-(2-(4-fluorophenyl)-5-(1-methylpiperidin-4-yl)-1H-pyrrol-3-yl)pyrimidine (105B)**

**[RUPB-38]**

Following the procedure as described for the synthesis of **105A** [RUPB-36], using benzyl 4-(5-(4-fluorophenyl)-4-(pyrimidin-4-yl)-1H-pyrrol-2-yl)piperidine-1-carboxylate **104B** (190 mg, 0.416 mmol, 1 eq) and LAH 2M solution in THF (0.83 mL, 1.66 mmol, 4 eq), the title compound **105B** was synthesized. The crude product was dissolved in 1N HCl and partitioned between EtOAc and water. The aqueous phase was separated, and the organic phase was extracted with water (2 x). The combined acidic aqueous phase was basified to pH 9 with 1N NaOH and EtOAc was added. The organic phase was separated, and the neutralised aqueous phase was extracted with EtOAc (3 x). The combined organic phase was dried over sodium sulphate and concentrated. Purification by silica gel chromatography (2%  $\rightarrow$  5%  $\rightarrow$  8%  $\rightarrow$  12% MeOH/ $\text{CHCl}_3$  with 0.25%  $\text{NH}_3$ ) afforded 4-(2-(4-fluorophenyl)-5-(1-methylpiperidin-4-yl)-1H-pyrrol-3-yl)pyrimidine **105B** [RUPB-38] (50 mg, 36% yield, >99% purity by LC-MS) as a yellow solid.

$^1\text{H}$  NMR (500 MHz,  $\text{DMSO}-d_6$ )  $\delta$  11.29 (d,  $J = 2.7$  Hz, 1H), 8.89 (d,  $J = 1.4$  Hz, 1H), 8.43 (d,  $J = 5.5$  Hz, 1H), 7.50 – 7.41 (m, 2H), 7.28 – 7.19 (m, 2H), 7.17 (dd,  $J = 5.5, 1.4$  Hz, 1H), 6.41 (d,  $J = 2.7$  Hz, 1H), 3.04 (s, 2H), 2.39 (s, 5H), 2.06 – 1.95 (m, 2H), 1.80 – 1.64 (m, 2H).

$^{13}\text{C}$  NMR (126 MHz, Methanol- $d_4$ )  $\delta$  162.81, 162.58 (d,  $J = 246.3$  Hz), 157.68, 155.13, 136.55, 132.43, 130.69 (d,  $J = 8.2$  Hz), 129.26 (d,  $J = 3.4$  Hz), 117.86, 117.76, 115.13 (d,  $J = 21.9$  Hz), 105.11, 54.52, 43.79, 32.80, 30.32. HRMS calculated for  $\text{C}_{20}\text{H}_{21}\text{FN}_4$  ( $\text{M}+\text{H}$ ) $^+$  337.1823, found 337.1845.

#### **tert-Butyl 4-(2-bromoacetyl)piperidine-1-carboxylate (106)**

tert-Butyl 4-acetylpiperidine-1-carboxylate **85** (8.16 g, 35.89 mmol, 1 eq) was dissolved in 40 mL MeOH. Bromine (5.73 g, density = 3.1 g/mL, 35.89 mmol, 1 eq) was separately dissolved in 5 mL MeOH. The methanolic solution of bromine was added to the methanolic solution of **85** in a portion wise manner over a period of 5 minutes and the reaction was allowed to stir at room temperature. After 30 minutes, the reaction was determined complete by TLC and the reaction was concentrated under reduced pressure. The residue was partitioned between EtOAc and water. The organic phase was separated, and the aqueous phase was extracted with EtOAc (2 x). The combined organic phase was dried over sodium sulphate and concentrated. Purification by silica gel chromatography (0%  $\rightarrow$  10%  $\rightarrow$  25% EtOAc/Hexanes) afforded tert-butyl 4-(2-bromoacetyl)piperidine-1-carboxylate **106** (5.32 g, 48% yield) as a clear yellow oil which crystallizes on standing.

#### **2-(3-chloropyridin-4-yl)-1-(4-fluorophenyl)ethan-1-one (108)**

Following the procedure as described for the synthesis of **102A**, using 3-chloro-4-methylpyridine **107** (475 mg, 3.72 mmol, 1 eq), NaHMDS 1M solution in THF (5.6 mL, 5.6 mmol, 1.5 eq) and ethyl 4-fluorobenzoate **90A** (600 mg, 5.58 mmol, 1.5 eq), the title compound **108** was synthesized. Purification by silica gel chromatography (10%  $\rightarrow$  25%  $\rightarrow$  50% EtOAc/Hexanes) afforded 2-(3-chloropyridin-4-yl)-1-(4-fluorophenyl)ethan-1-one **108** (350 mg, 38% yield, 89% purity by LC-MS) as a pale yellow crystalline solid.

$^1\text{H}$  NMR (500 MHz,  $\text{DMSO}-d_6$ )  $\delta$  8.61 (s, 1H), 8.48 (d,  $J = 4.8$  Hz, 1H), 8.19 – 8.12 (m, 2H), 7.46 – 7.36 (m, 3H), 4.64 (s, 2H).  $(\text{M}+\text{H})^+$  249.9

**tert-Butyl 4-(3-(3-chloropyridin-4-yl)-4-(4-fluorophenyl)-4-oxobutanoyl)piperidine-1-carboxylate (109)**

Following the procedure as described for the synthesis of **103A**, using 2-(3-chloropyridin-4-yl)-1-(4-fluorophenyl)ethan-1-one **108** (330 mg, 1.32 mmol, 1 eq), NaHMDS 1M solution in THF (1.6 mL, 1.6 mmol, 1.2 eq) and tert-butyl 4-(2-bromoacetyl)piperidine-1-carboxylate **106** (485 mg, 1.6 mmol, 1.2 eq), the title compound tert-butyl 4-(3-(3-chloropyridin-4-yl)-4-(4-fluorophenyl)-4-oxobutanoyl)piperidine-1-carboxylate **109** (534 mg, 32% purity by LC-MS) was synthesized and taken onto the next step without silica gel purification.  $(\text{M}+\text{H})^+$  475.0

**tert-Butyl 4-(4-(3-chloropyridin-4-yl)-5-(4-fluorophenyl)-1H-pyrrol-2-yl)piperidine-1-carboxylate (110)**

Following the procedure as described for the synthesis of compound **104A**, using crude tert-butyl 4-(3-(3-chloropyridin-4-yl)-4-(4-fluorophenyl)-4-oxobutanoyl)piperidine-1-carboxylate **109** (534 mg) and ammonium acetate (3 g, excess), the title compound **110** was synthesized. Purification by silica gel chromatography (10%  $\rightarrow$  25%  $\rightarrow$  50% EtOAc/Hexanes) and a second column (2%  $\rightarrow$  5%  $\rightarrow$  10% IPA/Hexanes) afforded tert-butyl 4-(4-(3-chloropyridin-4-yl)-5-(4-fluorophenyl)-1H-pyrrol-2-yl)piperidine-1-carboxylate **110** (194 mg, 32% yield over two steps, 51 % purity by LC-MS) as a deep yellow solid.

$^1\text{H}$  NMR (500 MHz,  $\text{DMSO}-d_6$ )  $\delta$  11.20 (d,  $J = 2.6$  Hz, 1H), 8.55 (s, 1H), 8.33 (d,  $J = 5.0$  Hz, 1H), 7.22 – 7.07 (m, 5H), 6.04 – 6.00 (m, 1H), 4.04 (dd,  $J = 19.3, 9.6$  Hz, 2H), 2.91 – 2.70 (m, 3H), 1.97 – 1.87 (m, 2H), 1.51 (qd,  $J = 12.6, 4.2$  Hz, 2H), 1.40 (s, 9H).  $(\text{M}+\text{H})^+$  456.0

**3-chloro-4-(2-(4-fluorophenyl)-5-(piperidin-4-yl)-1H-pyrrol-3-yl)pyridine (111)**

tert-Butyl 4-(4-(3-chloropyridin-4-yl)-5-(4-fluorophenyl)-1H-pyrrol-2-yl)piperidine-1-carboxylate **110** (194 mg, 0.43 mmol, 1 eq) was dissolved in 7 mL MeOH and 4N HCl in 1,4 dioxane (3 mL) was added to it. The reaction was stirred for 1 hour at room temperature and was determined complete by LC-MS analysis. The reaction was concentrated under reduced

pressure and the residue was partitioned between water and EtOAc. The aqueous phase was separated, and the organic phase was extracted with water (2 x). The combined aqueous phase was basified to pH 8 with saturated NaHCO<sub>3</sub> and the aqueous phase was extracted with EtOAc (3 x). The combined organic phase was washed with brine, dried over sodium sulphate, concentrated to give the title compound 3-chloro-4-(2-(4-fluorophenyl)-5-(piperidin-4-yl)-1H-pyrrol-3-yl)pyridine **111** (100 mg, 98% purity by LC-MS) which was taken onto the next step without silica gel purification. (M+H)<sup>+</sup> 356.1

**3-chloro-4-(2-(4-fluorophenyl)-5-(1-methylpiperidin-4-yl)-1H-pyrrol-3-yl)pyridine (112)**  
**[RUPB-37]**

3-chloro-4-(2-(4-fluorophenyl)-5-(piperidin-4-yl)-1H-pyrrol-3-yl)pyridine **111** (100 mg, 0.281 mmol, 1 eq) was dissolved in 6 mL MeOH and 1 mL AcOH. Formaldehyde 37% solution in water (1 mL, excess) was added and the reaction was stirred for 1 hour at room temperature. NaBH<sub>4</sub> (55 mg, 1.41 mmol, 5 eq) was added to the imine generated and the reaction was allowed to stir for 1 hour at room temperature. The reaction was deemed complete, quenched by the addition of 2 mL water and concentrated under reduced pressure. The residue was partitioned between 1N HCl and EtOAc. The aqueous phase was separated, and the organic phase was extracted with water (3 x). The combined aqueous phase was basified to pH 9 with 1N NaOH and extracted with EtOAc (3 x). The combined organic phase was washed with brine (1 x), dried over sodium sulphate and concentrated. Purification by silica gel chromatography (2% → 5% → 8% → 12% MeOH/CHCl<sub>3</sub> with 0.25% NH<sub>3</sub>) afforded the title compound 3-chloro-4-(2-(4-fluorophenyl)-5-(1-methylpiperidin-4-yl)-1H-pyrrol-3-yl)pyridine **112 [RUPB-37]** (83 mg, 80% yield, 98% purity by LC-MS) as a yellow solid.

<sup>1</sup>H NMR (500 MHz, DMSO-*d*<sub>6</sub>) δ 11.18 (d, *J* = 2.7 Hz, 1H), 8.55 (s, 1H), 8.33 (d, *J* = 5.0 Hz, 1H), 7.22 – 7.07 (m, 5H), 6.00 (dd, *J* = 2.7, 0.7 Hz, 1H), 2.86 (dt, *J* = 11.6, 3.0 Hz, 2H), 2.54 (ddt, *J* = 11.8, 8.0, 4.2 Hz, 1H), 2.20 (s, 3H), 2.05 – 1.90 (m, 4H), 1.71 – 1.58 (m, 2H).

<sup>13</sup>C NMR (126 MHz, Methanol-*d*<sub>4</sub>) δ 161.76 (d, *J* = 245.1 Hz), 148.97, 146.30, 145.49, 136.86, 131.13, 129.49 (d, *J* = 3.3 Hz), 128.89, 128.59 (d, *J* = 8.0 Hz), 126.76, 115.32, 114.96 (d, *J*

= 21.8 Hz), 106.21 , 55.10 , 44.67 , 33.75 , 31.26 . HRMS calculated for  $C_{21}H_{21}ClFN_3$  ( $M+H$ )<sup>+</sup> 370.1486, found 370.1504; 372.1474.

**Benzyl 4-(5-(4-fluorophenyl)-1-methyl-4-(pyridin-4-yl)-1H-pyrrol-2-yl)piperidine-1-carboxylate (113)**

Crude benzyl 4-(4-(4-fluorophenyl)-4-oxo-3-(pyridin-4-yl)butanoyl)piperidine-1-carboxylate **92A** (200 mg) was dissolved in 10 mL AcOH and 5 mL EtOH. Methylamine 2M solution in THF (12 mL) was added and the reaction was heated to reflux. After 3 hours, the reaction was determined complete by LC-MS analysis and was concentrated under reduced pressure. The concentrate was partitioned between EtOAc and water. The organic phase was separated, and the aqueous phase was extracted with EtOAc (3 x). The combined organic phase was dried over sodium sulphate and concentrated. Purification by silica gel chromatography (10% → 25% → 50% EtOAc/Hexanes) afforded benzyl 4-(5-(4-fluorophenyl)-1-methyl-4-(pyridin-4-yl)-1H-pyrrol-2-yl)piperidine-1-carboxylate **113** (160 mg, 41% yield, 64% purity by LC-MS) as a dark yellow solid that was taken onto the next step without further purification. ( $M+H$ )<sup>+</sup> 470.0

**4-(2-(4-fluorophenyl)-1-methyl-5-(1-methylpiperidin-4-yl)-1H-pyrrol-3-yl)pyridine (114) [RUPB-14]**

Following the procedure as described for the synthesis of **94A** [TSP], using benzyl 4-(5-(4-fluorophenyl)-1-methyl-4-(pyridin-4-yl)-1H-pyrrol-2-yl)piperidine-1-carboxylate **113** (160 mg, 0.341 mmol, 1 eq) and LAH 2M solution in THF (0.68 mL, 1.36 mmol, 4 eq), the title compound **114** was synthesized. The product was purified using silica gel chromatography (0% → 1% → 2% MeOH/EtOAc with 0.25%  $NH_3$ ). Traces of compound **94A** [TSP] were still present in the crude product. Purification by reverse phase chromatography gave the bis HCl salt of **114**. The salt was dissolved in 1N NaOH and partitioned between EtOAc and water. The organic phase was separated, and the aqueous phase was extracted with EtOAc (3 x). The organic phase was combined, dried over sodium sulphate and concentrated to give 4-(2-(4-fluorophenyl)-1-methyl-5-(1-methylpiperidin-4-yl)-1H-pyrrol-3-yl)pyridine **114** [RUPB-14] (20 mg, 27% yield, 100% purity by LC-MS) as a pale-yellow solid.



$^1\text{H}$  NMR (400 MHz,  $\text{DMSO-}d_6$ )  $\delta$  8.23 (d,  $J = 5.4$  Hz, 2H), 7.37 – 7.25 (m, 4H), 6.97 – 6.92 (m, 2H), 6.28 (d,  $J = 0.6$  Hz, 1H), 2.85 (dt,  $J = 11.9, 3.0$  Hz, 2H), 2.55 (ddt,  $J = 11.7, 8.6, 3.6$  Hz, 1H), 2.19 (s, 3H), 2.05 – 1.93 (m, 2H), 1.86 (ddd,  $J = 13.2, 3.5, 1.6$  Hz, 2H), 1.62 (qd,  $J = 12.5, 3.7$  Hz, 2H).

$^{13}\text{C}$  NMR (126 MHz, Methanol- $d_4$ )  $\delta$  162.85 (d,  $J = 247.2$  Hz), 147.99, 145.65, 138.40, 132.86 (d,  $J = 8.3$  Hz), 131.11, 129.04 (d,  $J = 3.5$  Hz), 121.42, 118.05, 115.57 (d,  $J = 21.7$  Hz), 103.03, 55.34, 44.94, 32.85, 31.61, 30.12. HRMS calculated for  $\text{C}_{22}\text{H}_{24}\text{FN}_3$  ( $\text{M}+\text{H}$ ) $^+$  350.2032, found 350.2049.

Since the pyrrole N-Me protons are obscured by the water signal, **[RUPB-14]** bis HCl salt was prepared to view all the proton signals.

$^1\text{H}$  NMR (400 MHz,  $\text{DMSO-}d_6$ )  $\delta$  11.02 (s, 1H), 8.53 – 8.45 (m, 2H), 7.54 – 7.35 (m, 6H), 6.67 (s, 1H), 3.47 (d,  $J = 12.6$  Hz, 2H), 3.35 (s, 3H), 3.07 (dt,  $J = 13.4, 10.3$  Hz, 2H), 2.96 (td,  $J = 11.7, 5.8$  Hz, 1H), 2.72 (d,  $J = 4.5$  Hz, 3H), 2.16 – 1.93 (m, 4H).

**4-(4-bromo-2-(4-fluorophenyl)-5-(1-methylpiperidin-4-yl)-1H-pyrrol-3-yl)pyridine (115) [RUPB-15]**

4-(2-(4-fluorophenyl)-5-(1-methylpiperidin-4-yl)-1H-pyrrol-3-yl)pyridine **94A** [TSP] (1.5 g, 4.47 mmol, 1 eq) was dissolved in 20 mL anhydrous DMF and cooled to 0°C. NBS (637 mg, 3.58 mmol, 0.8 eq) was added portion wise to the solution of **94A** over 5 minutes and the reaction was stirred maintaining the temperature at 0°C. The reaction reached completion in 1 hour as determined by LC-MS analysis. The product immediately precipitated out after the addition of ice-cold water. The reaction mixture was filtered, and the residue was collected. Purification by recrystallization using MeOH afforded 4-(4-bromo-2-(4-fluorophenyl)-5-(1-methylpiperidin-4-yl)-1H-pyrrol-3-yl)pyridine **115** [RUPB-15] (1.45g, 78% yield, 99% purity by LC-MS) as an off-white solid.

$^1\text{H}$  NMR (400 MHz,  $\text{DMSO-}d_6$ )  $\delta$  11.41 (s, 1H), 8.50 – 8.42 (m, 2H), 7.22 – 7.10 (m, 6H), 2.87 (d,  $J = 6.3$  Hz, 2H), 2.69 (dd,  $J = 8.2, 4.1$  Hz, 1H), 2.19 (s, 3H), 2.03 – 1.86 (m, 4H), 1.67 (p,  $J = 5.2, 4.0$  Hz, 2H).

$^{13}\text{C}$  NMR (126 MHz, DMSO- $d_6$ )  $\delta$  161.66 (d,  $J$  = 244.5 Hz), 149.87, 142.92, 135.04, 130.38 (d,  $J$  = 8.2 Hz), 128.59 (d,  $J$  = 3.0 Hz), 128.15, 125.41, 117.84 (d,  $J$  = 2.9 Hz), 115.74 (d,  $J$  = 21.6 Hz), 94.97 (d,  $J$  = 2.1 Hz), 56.17, 46.63, 34.36 (d,  $J$  = 3.0 Hz), 30.99. HRMS calculated for  $\text{C}_{21}\text{H}_{21}\text{BrFN}_3$  ( $\text{M}+\text{H}$ ) $^+$  414.0981, found 414.0999; 416.0977.

**4-(2-(4-fluorophenyl)-5-(1-methylpiperidin-4-yl)-4-vinyl-1H-pyrrol-3-yl)pyridine (116)**  
**[RUPB-17]**

4-(4-bromo-2-(4-fluorophenyl)-5-(1-methylpiperidin-4-yl)-1H-pyrrol-3-yl)pyridine **115** **[RUPB-15]** (224 mg, 0.542 mmol, 1 eq), potassium vinyltrifluoroborate (145 mg, 1.084 mmol, 2 eq) and  $\text{Pd}(\text{dppf})\text{Cl}_2$  (44 mg, 0.054 mmol, 0.1 eq) were dissolved in 4 mL 1,2 DME in a 5 mL microwave vial. Saturated  $\text{Na}_2\text{CO}_3$  (1 mL) was added and the vial was sealed shut. It was then heated in the microwave at 120°C. After 30 minutes, the reaction was determined complete by LC-MS analysis. The reaction mixture was filtered over celite and the filtrate was concentrated. Purification by silica gel chromatography (2%  $\rightarrow$  5%  $\rightarrow$  10% EtOAc/MeOH with 0.25%  $\text{NH}_3$ ) was carried out. A second purification by silica gel chromatography (4%  $\rightarrow$  8% MeOH/ $\text{CHCl}_3$  with 0.25%  $\text{NH}_3$ ) afforded 4-(2-(4-fluorophenyl)-5-(1-methylpiperidin-4-yl)-4-vinyl-1H-pyrrol-3-yl)pyridine **116** **[RUPB-17]** (90 mg, 46% yield, 98% purity by LC-MS) as a yellowish-white solid.

$^1\text{H}$  NMR (400 MHz, DMSO- $d_6$ )  $\delta$  11.03 (s, 1H), 8.48 – 8.40 (m, 2H), 7.19 – 7.12 (m, 2H), 7.12 – 7.05 (m, 4H), 6.46 (dd,  $J$  = 17.8, 11.5 Hz, 1H), 4.94 (dd,  $J$  = 11.5, 2.0 Hz, 1H), 4.80 (dd,  $J$  = 17.8, 2.1 Hz, 1H), 2.91 – 2.82 (m, 2H), 2.76 (dt,  $J$  = 11.7, 6.1 Hz, 1H), 2.19 (s, 3H), 2.05 – 1.87 (m, 4H), 1.65 (d,  $J$  = 9.8 Hz, 2H).

$^{13}\text{C}$  NMR (126 MHz, Methanol- $d_4$ )  $\delta$  161.84 (d,  $J$  = 245.3 Hz), 148.12, 146.49, 134.55, 129.80 (d,  $J$  = 8.1 Hz), 129.32 (d,  $J$  = 1.7 Hz), 128.83 (d,  $J$  = 3.3 Hz), 128.27, 125.88, 117.18, 117.08, 114.80 (d,  $J$  = 21.8 Hz), 112.89, 55.60, 44.98, 32.87, 31.20. HRMS calculated for  $\text{C}_{23}\text{H}_{24}\text{FN}_3$  ( $\text{M}+\text{H}$ ) $^+$  362.2032, found 362.2050.

**4-(4-ethyl-2-(4-fluorophenyl)-5-(1-methylpiperidin-4-yl)-1H-pyrrol-3-yl)pyridine (117)****[RUPB-24]****4-(2-(4-fluorophenyl)-5-(1-methylpiperidin-4-yl)-4-vinyl-1H-pyrrol-3-yl)pyridine 116**

**[RUPB-17]** (44 mg, 0.122 mmol, 1 eq) was dissolved in 6 mL MeOH. Palladium on carbon (30 mg, excess) was added to the methanolic solution of **116**. The reaction mixture was set up for hydrogenation using a hydrogen balloon setup. The reaction was stirred for 3 hours at room temperature and was determined complete by LC-MS analysis. The reaction mixture was filtered over celite and the filtrate was concentrated. Purification by silica gel chromatography (8% MeOH/ CHCl<sub>3</sub> with 0.25% NH<sub>3</sub>) afforded 4-(4-ethyl-2-(4-fluorophenyl)-5-(1-methylpiperidin-4-yl)-1H-pyrrol-3-yl)pyridine **117** **[RUPB-24]** (15 mg, 34% yield, 96% purity by LC-MS) as an off-white solid.

<sup>1</sup>H NMR (400 MHz, DMSO-*d*<sub>6</sub>)  $\delta$  10.72 (s, 1H), 8.48 – 8.39 (m, 2H), 7.20 – 7.00 (m, 6H), 2.89 (d, *J* = 10.0 Hz, 2H), 2.66 – 2.52 (m, 1H), 2.35 (q, *J* = 7.5 Hz, 2H), 2.22 (s, 3H), 2.09 – 1.88 (m, 4H), 1.62 (d, *J* = 11.1 Hz, 2H), 0.86 (t, *J* = 7.4 Hz, 3H).

<sup>13</sup>C NMR (126 MHz, Methanol-*d*<sub>4</sub>)  $\delta$  161.57 (d, *J* = 244.8 Hz), 148.21, 147.21, 132.41, 129.36 (d, *J* = 7.8 Hz), 129.35, 127.51, 125.58, 120.12, 117.78, 114.72 (d, *J* = 21.7 Hz), 55.62, 44.77, 32.67, 31.38, 16.77, 15.99. HRMS calculated for C<sub>23</sub>H<sub>26</sub>FN<sub>3</sub> (M+H)<sup>+</sup> 364.2189, found 364.2201.

**5-(4-fluorophenyl)-2-(1-methylpiperidin-4-yl)-4-(pyridin-4-yl)-1H-pyrrole-3-carbonitrile (118) [RUPB-18]****4-(4-bromo-2-(4-fluorophenyl)-5-(1-methylpiperidin-4-yl)-1H-pyrrol-3-yl)pyridine 115**

**[RUPB-15]** (110 mg, 0.267 mmol, 1 eq) and Zn(CN)<sub>2</sub> (624 mg, 5.31 mmol, 20 eq) were dissolved in 6 mL anhydrous DMF in a microwave vial. The solution was degassed under N<sub>2</sub> for 10 minutes. Pd(PPh<sub>3</sub>)<sub>2</sub>Cl<sub>2</sub> (37 mg, 0.05 mmol, 0.19 eq) was added and the reaction was heated in the microwave at 180°C. After 1.5 hours, the reaction was determined complete by LC-MS analysis. The reaction was partitioned between water and EtOAc and the organic phase was separated. The aqueous phase was extracted with EtOAc (3 x). The combined organic

phase was washed with brine (1 x), dried over sodium sulphate and concentrated. Excess DMF was removed by forming an azeotropic mixture with toluene. The resulting crude product was purified by silica gel chromatography (1% → 2% → 4% EtOAc/MeOH with 0.25% NH<sub>3</sub>). A second purification by silica gel chromatography (8% MeOH/CHCl<sub>3</sub> with 0.25% NH<sub>3</sub>) afforded 5-(4-fluorophenyl)-2-(1-methylpiperidin-4-yl)-4-(pyridin-4-yl)-1H-pyrrole-3-carbonitrile **118** [RUPB-18] (52 mg, 54% yield, 97% purity by LC-MS) as a crystalline yellow solid.

<sup>1</sup>H NMR (400 MHz, DMSO-*d*<sub>6</sub>) δ 12.03 (s, 1H), 8.53 – 8.47 (m, 2H), 7.32 – 7.26 (m, 2H), 7.23 – 7.16 (m, 4H), 2.88 (dd, *J* = 7.1, 2.0 Hz, 2H), 2.81 – 2.69 (m, 1H), 2.19 (s, 3H), 2.01 – 1.88 (m, 4H), 1.87 – 1.75 (m, 2H).

<sup>13</sup>C NMR (126 MHz, Methanol-*d*<sub>4</sub>) δ 162.70 (d, *J* = 247.2 Hz), 148.76, 146.18, 142.66, 130.49 (d, *J* = 8.3 Hz), 129.92, 127.12 (d, *J* = 3.4 Hz), 123.94, 119.18, 115.91, 115.39 (d, *J* = 22.1 Hz), 89.75, 55.12, 44.86, 34.66, 30.66. HRMS calculated for C<sub>22</sub>H<sub>21</sub>FN<sub>4</sub> (M+H)<sup>+</sup> 361.1825, found 361.1846.

**5-(4-fluorophenyl)-2-(1-methylpiperidin-4-yl)-4-(pyridin-4-yl)-1H-pyrrole-3-carboxamide (119) [RUPB-19]**

5-(4-fluorophenyl)-2-(1-methylpiperidin-4-yl)-4-(pyridin-4-yl)-1H-pyrrole-3-carbonitrile **118** [RUPB-18] (51 mg, 0.142 mmol, 1 eq) was dissolved in 3.5 mL TFA in a microwave vial. Concentrated H<sub>2</sub>SO<sub>4</sub> (0.4 mL) and water (0.1 mL) were added and the reaction was heated in the microwave at 100°C for 1.5 hours. Total conversion to the primary amide was observed by LC-MS analysis. The reaction was poured into ice-cold water and 1M NaOH was added until the solution was basic at pH 9. The product precipitated out and the precipitate was collected by filtration. EtOAc was added to the filtrate and the organic phase was separated. The aqueous phase was extracted with EtOAc (2 x). The organic phase was combined, dried over sodium sulphate, concentrated and combined with the precipitate from the filtration. Purification by silica gel chromatography (10% → 20% (25% MeOH/MeCN)/DCM with 0.25% NH<sub>3</sub>) was carried out. A second purification by silica gel chromatography (10% → 15% → 20% MeOH/EtOAc with 0.25% NH<sub>3</sub>) afforded 5-(4-fluorophenyl)-2-(1-methylpiperidin-4-yl)-4-

(pyridin-4-yl)-1H-pyrrole-3-carboxamide **119** [RUPB-19] (20 mg, 37% yield, 95% purity by LC-MS) as a crystalline yellow solid.

$^1\text{H}$  NMR (400 MHz, DMSO- $d_6$ )  $\delta$  11.18 (s, 1H), 8.40 – 8.37 (m, 2H), 7.23 – 7.11 (m, 4H), 7.11 – 7.08 (m, 2H), 7.01 (s, 1H), 6.87 (s, 1H), 2.92 – 2.81 (m, 3H), 2.18 (s, 3H), 1.99 – 1.86 (m, 4H), 1.73 (d,  $J$  = 11.1 Hz, 2H).

$^{13}\text{C}$  NMR (126 MHz, Methanol- $d_4$ )  $\delta$  170.30, 162.24 (d,  $J$  = 246.2 Hz), 148.20, 144.76, 137.04, 130.33 (d,  $J$  = 8.2 Hz), 128.99, 128.18 (d,  $J$  = 3.4 Hz), 125.33, 116.91, 115.78, 115.01 (d,  $J$  = 21.9 Hz), 54.94, 43.92, 32.61, 30.08. HRMS calculated for  $\text{C}_{22}\text{H}_{23}\text{FN}_4\text{O}$  ( $\text{M}+\text{H}$ ) $^+$  379.1934, found 379.1954

**Benzyl 4-(3-((dimethylamino)methyl)-5-(4-fluorophenyl)-4-(pyridin-4-yl)-1H-pyrrol-2-yl)piperidine-1-carboxylate (120A)**

Formaldehyde 37% w/w solution in water (1.7 mL, excess) was dissolved in 8 mL MeOH and 1 mL AcOH and dimethylamine 2M solution in THF (1.8 mL, excess) was added to this. The reaction was stirred for 1 hour under  $\text{N}_2$ . Benzyl 4-(5-(4-fluorophenyl)-4-(pyridin-4-yl)-1H-pyrrol-2-yl)piperidine-1-carboxylate **93A** (90 mg, 0.198 mmol, 1 eq) was dissolved in 8 mL MeOH and added dropwise to the Mannich base generated by means of a syringe. The reaction was warmed to 60°C. The reaction was found to progress ahead each day by LC-MS analysis and stalled after 12 days. 1N NaOH was added until pH 9 and it was concentrated under reduced pressure. The concentrate was partitioned between water and EtOAc. The organic phase was separated, and the aqueous phase was extracted with EtOAc (3 x). The combined organic phase was dried over sodium sulphate and concentrated. Purification by silica gel chromatography (1%  $\rightarrow$  2%  $\rightarrow$  4%  $\rightarrow$  6%  $\rightarrow$  8%  $\rightarrow$  10% MeOH/DCM with 0.25%  $\text{NH}_3$ ) gave benzyl 4-(3-((dimethylamino)methyl)-5-(4-fluorophenyl)-4-(pyridin-4-yl)-1H-pyrrol-2-yl)piperidine-1-carboxylate **120A** (65 mg, 64% yield, 97% purity by LC-MS).

$^1\text{H}$  NMR (400 MHz, DMSO- $d_6$ )  $\delta$  10.92 (s, 1H), 8.43 – 8.32 (m, 2H), 7.37 (d,  $J$  = 4.1 Hz, 4H), 7.35 – 7.29 (m, 1H), 7.29 – 7.26 (m, 2H), 7.21 – 7.16 (m, 2H), 7.13 – 7.05 (m, 2H), 5.09 (d,  $J$

= 7.1 Hz, 2H), 4.13 (d,  $J$  = 12.9 Hz, 2H), 3.35 – 3.32 (m, 2H), 3.14 – 2.92 (m, 3H), 2.16 – 2.03 (m, 6H), 1.93 – 1.78 (m, 2H), 1.64 (d,  $J$  = 12.6 Hz, 2H). (M+H)<sup>+</sup> 513.10

**1-(5-(4-fluorophenyl)-2-(1-methylpiperidin-4-yl)-4-(pyridin-4-yl)-1H-pyrrol-3-yl)-N,N-dimethylmethanamine (121A) [RUPB-22]**

Benzyl 4-(3-((dimethylamino)methyl)-5-(4-fluorophenyl)-4-(pyridin-4-yl)-1H-pyrrol-2-yl)piperidine-1-carboxylate **120A** (65 mg, 0.127 mmol, 1 eq) was dissolved in 6 mL anhydrous THF. Lithium aluminium hydride 2M solution in THF (0.25 mL, 0.508 mmol, 4 eq) was added dropwise to the solution of **120A** and stirred at room temperature for 30 minutes. The reaction was determined complete by LC-MS analysis. The Feiser & Feiser quench (0.02 mL water, 0.02 mL 15% NaOH and 0.06 mL water in a sequential manner) was employed and the reaction mixture was stirred for an additional 45 minutes. The reaction was filtered over celite and the filtrate was concentrated. Purification by silica gel chromatography (10% → 12% → 15% MeOH/EtOAc with 0.25% NH<sub>3</sub>) produced an almost pure product. That product was partitioned between 1N HCl and EtOAc. The aqueous phase was separated, and the organic phase was extracted with water (2 x). The combined acidic aqueous phase was basified by the addition of 1N NaOH until the pH was 9 and then EtOAc was added. The organic phase was separated, and the neutralised aqueous phase was extracted with EtOAc (3 x), dried over sodium sulphate and concentrated to give 1-(5-(4-fluorophenyl)-2-(1-methylpiperidin-4-yl)-4-(pyridin-4-yl)-1H-pyrrol-3-yl)-N,N-dimethylmethanamine **121A** [RUPB-22] (30 mg, 60% yield, 98% purity by LC-MS) as a white solid.

<sup>1</sup>H NMR (400 MHz, DMSO-*d*<sub>6</sub>) δ 10.89 (s, 1H), 8.40 – 8.35 (m, 2H), 7.31 – 7.26 (m, 2H), 7.23 – 7.17 (m, 2H), 7.12 – 7.05 (m, 2H), 3.03 (s, 2H), 2.89 – 2.82 (m, 2H), 2.72 – 2.62 (m, 1H), 2.17 (s, 3H), 2.07 (s, 6H), 2.00 – 1.86 (m, 4H), 1.58 (d,  $J$  = 13.5 Hz, 2H).

<sup>13</sup>C NMR (126 MHz, Methanol-*d*<sub>4</sub>) δ 161.78 (d,  $J$  = 244.3 Hz), 148.08, 146.71, 135.77, 129.78 (d,  $J$  = 8.0 Hz), 129.18 (d,  $J$  = 3.2 Hz), 128.24, 125.98, 118.83, 114.81 (d,  $J$  = 21.8 Hz), 113.88, 55.67, 51.94, 45.00, 43.54, 32.68, 31.30. HRMS calculated for C<sub>24</sub>H<sub>29</sub>FN<sub>4</sub>. (M+H)<sup>+</sup> 393.2455, found 393.2485.

**Benzyl 4-(5-(4-fluorophenyl)-3-((methylamino)methyl)-4-(pyridin-4-yl)-1H-pyrrol-2-yl)piperidine-1-carboxylate (120B)**

Following the procedure as described for the synthesis of **120A**, using benzyl 4-(5-(4-fluorophenyl)-4-(pyridin-4-yl)-1H-pyrrol-2-yl)piperidine-1-carboxylate **93A** (115 mg, 0.252 mmol, 1 eq), methylamine 2M solution in THF (0.7mL, 1.4 mmol, 5.5 eq) and formaldehyde 37% w/w solution in water (0.1 mL), the title compound benzyl 4-(5-(4-fluorophenyl)-3-((methylamino)methyl)-4-(pyridin-4-yl)-1H-pyrrol-2-yl)piperidine-1-carboxylate **120B** (65 mg, 52% yield, 98% purity by LC-MS) was isolated.

<sup>1</sup>H NMR (400 MHz, DMSO-*d*<sub>6</sub>) δ 10.87 (s, 1H), 8.43 – 8.37 (m, 2H), 7.37 (d, *J* = 4.1 Hz, 4H), 7.35 – 7.29 (m, 1H), 7.27 – 7.24 (m, 2H), 7.20 – 7.14 (m, 2H), 7.12 – 7.06 (m, 2H), 5.09 (d, *J* = 5.3 Hz, 2H), 4.13 (d, *J* = 13.4 Hz, 2H), 3.37 (d, *J* = 2.8 Hz, 2H), 2.97 (tt, *J* = 12.4, 3.8 Hz, 3H), 2.24 (s, 3H), 1.91 – 1.76 (m, 2H), 1.69 (d, *J* = 12.6 Hz, 2H). (M+H)<sup>+</sup> 499.15

**1-(5-(4-fluorophenyl)-2-(1-methylpiperidin-4-yl)-4-(pyridin-4-yl)-1H-pyrrol-3-yl)-N-methylmethanamine (121B) [RUPB-23]**

Following the procedure as described for the synthesis of **121A [RUPB-22]**, using benzyl 4-(5-(4-fluorophenyl)-3-((methylamino)methyl)-4-(pyridin-4-yl)-1H-pyrrol-2-yl)piperidine-1-carboxylate **120B** (60 mg, 0.120 mmol, 1 eq) and Lithium aluminium hydride 2M solution in THF (0.24 mL, 0.48 mmol, 4 eq), the title compound 1-(5-(4-fluorophenyl)-2-(1-methylpiperidin-4-yl)-4-(pyridin-4-yl)-1H-pyrrol-3-yl)-N-methylmethanamine **121B [RUPB-23]** (15 mg, 33% yield, 98% purity by LC-MS) was isolated as a crystalline white solid.

<sup>1</sup>H NMR (400 MHz, DMSO-*d*<sub>6</sub>) δ 10.89 (s, 1H), 8.42 – 8.38 (m, 2H), 7.27 – 7.23 (m, 2H), 7.20 – 7.16 (m, 2H), 7.12 – 7.06 (m, 2H), 3.36 (s, 2H), 2.87 – 2.82 (m, 2H), 2.71 – 2.63 (m, 1H), 2.25 (s, 3H), 2.18 (s, 3H), 1.97 – 1.87 (m, 4H), 1.64 (q, *J* = 4.8, 3.8 Hz, 2H).

<sup>13</sup>C NMR (126 MHz, Methanol-*d*<sub>4</sub>) δ 161.86 (d, *J* = 245.8 Hz), 148.57, 145.97, 135.91, 129.70 (d, *J* = 8.0 Hz), 128.79 (d, *J* = 3.3 Hz), 128.50, 125.58, 118.12, 114.87 (d, *J* = 21.9 Hz), 109.99, 55.53, 44.99, 43.49, 33.46, 32.56, 31.46. HRMS calculated for C<sub>23</sub>H<sub>27</sub>FN<sub>4</sub> (M+H)<sup>+</sup> 379.2298, found 379.2312.

**1-(5-(4-fluorophenyl)-2-(piperidin-4-yl)-4-(pyridin-4-yl)-1H-pyrrol-3-yl)ethan-1-one (122)**

Acetyl chloride (0.02 mL, density = 1.104g/mL, 0.296 mmol, 1.5 eq) was dissolved in 2 mL 1,2 DCE and cooled to 0°C under N<sub>2</sub>. AlCl<sub>3</sub> (40 mg, 0.296 mmol, 1.5 eq) was added to the acetyl chloride solution and stirred for 20 minutes while maintaining the temperature at 0°C. Benzyl 4-(5-(4-fluorophenyl)-4-(pyridin-4-yl)-1H-pyrrol-2-yl)piperidine-1-carboxylate **93A** (90 mg, 0.198 mmol, 1 eq) was dissolved in 5 mL 1,2 DCE and added to the reaction mixture by means of a syringe. The reaction was warmed to room temperature and stirred overnight. A mixture of products **122** and **123** was observed by LC-MS analysis. The reaction was quenched by the addition of ice-cold water. The reaction mixture was partitioned between water and DCM. The aqueous phase was separated, and the organic phase was extracted with water (3 x). The combined aqueous phase was basified by the addition of 1N NaOH till pH 9 and partitioned between water and DCM. The organic phase was separated, and the aqueous phase was extracted with DCM (3 x). The combined organic phase was dried over sodium sulphate and concentrated to give a crude mixture of **122** and **123**. The crude mixture was dissolved in 2 mL 1,4-dioxane in a sealed vial and concentrated HCl (1 mL) was added. The reaction was heated to reflux for 3 hours for total conversion of **123** to **122**. The reaction mixture was basified by the addition of 1N NaOH and partitioned between water and EtOAc. The organic phase was separated, and the aqueous phase was extracted with EtOAc (3 x). The combined organic phase was dried over celite and concentrated to give 1-(5-(4-fluorophenyl)-2-(piperidin-4-yl)-4-(pyridin-4-yl)-1H-pyrrol-3-yl)ethan-1-one **122** (56 mg, 79% yield over 2 steps, 84% purity by LC-MS) which was taken onto the next step without further purification. (M+H)<sup>+</sup> 363.85

**1-(5-(4-fluorophenyl)-2-(1-methylpiperidin-4-yl)-4-(pyridin-4-yl)-1H-pyrrol-3-yl)ethan-1-one (124)**

1-(5-(4-fluorophenyl)-2-(piperidin-4-yl)-4-(pyridin-4-yl)-1H-pyrrol-3-yl)ethan-1-one **122** (56 mg, 0.154 mmol, 1 eq) was dissolved in 5 mL MeOH and 1 mL AcOH. Formaldehyde 37% w/w in H<sub>2</sub>O (1 mL, excess) was added to the solution of **122**. The reaction was stirred at room



temperature for 1 hour. Sodium borohydride (50 mg, 1.31 mmol, 8.5 eq) was added portion wise to the reaction mixture over 10 minutes. After 1 hour, the reaction was determined complete by LC-MS analysis. The reaction was quenched by the addition of 2 mL water and was concentrated under reduced pressure. The concentrate was partitioned between EtOAc and water. The organic phase was separated, and the aqueous phase was extracted with EtOAc (3 x). The combined organic phase was dried over sodium sulphate and concentrated to give 1-(5-(4-fluorophenyl)-2-(1-methylpiperidin-4-yl)-4-(pyridin-4-yl)-1H-pyrrol-3-yl)ethan-1-one **124** (55 mg, 95% yield, 86% purity by LC-MS) which was taken onto the next step without further purification. (M+H)<sup>+</sup> 378.25

**1-(5-(4-fluorophenyl)-2-(1-methylpiperidin-4-yl)-4-(pyridin-4-yl)-1H-pyrrol-3-yl)ethan-1-ol (125) [RUPB-20]**

To a solution of 1-(5-(4-fluorophenyl)-2-(1-methylpiperidin-4-yl)-4-(pyridin-4-yl)-1H-pyrrol-3-yl)ethan-1-one **124** (55 mg, 0.146 mmol, 1 eq) in 7 mL MeOH, sodium borohydride (50 mg, 1.322 mmol, 9 eq) was added portion wise. The reaction was stirred at room temperature over the weekend during which it achieved completion as determined by LC-MS analysis. 2 mL water was added to quench the reaction and it was concentrated under reduced pressure. The concentrate was partitioned between water and EtOAc. The organic phase was separated, and the aqueous phase was extracted with EtOAc (3 x). The combined organic phase was dried over sodium sulphate and concentrated. Purification by silica gel chromatography (8% MeOH/CHCl<sub>3</sub> with 0.25% NH<sub>3</sub>) afforded 1-(5-(4-fluorophenyl)-2-(1-methylpiperidin-4-yl)-4-(pyridin-4-yl)-1H-pyrrol-3-yl)ethan-1-ol **125** [RUPB-20] (30 mg, 55% yield, 95% purity by LC-MS) as a deep yellow solid.

<sup>1</sup>H NMR (400 MHz, DMSO-*d*<sub>6</sub>) δ 10.78 (s, 1H), 8.44 – 8.39 (m, 2H), 7.17 – 7.14 (m, 2H), 7.14 – 7.02 (m, 4H), 4.69 (d, *J* = 2.6 Hz, 1H), 4.63 (qd, *J* = 6.6, 2.7 Hz, 1H), 2.99 (d, *J* = 11.6 Hz, 1H), 2.87 (d, *J* = 6.7 Hz, 2H), 2.19 (s, 3H), 1.93 (p, *J* = 10.9, 10.4 Hz, 4H), 1.74 – 1.59 (m, 2H), 1.20 (d, *J* = 6.6 Hz, 3H).

$^{13}\text{C}$  NMR (126 MHz, Methanol- $d_4$ )  $\delta$  161.64 (d,  $J$  = 244.9 Hz), 148.04, 146.88, 133.75, 129.56 (d,  $J$  = 8.0 Hz), 129.10 (d,  $J$  = 3.4 Hz), 127.51, 126.48, 121.85, 117.35, 114.71 (d,  $J$  = 21.7 Hz), 62.83, 55.67, 44.88, 32.98, 31.30, 23.48. HRMS calculated for  $\text{C}_{23}\text{H}_{26}\text{FN}_3\text{O}$  ( $\text{M}+\text{H}$ ) $^+$  380.2138, found 380.2150.

**Benzyl 4-(5-(4-fluorophenyl)-3-formyl-4-(pyridin-4-yl)-1H-pyrrol-2-yl)piperidine-1-carboxylate (126)**

Anhydrous DMF (5 mL, excess) was cooled to 0°C under  $\text{N}_2$  and  $\text{POCl}_3$  (0.2 mL, excess) was added to it. The reaction was stirred for 45 minutes. Benzyl 4-(5-(4-fluorophenyl)-4-(pyridin-4-yl)-1H-pyrrol-2-yl)piperidine-1-carboxylate **93A** (90 mg, 0.198 mmol, 1 eq) was dissolved in 5 mL dry DMF and added to the Vilsmeier salt by means of a syringe. The reaction was warmed to 60°C and the reaction was determined complete in 30 minutes by LC-MS analysis. The reaction was quenched by the addition of 1N NaOH until basic and concentrated under reduced pressure. The concentrate was partitioned between water and EtOAc. The organic phase was separated, and the aqueous phase was extracted with EtOAc (3 x). The combined organic phase was washed with brine, dried over sodium sulphate and concentrated. Excess DMF was removed by forming an azeotropic mixture with toluene. Purification by silica gel chromatography (25%  $\rightarrow$  50% EtOAc/Hexanes) afforded Benzyl 4-(5-(4-fluorophenyl)-3-formyl-4-(pyridin-4-yl)-1H-pyrrol-2-yl)piperidine-1-carboxylate **126** (60 mg, 63% yield, 94% purity by LC/MS).

$^1\text{H}$  NMR (500 MHz, DMSO- $d_6$ )  $\delta$  11.79 (s, 1H), 9.77 (d,  $J$  = 2.2 Hz, 1H), 8.54 – 8.40 (m, 2H), 7.43 – 7.28 (m, 5H), 7.26 – 7.05 (m, 6H), 5.10 (d,  $J$  = 5.2 Hz, 2H), 4.16 (d,  $J$  = 13.1 Hz, 2H), 3.72 – 3.57 (m, 1H), 2.97 – 2.84 (m, 2H), 1.94 – 1.82 (m, 2H), 1.81 – 1.72 (m, 2H). ( $\text{M}+\text{H}$ ) $^+$  483.95

**5-(4-fluorophenyl)-2-(piperidin-4-yl)-4-(pyridin-4-yl)-1H-pyrrole-3-carbaldehyde (127)**  
**and 5-(4-fluorophenyl)-2-(1-methylpiperidin-4-yl)-4-(pyridin-4-yl)-1H-pyrrole-3-**  
**carbaldehyde (128)**

Benzyl 4-(5-(4-fluorophenyl)-3-formyl-4-(pyridin-4-yl)-1H-pyrrol-2-yl)piperidine-1-carboxylate **126** (60 mg, 0.124 mmol, 1 eq) was dissolved in 10 mL MeOH. Palladium on carbon (50 mg) was added to the methanolic solution of **126**. The reaction mixture was set up for hydrogenation using a hydrogen balloon setup. The reaction was stirred for 3 hours at room temperature and was determined complete by LC-MS analysis. The reaction mixture was filtered over celite and the filtrate was concentrated to give a 1:1 mixture of 5-(4-fluorophenyl)-2-(piperidin-4-yl)-4-(pyridin-4-yl)-1H-pyrrole-3-carbaldehyde **127** and 5-(4-fluorophenyl)-2-(1-methylpiperidin-4-yl)-4-(pyridin-4-yl)-1H-pyrrole-3-carbaldehyde **128** (65 mg) which was taken onto the next step without further purification. (M+H)<sup>+</sup> 349.95; 363.85

**(5-(4-fluorophenyl)-2-(piperidin-4-yl)-4-(pyridin-4-yl)-1H-pyrrol-3-yl)methanol (129)**  
**and (5-(4-fluorophenyl)-2-(1-methylpiperidin-4-yl)-4-(pyridin-4-yl)-1H-pyrrol-3-**  
**yl)methanol (130)**

A 1:1 mixture of 5-(4-fluorophenyl)-2-(piperidin-4-yl)-4-(pyridin-4-yl)-1H-pyrrole-3-carbaldehyde **127** and 5-(4-fluorophenyl)-2-(1-methylpiperidin-4-yl)-4-(pyridin-4-yl)-1H-pyrrole-3-carbaldehyde **128** (65 mg) was dissolved in 8 mL MeOH and sodium borohydride (50 mg, excess) was added. The reaction was determined complete by LC-MS analysis after stirring for 1 hour. 4 mL water was added to quench the reaction and it was concentrated under reduced pressure. The concentrate was partitioned between EtOAc and water. The organic phase was separated, and the aqueous phase was extracted with EtOAc (3 x). The combined organic phase was dried over sodium sulphate and concentrated to give a mixture of (5-(4-fluorophenyl)-2-(piperidin-4-yl)-4-(pyridin-4-yl)-1H-pyrrol-3-yl)methanol **129** and (5-(4-fluorophenyl)-2-(1-methylpiperidin-4-yl)-4-(pyridin-4-yl)-1H-pyrrol-3-yl)methanol **130** (50 mg) which was taken onto the next step without further purification. (M+H)<sup>+</sup> 351.65; 365.75

**(5-(4-fluorophenyl)-2-(1-methylpiperidin-4-yl)-4-(pyridin-4-yl)-1H-pyrrol-3-yl)methanol (130) [RUPB-21]**

A mixture of (5-(4-fluorophenyl)-2-(piperidin-4-yl)-4-(pyridin-4-yl)-1H-pyrrol-3-yl)methanol **129** and (5-(4-fluorophenyl)-2-(1-methylpiperidin-4-yl)-4-(pyridin-4-yl)-1H-pyrrol-3-yl)methanol **130** (50 mg) was dissolved in 8 mL MeOH and 2 mL AcOH. Formaldehyde 37% w/w solution (1 mL, excess) was added to this solution and the reaction was stirred at room temperature for 1 hour. Sodium borohydride (35 mg, excess) was then added to the reaction mixture and the reaction was again stirred over the weekend to achieve total conversion of **129** to **130**. 1 mL water was added to quench the reaction and it was concentrated under reduced pressure. The concentrate was partitioned between EtOAc and water. The organic phase was separated, and the aqueous phase was extracted with EtOAc (3 x). The combined organic phase was dried over sodium sulphate and concentrated. New mass peak corresponding to possible hydroxymethylation of the piperidine nitrogen was seen. The crude mixture was dissolved in 5 mL 7N NH<sub>3</sub> solution in MeOH and stirred overnight resulting in total conversion to the desired product **130**. The reaction was concentrated under reduced pressure. Purification by silica gel chromatography (8% → 10% MeOH/CHCl<sub>3</sub> with 0.25% NH<sub>3</sub>) afforded (5-(4-fluorophenyl)-2-(1-methylpiperidin-4-yl)-4-(pyridin-4-yl)-1H-pyrrol-3-yl)methanol **130** [RUPB-21] (20 mg, 100% purity by LC-MS) as a deep yellow solid.

<sup>1</sup>H NMR (400 MHz, DMSO-*d*<sub>6</sub>) δ 10.90 (s, 1H), 8.41 – 8.37 (m, 2H), 7.25 – 7.16 (m, 4H), 7.15 – 7.07 (m, 2H), 4.61 – 4.55 (m, 1H), 4.18 (d, *J* = 4.7 Hz, 2H), 2.85 (d, *J* = 6.8 Hz, 2H), 2.72 (dq, *J* = 8.4, 4.2 Hz, 1H), 2.18 (s, 3H), 2.00 – 1.86 (m, 4H), 1.67 (q, *J* = 4.7, 4.1 Hz, 2H). <sup>13</sup>C NMR (126 MHz, Methanol-*d*<sub>4</sub>) δ 161.87 (d, *J* = 245.2 Hz), 148.12, 145.97, 135.97, 129.80 (d, *J* = 8.0 Hz), 129.13 (d, *J* = 3.2 Hz), 127.97, 125.43, 118.40, 117.26, 114.88 (d, *J* = 21.9 Hz), 55.64, 53.51, 44.98, 32.74, 31.41. HRMS calculated for C<sub>22</sub>H<sub>24</sub>FN<sub>3</sub>O (M+H)<sup>+</sup> 366.1981, found 366.2009.

**Benzyl 4-(5-(4-fluorophenyl)-3-((methylthio)methyl)-4-(pyridin-4-yl)-1H-pyrrol-2-yl)piperidine-1-carboxylate (131)**

Benzyl 4-(5-(4-fluorophenyl)-4-(pyridin-4-yl)-1H-pyrrol-2-yl)piperidine-1-carboxylate **93A** (100 mg, 0.22 mmol, 1 eq), Cu(PPh<sub>3</sub>)<sub>3</sub>Cl (31 mg, 0.033 mmol, 0.15 eq), NH<sub>4</sub>OAc (68 mg, 0.88 mmol, 4 eq) and NaOMe 0.5M solution in methanol (0.44 mL, 0.22 mmol, 1 eq) were dissolved in DMSO (1.5 mL). The reaction was heated in the microwave for 48 hours at 140°C after slow progression of heating the reaction in the hood. The reaction stalled after achieving 50% completion. 4 mL water was added to quench the reaction. The quenched mixture was partitioned between EtOAc and water. The organic phase was separated, and the aqueous phase was extracted with EtOAc (3 x). The combined organic phase was dried over sodium sulphate and concentrated. Purification by silica gel chromatography (10% → 25% → 40% EtOAc/Hexanes) afforded benzyl 4-(5-(4-fluorophenyl)-3-((methylthio)methyl)-4-(pyridin-4-yl)-1H-pyrrol-2-yl)piperidine-1-carboxylate **131** (90 mg, 80% yield, 97% purity by LC-MS).

<sup>1</sup>H NMR (400 MHz, DMSO-*d*<sub>6</sub>) δ 10.96 (s, 1H), 8.46 – 8.42 (m, 2H), 7.41 – 7.28 (m, 5H), 7.22 – 7.04 (m, 6H), 5.09 (s, 2H), 4.20 – 4.08 (m, 2H), 3.53 (s, 2H), 2.99 (ddt, *J* = 12.5, 9.0, 3.7 Hz, 3H), 1.95 (s, 3H), 1.84 (qd, *J* = 12.6, 4.2 Hz, 2H), 1.68 (d, *J* = 12.4 Hz, 2H). (M+H)<sup>+</sup> 516.30

**Benzyl 4-(5-(4-fluorophenyl)-3-((methylsulfonyl)methyl)-4-(pyridin-4-yl)-1H-pyrrol-2-yl)piperidine-1-carboxylate (132)**

Benzyl 4-(5-(4-fluorophenyl)-3-((methylthio)methyl)-4-(pyridin-4-yl)-1H-pyrrol-2-yl)piperidine-1-carboxylate **131** (90 mg, 0.175 mmol, 1 eq) was dissolved in 6 mL THF and cooled to 0°C. The reagent, mCPBA (60 mg, 0.349 mmol, 2 eq), was added portion wise and the reaction was stirred maintaining the temperature at 0°C. After 30 minutes, the reaction reached completion as determined by LC-MS analysis. 3 mL saturated NaHCO<sub>3</sub> was added to quench the reaction. The reaction mixture was partitioned between water and EtOAc. The EtOAc phase was separated, and the aqueous phase was extracted with EtOAc (3 x). The combined organic phase was dried over sodium sulphate and concentrated. Purification by silica gel chromatography (25% → 50% → 75% → 100% EtOAc/Hexanes) gave benzyl 4-(5-

(4-fluorophenyl)-3-((methylsulfonyl)methyl)-4-(pyridin-4-yl)-1H-pyrrol-2-yl)piperidine-1-carboxylate **132** (81 mg, 85% yield, 99% purity by LC-MS).

<sup>1</sup>H NMR (500 MHz, DMSO-*d*<sub>6</sub>) δ 11.23 (s, 1H), 8.49 – 8.40 (m, 2H), 7.37 (d, *J* = 4.4 Hz, 4H), 7.35 – 7.29 (m, 1H), 7.27 – 7.20 (m, 2H), 7.16 (ddt, *J* = 8.5, 5.3, 2.6 Hz, 2H), 7.13 – 7.06 (m, 2H), 5.09 (d, *J* = 12.1 Hz, 2H), 4.27 (s, 2H), 4.21 – 4.08 (m, 2H), 3.08 (tt, *J* = 12.2, 3.9 Hz, 1H), 2.84 (d, *J* = 27.5 Hz, 2H), 2.73 (s, 3H), 1.84 (qd, *J* = 12.5, 4.2 Hz, 2H), 1.75 (t, *J* = 7.6 Hz, 2H). (M+H)<sup>+</sup> 548.0

**4-(2-(4-fluorophenyl)-4-((methylsulfonyl)methyl)-5-(piperidin-4-yl)-1H-pyrrol-3-yl)pyridine (133) and 4-(2-(4-fluorophenyl)-5-(1-methylpiperidin-4-yl)-4-((methylsulfonyl)methyl)-1H-pyrrol-3-yl)pyridine (134)**

Following the procedure as described for the synthesis of **127** and **128**, using benzyl 4-(5-(4-fluorophenyl)-3-((methylsulfonyl)methyl)-4-(pyridin-4-yl)-1H-pyrrol-2-yl)piperidine-1-carboxylate **132** (75 mg, 0.137 mmol, 1 eq) and palladium on carbon (50 mg, excess), the title compounds 4-(2-(4-fluorophenyl)-4-((methylsulfonyl)methyl)-5-(piperidin-4-yl)-1H-pyrrol-3-yl)pyridine **133** and 4-(2-(4-fluorophenyl)-5-(1-methylpiperidin-4-yl)-4-((methylsulfonyl)methyl)-1H-pyrrol-3-yl)pyridine **134** were isolated as a mixture (59 mg). (M+H)<sup>+</sup> 413.95; 427.85

**4-(2-(4-fluorophenyl)-5-(1-methylpiperidin-4-yl)-4-((methylsulfonyl)methyl)-1H-pyrrol-3-yl)pyridine (134) [RUPB-25]**

Following the procedure as described for the synthesis of **130** [RUPB-21], using a mixture of 4-(2-(4-fluorophenyl)-4-((methylsulfonyl)methyl)-5-(piperidin-4-yl)-1H-pyrrol-3-yl)pyridine **133** and 4-(2-(4-fluorophenyl)-5-(1-methylpiperidin-4-yl)-4-((methylsulfonyl)methyl)-1H-pyrrol-3-yl)pyridine **134** (59 mg), HCHO 37% w/w solution in water (1.5 mL, excess) and NaBH<sub>4</sub> (30 mg, excess), the total conversion of **133** to **134** was achieved. The crude product was dissolved in 1M HCl and partitioned between EtOAc and water. The aqueous phase was separated, and the organic phase was extracted with water (2 x). The combined acidic aqueous phase was basified to pH 9 with 1N NaOH and EtOAc was added to this. The organic phase

was separated, and the neutralised aqueous phase was extracted with EtOAc (3 x). The combined organic phase was dried over sodium sulphate and concentrated to give purified 4-(2-(4-fluorophenyl)-5-(1-methylpiperidin-4-yl)-4-((methylsulfonyl)methyl)-1H-pyrrol-3-yl)pyridine **134** [RUPB-25] (20 mg, 98% purity by LC-MS) as an amorphous white solid.

<sup>1</sup>H NMR (400 MHz, DMSO-*d*<sub>6</sub>) δ 10.72 (s, 1H), 8.48 – 8.39 (m, 2H), 7.20 – 7.00 (m, 6H), 2.95 – 2.83 (m, 2H), 2.66 – 2.52 (m, 1H), 2.35 (q, *J* = 7.5 Hz, 2H), 2.22 (s, 3H), 2.09 – 1.88 (m, 4H), 1.62 (d, *J* = 11.1 Hz, 2H), 0.86 (t, *J* = 7.4 Hz, 3H).

<sup>13</sup>C NMR (126 MHz, Methanol-*d*<sub>4</sub>) δ 161.91 (d, *J* = 245.6 Hz), 148.59, 145.58, 138.08, 129.80 (d, *J* = 8.0 Hz), 128.96, 128.56 (d, *J* = 3.3 Hz), 125.91, 118.90, 114.87 (d, *J* = 21.9 Hz), 103.62, 55.59, 50.13, 44.95, 38.76, 32.82, 31.04. LRMS for C<sub>23</sub>H<sub>26</sub>FN<sub>3</sub>O<sub>2</sub>S found (M+H)<sup>+</sup> 427.95

#### **2-bromo-1-(4-fluorophenyl)-2-(pyridin-4-yl)ethan-1-one hydrobromide (135)**

1-(4-fluorophenyl)-2-(pyridin-4-yl)ethan-1-one **91A** (1.274 g, 5.92 mmol, 1 eq) was dissolved in 10 mL AcOH. A stock solution of bromine (2.12 g, 0.6 mL, density = 3.1 g/mL) in 2 mL AcOH was prepared. 1.045 mL of the stock solution of bromine (amounting to 852 mg, 5.328 mmol, 0.9 eq of Br<sub>2</sub>) was added to the solution of **91A** in a dropwise manner by means of a syringe. The reaction was stirred at room temperature for 45 minutes which resulted in complete bromination of **91A** as determined by the LC-MS. The hydrobromide salt of the product was seen to precipitate out of the solution. 3 mL EtOAc was added and stirred for 10 minutes to achieve total precipitation of the product. The reaction mixture was filtered, and the residue was dried and collected to give 2-bromo-1-(4-fluorophenyl)-2-(pyridin-4-yl)ethan-1-one hydrobromide **135** (1.88 g, 85% yield, 98% purity by LC-MS) as a beige-yellow crystalline solid which was taken onto the next step without any purification. (M+H)<sup>+</sup> 294.95; 295.95

#### **Benzyl 4-(2-(ethoxycarbonyl)-4-(4-fluorophenyl)-4-oxo-3-(pyridin-4-yl)butanoyl)piperidine-1-carboxylate (137)**

Benzyl 4-(3-ethoxy-3-oxopropanoyl)piperidine-1-carboxylate **136** (1.1 g, 3.299 mmol, 1 eq) was dissolved in 14 mL THF. NaH 60% dispersion in mineral oil (237.48 mg, 9.899 mmol, 3 eq) and 2-bromo-1-(4-fluorophenyl)-2-(pyridin-4-yl)ethan-1-one hydrobromide **135** (1.234 g,

3.299 mmol, 1 eq) were added in a sequential manner and the reaction was stirred overnight. LC-MS analysis revealed that the reaction was complete, and 3 mL water was added to quench the reaction. The reaction was concentrated under reduced pressure and the concentrate was partitioned between EtOAc and water. The organic phase was separated, and the aqueous phase was extracted with EtOAc (3 x). The combined organic phase was dried over sodium sulphate and concentrated to give crude benzyl 4-(2-(ethoxycarbonyl)-4-(4-fluorophenyl)-4-oxo-3-(pyridin-4-yl)butanoyl)piperidine-1-carboxylate **137** (1.3 g) which was taken onto the next step without any purification.

<sup>1</sup>H NMR (500 MHz, DMSO-*d*<sub>6</sub>)  $\delta$  11.46 (s, 1H), 8.44 – 8.38 (m, 2H), 7.38 – 7.23 (m, 5H), 7.18 – 7.04 (m, 6H), 5.18 – 4.99 (m, 2H), 4.16 (d, *J* = 13.0 Hz, 2H), 3.94 (q, *J* = 7.1 Hz, 2H), 3.64 (tt, *J* = 12.2, 3.7 Hz, 1H), 2.87 (d, *J* = 40.2 Hz, 2H), 1.85 (qd, *J* = 12.5, 3.7 Hz, 2H), 1.76 (d, *J* = 12.2 Hz, 2H), 0.92 (t, *J* = 7.1 Hz, 3H). (M+H)<sup>+</sup> 547.10

**Benzyl 4-(3-(ethoxycarbonyl)-5-(4-fluorophenyl)-4-(pyridin-4-yl)-1H-pyrrol-2-yl)piperidine-1-carboxylate (138)**

Following the procedure as described for the synthesis of benzyl 4-(5-(4-fluorophenyl)-4-(pyridin-4-yl)-1H-pyrrol-2-yl)piperidine-1-carboxylate **93A**, using crude benzyl 4-(2-(ethoxycarbonyl)-4-(4-fluorophenyl)-4-oxo-3-(pyridin-4-yl)butanoyl)piperidine-1-carboxylate **137** (1.3 g) and NH<sub>4</sub>OAc (3 g, excess), the title compound **138** was synthesized. Purification by silica gel chromatography (50% EtOAc/Hexanes) afforded benzyl 4-(3-(ethoxycarbonyl)-5-(4-fluorophenyl)-4-(pyridin-4-yl)-1H-pyrrol-2-yl)piperidine-1-carboxylate **138** (600 mg, 39% over two steps, 97% purity by LC-MS). (M+H)<sup>+</sup> 527.95

**Ethyl 5-(4-fluorophenyl)-2-(1-methylpiperidin-4-yl)-4-(pyridin-4-yl)-1H-pyrrole-3-carboxylate (139) [RUPB-16]**

Following the procedure as described for the synthesis of 4-(2-(4-fluorophenyl)-5-(1-methylpiperidin-4-yl)-1H-pyrrol-3-yl)pyridine **94A** [TSP], using benzyl 4-(3-(ethoxycarbonyl)-5-(4-fluorophenyl)-4-(pyridin-4-yl)-1H-pyrrol-2-yl)piperidine-1-carboxylate **138** (358 mg, 0.679 mmol, 1 eq) and LAH 2M solution in THF (1.35 mL, 2.7 mmol,



4 eq), the title compound **139** was synthesized without any reduction of the ester moiety. Purification by silica gel chromatography (8% MeOH/CHCl<sub>3</sub> with 0.25% NH<sub>3</sub>) afforded ethyl 5-(4-fluorophenyl)-2-(1-methylpiperidin-4-yl)-4-(pyridin-4-yl)-1H-pyrrole-3-carboxylate **139** [RUPB-16] (121 mg, 44% yield, 100% purity by LC-MS) as a clear white solid.

<sup>1</sup>H NMR (400 MHz, DMSO-*d*<sub>6</sub>) δ 11.44 (s, 1H), 8.41 – 8.37 (m, 2H), 7.19 – 7.12 (m, 2H), 7.12 – 7.05 (m, 4H), 3.94 (q, *J* = 7.1 Hz, 2H), 3.35 (td, *J* = 8.9, 4.1 Hz, 1H), 2.93 – 2.83 (m, 2H), 2.18 (s, 3H), 2.06 – 1.84 (m, 4H), 1.70 (dd, *J* = 9.6, 3.8 Hz, 2H), 0.92 (t, *J* = 7.1 Hz, 3H). <sup>13</sup>C NMR (126 MHz, Methanol-*d*<sub>4</sub>) δ 165.45, 162.06 (d, *J* = 246.1 Hz), 147.60, 146.53, 143.50, 130.18 (d, *J* = 8.2 Hz), 128.87, 127.90 (d, *J* = 3.4 Hz), 126.57, 119.45, 114.79 (d, *J* = 21.8 Hz), 110.15, 59.20, 55.62, 45.00, 33.36, 30.64, 12.77. HRMS calculated for C<sub>24</sub>H<sub>26</sub>FN<sub>3</sub>O<sub>2</sub> (M+H)<sup>+</sup> 408.2087, found 408.2106.

#### 6-fluoro-4-(pyridin-4-yl)-1H-indole (141)

4-bromo-6-fluoro-1H-indole **140** (700 mg, 3.27 mmol, 1 eq) and pyridin-4-ylboronic acid (800 mg, 6.54 mmol, 2 eqs) were dissolved in 12 mL 1,4 dioxane and 2M Na<sub>2</sub>CO<sub>3</sub> (8 mL) in a microwave vial and degassed for 10 minutes under nitrogen. Pd(dppf)Cl<sub>2</sub> (240 mg, 0.327 mmol, 0.1 eq) was added and the reaction was heated in the microwave at 125°C for 30 minutes. The reaction was determined complete by LC-MS analysis. The reaction mixture was partitioned between EtOAc and water and the organic phase was separated. The aqueous phase was extracted with EtOAc (2 x). The combined organic phase was dried over sodium sulphate, filtered over celite and the filtrate was concentrated under reduced pressure. Purification by silica gel chromatography (25% → 50% → 75% EtOAc/Hexanes) afforded 6-fluoro-4-(pyridin-4-yl)-1H-indole **141** (615 mg, 89% yield, 93% purity by LC-MS) as a pale brown solid.

<sup>1</sup>H NMR (500 MHz, DMSO-*d*<sub>6</sub>) δ 11.43 (s, 1H), 8.70 – 8.64 (m, 2H), 7.71 – 7.66 (m, 2H), 7.47 (dd, *J* = 3.2, 2.4 Hz, 1H), 7.28 (ddd, *J* = 9.6, 2.3, 0.9 Hz, 1H), 7.10 (dd, *J* = 10.6, 2.3 Hz, 1H), 6.60 (ddd, *J* = 3.1, 1.9, 0.9 Hz, 1H). (M+H)<sup>+</sup> 212.90

**6-fluoro-4-(pyridin-4-yl)-1-tosyl-1H-indole (142)**

6-fluoro-4-(pyridin-4-yl)-1H-indole **141** (600 mg, 2.83 mmol, 1 eq) was dissolved in 8 mL anhydrous DMF and cooled to 0°C under nitrogen. NaH 60% dispersion in mineral oil (115 mg, 4.80 mmol, 1.7 eqs,) was added and the reaction was stirred for 1 hour at 0°C. Tosyl chloride (700 mg, 3.67 mmol, 1.3 eqs) was added and the reaction was warmed to room temperature. After 2 hours, the reaction was determined complete by LC-MS analysis and quenched by the addition of 1 mL water. The reaction was concentrated under reduced pressure and the concentrate was partitioned between EtOAc and water. The organic phase was separated, and the aqueous phase was extracted with EtOAc (2 x). The combined organic phase was dried over sodium sulphate and concentrated under reduced pressure. Purification by silica gel chromatography (0% → 1% → 2% → 5% MeOH/Dichloromethane) gave 6-fluoro-4-(pyridin-4-yl)-1-tosyl-1H-indole **142** (1.0 g, 97% yield, 94% purity by LC-MS) as a pale yellow solid.

<sup>1</sup>H NMR (500 MHz, DMSO-*d*<sub>6</sub>) δ 8.70 – 8.62 (m, 2H), 7.99 – 7.91 (m, 3H), 7.82 (ddd, *J* = 9.5, 2.3, 0.8 Hz, 1H), 7.61 – 7.56 (m, 2H), 7.44 – 7.33 (m, 3H), 6.90 (dd, *J* = 3.8, 0.8 Hz, 1H). (M+H)<sup>+</sup> 367.1

**2-bromo-6-fluoro-4-(pyridin-4-yl)-1-tosyl-1H-indole (143)**

6-fluoro-4-(pyridin-4-yl)-1-tosyl-1H-indole **142** (700 mg, 1.91 mmol, 1 eq) was dissolved in 10 mL anhydrous THF and cooled to -78°C under nitrogen. TMEDA (0.32 mL, density = 0.775 g/mL, 2.1 mmol, 1.1 eqs) was added by means of a syringe. After 5 minutes, LDA 2M solution in THF (1.63 mL, 3.26 mmol, 1.7 eqs) was added dropwise over 2 minutes by means of a syringe and the reaction was stirred at -78°C for 1.5 hours. 1,2-dibromo-1,1,2,2-tetrachloroethane (935 mg, 2.87 mmol, 1.5 eqs) was dissolved in 2 mL THF and added to the reaction mixture by means of a cannula. The reaction was stirred further for 2 hours maintaining the temperature at -78°C and was deemed complete by LC-MS analysis. The reaction was quenched by the addition of 1 mL water and was concentrated under reduced pressure. The concentrate was partitioned between EtOAc and water and the organic phase was separated.

The aqueous phase was extracted with EtOAc (3 x). The combined organic phase was washed with brine (1 x), dried over sodium sulphate and concentrated under reduced pressure. Purification by silica gel chromatography (10% → 25% → 50% → 75% EtOAc/Hexanes) yielded 2-bromo-6-fluoro-4-(pyridin-4-yl)-1-tosyl-1H-indole **143** (400 mg, 47% yield, 82% purity by LC-MS) as a yellow oil.

<sup>1</sup>H NMR (500 MHz, DMSO-*d*<sub>6</sub>) δ 8.70 – 8.63 (m, 2H), 8.04 (ddd, *J* = 10.1, 2.3, 0.8 Hz, 1H), 7.90 – 7.84 (m, 2H), 7.62 – 7.55 (m, 2H), 7.47 – 7.38 (m, 3H), 7.11 (d, *J* = 0.8 Hz, 1H), 2.34 (s, 3H). (M+H)<sup>+</sup> 445.55, 446.1

**tert-Butyl 4-(6-fluoro-4-(pyridin-4-yl)-1-tosyl-1H-indol-2-yl)-3,6-dihydropyridine-1(2H)-carboxylate (144)**

2-bromo-6-fluoro-4-(pyridin-4-yl)-1-tosyl-1H-indole **143** (400 mg, 0.898 mmol, 1 eq) and tert-butyl 4-(4,4,5,5-tetramethyl-1,3,2-dioxaborolan-2-yl)-3,6-dihydropyridine-1(2H)-carboxylate (555 mg, 1.795 mmol, 2 eq) were dissolved in 10 mL 1,4 dioxane and 2M Na<sub>2</sub>CO<sub>3</sub> (7 mL) in a microwave vial and degassed under nitrogen for 10 minutes. Pd(dppf)Cl<sub>2</sub> (66 mg, 0.089 mmol, 0.1 eq) was added and the reaction was heated at 125°C for 15 minutes in the microwave. The reaction was determined complete by LC-MS analysis and was partitioned between EtOAc and water. The organic phase was separated, and the aqueous phase was extracted with EtOAc (3 x). The combined organic phase was dried over sodium sulphate and concentrated under reduced pressure. Purification by silica gel chromatography (10% → 25% → 50% EtOAc/Hexanes) afforded tert-butyl 4-(6-fluoro-4-(pyridin-4-yl)-1-tosyl-1H-indol-2-yl)-3,6-dihydropyridine-1(2H)-carboxylate **144** (520 mg, 76% yield, 72% purity by LC-MS) as a deep maroon oil.

<sup>1</sup>H NMR (500 MHz, DMSO-*d*<sub>6</sub>) δ 8.74 – 8.58 (m, 2H), 8.04 – 7.85 (m, 1H), 7.73 – 7.25 (m, 6H), 6.83 – 6.66 (m, 1H), 5.80 (s, 1H), 4.11 – 3.83 (m, 2H), 3.57 (dt, *J* = 16.0, 5.8 Hz, 2H), 2.35 – 2.22 (m, 4H), 1.55 – 1.30 (m, 11H). (M+H)<sup>+</sup> 547.9

**tert-Butyl 4-(6-fluoro-4-(pyridin-4-yl)-1H-indol-2-yl)-3,6-dihydropyridine-1(2H)-carboxylate (145)**

tert-Butyl 4-(6-fluoro-4-(pyridin-4-yl)-1-tosyl-1H-indol-2-yl)-3,6-dihydropyridine-1(2H)-carboxylate **144** (400 mg, 0.73 mmol, 1 eq, 72% purity) was dissolved in 3 mL 1,4 dioxane in a microwave vial. 1N NaOH (1.5 mL) was added and the reaction was heated at 125°C for 3 hours in the microwave. The reaction was concentrated under reduced pressure and the concentrate was partitioned between EtOAc and water. The organic phase was separated, and the aqueous phase was extracted with EtOAc (3 x). The combined organic phase was dried over sodium sulphate and concentrated under reduced pressure. Purification by silica gel chromatography (10% → 25% → 50% → 75% → 100% EtOAc/Hexanes) gave tert-butyl 4-(6-fluoro-4-(pyridin-4-yl)-1H-indol-2-yl)-3,6-dihydropyridine-1(2H)-carboxylate **145** (150 mg, 54% yield, 85% purity by LC-MS).

<sup>1</sup>H NMR (500 MHz, DMSO-*d*<sub>6</sub>) δ 11.56 (d, *J* = 1.8 Hz, 1H), 8.70 – 8.63 (m, 2H), 7.71 – 7.65 (m, 2H), 7.16 (ddd, *J* = 9.4, 2.3, 0.9 Hz, 1H), 7.10 – 7.03 (m, 1H), 6.63 (d, *J* = 1.5 Hz, 1H), 6.32 (s, 1H), 4.04 (s, 2H), 3.52 (t, *J* = 5.7 Hz, 2H), 1.41 (s, 11H). (M+H)<sup>+</sup> 394.15

**tert-Butyl 4-(6-fluoro-4-(pyridin-4-yl)-1H-indol-2-yl)piperidine-1-carboxylate (146)**

tert-Butyl 4-(6-fluoro-4-(pyridin-4-yl)-1H-indol-2-yl)-3,6-dihydropyridine-1(2H)-carboxylate **145** (130 mg, 0.33 mmol, 1 eq) was dissolved in 6 mL EtOH and 3 mL AcOH. Palladium on carbon (50 mg) was added and the reaction was set up for hydrogenation using a hydrogen balloon setup. The reaction was stirred for 3 hours at room temperature and was determined complete by LC-MS analysis. The reaction mixture was filtered over celite and the filtrate was concentrated under reduced pressure. The subsequent concentrate was partitioned between EtOAc and water. The pH of the biphasic mixture was brought to 9 by the addition of 1N NaOH. The organic phase was separated, and the aqueous phase was extracted with EtOAc (3 x). The combined organic phase was dried over sodium sulphate and concentrated under reduced pressure. Purification by silica gel chromatography (10% → 25% → 50% → 75% → 100%

EtOAc/Hexanes) gave tert-butyl 4-(6-fluoro-4-(pyridin-4-yl)-1H-indol-2-yl)piperidine-1-carboxylate **146** (93 mg, 72% yield, 91% purity by LC-MS).

<sup>1</sup>H NMR (500 MHz, DMSO-*d*<sub>6</sub>) δ 11.36 (d, *J* = 2.2 Hz, 1H), 8.68 – 8.62 (m, 2H), 7.70 – 7.63 (m, 2H), 7.15 (ddd, *J* = 9.5, 2.3, 0.9 Hz, 1H), 7.05 (dd, *J* = 10.7, 2.3 Hz, 1H), 6.36 (dt, *J* = 1.8, 0.8 Hz, 1H), 4.03 (d, *J* = 11.2 Hz, 2H), 2.96 – 2.72 (m, 3H), 1.99 – 1.87 (m, 2H), 1.62 – 1.48 (m, 2H), 1.39 (s, 9H). (M+H)<sup>+</sup> 395.75

#### **6-fluoro-2-(piperidin-4-yl)-4-(pyridin-4-yl)-1H-indole (147)**

tert-Butyl 4-(6-fluoro-4-(pyridin-4-yl)-1H-indol-2-yl)piperidine-1-carboxylate **146** (85 mg, 0.215 mmol, 1 eq) was dissolved in 6 mL MeOH and 4N HCl in 1,4 dioxane (1 mL). The reaction was stirred overnight at room temperature and was deemed complete by LC-MS analysis. The reaction was concentrated under reduced pressure to give crude 6-fluoro-2-(piperidin-4-yl)-4-(pyridin-4-yl)-1H-indole **147** (68 mg, 86% yield, 92% purity by LC-MS) which was taken onto the next step without further purification. (M+H)<sup>+</sup> 294.85

#### **6-fluoro-2-(1-methylpiperidin-4-yl)-4-(pyridin-4-yl)-1H-indole (148) [RUPB-39]**

Crude 6-fluoro-2-(piperidin-4-yl)-4-(pyridin-4-yl)-1H-indole **147** (68 mg, 0.23 mmol, 1 eq) was dissolved in 7 mL MeOH and 1 mL AcOH. Formaldehyde 37% solution in water (1 mL, excess) was added and the reaction was stirred for 1.5 hours at room temperature. NaBH<sub>4</sub> (70 mg, 1.85 mmol, 8 eqs) was added to the imine generated and the reaction was allowed to stir for 30 minutes at room temperature. The reaction was deemed complete, quenched by the addition of 2 mL water and concentrated under reduced pressure. The residue was partitioned between 1N HCl and EtOAc. The aqueous phase was separated, and the organic phase was extracted with water (3 x). The combined aqueous phase was basified with 1N NaOH to pH 9 and extracted with EtOAc (3 x). The combined organic phase was washed with brine (1 x), dried over sodium sulphate and concentrated. Purification by silica gel chromatography (4% → 8% → 12% MeOH/CHCl<sub>3</sub> with 0.25% NH<sub>3</sub>) afforded the title compound 6-fluoro-2-(1-methylpiperidin-4-yl)-4-(pyridin-4-yl)-1H-indole **148** [RUPB-39] (35 mg, 50% yield, 99% purity by LC-MS) as a yellow solid.

$^1\text{H}$  NMR (500 MHz,  $\text{DMSO-}d_6$ )  $\delta$  11.35 (d,  $J = 2.2$  Hz, 1H), 8.65 (d,  $J = 5.1$  Hz, 2H), 7.74 – 7.61 (m, 2H), 7.15 (dd,  $J = 9.5, 2.2$  Hz, 1H), 7.04 (dd,  $J = 10.7, 2.3$  Hz, 1H), 6.41 – 6.27 (m, 1H), 3.15 (s, 1H), 2.87 (dt,  $J = 11.3, 3.6$  Hz, 2H), 2.67 (tt,  $J = 11.7, 3.7$  Hz, 1H), 2.21 (s, 3H), 2.11 – 1.90 (m, 4H), 1.70 (qd,  $J = 12.3, 3.7$  Hz, 2H).

$^{13}\text{C}$  NMR (126 MHz,  $\text{Methanol-}d_4$ )  $\delta$  159.12 (d,  $J = 235.1$  Hz), 149.36 (d,  $J = 2.2$  Hz), 148.89, 145.27 (d,  $J = 3.3$  Hz), 136.96 (d,  $J = 12.6$  Hz), 129.97 (d,  $J = 9.5$  Hz), 123.47, 122.80, 106.65 (d,  $J = 25.5$  Hz), 97.32 (d,  $J = 25.8$  Hz), 95.40, 55.00, 44.74, 34.41, 30.92.

HRMS calculated for  $\text{C}_{19}\text{H}_{20}\text{FN}_3$  ( $\text{M}+\text{H}$ ) $^+$  310.1720, found 310.1732.

## C. BIOLOGICAL EVALUATION

### 1. PKG Expression

Full length *Pf*PKG was cloned into the pTrcHisC vector for expression in BL21 (DE3) Star cells. An LB culture containing 50 ug/ml carbenicillin (250 mL) was grown overnight at 37°C. The following day the culture was cooled on ice for about 10-15 minutes and divided equally into two new 125 mL cultures. 125 ml of fresh LB broth containing carbenicillin was added to each flask bringing the volume of each flask to 250 ml. Cultures were shaken at 18°C before induction with IPTG (1.0 mM) for 18 – 24 hours. The bacterial pellet was frozen at -80°C until protein purification. Cells were lysed with Bacterial Protein Extraction Reagent (Thermo Scientific) on ice for 10-15 min. Supernatant was obtained after centrifugation of lysate at 21,000 x g for 15 min at 4°C. Supernatant was incubated for 30 min at 4°C with rotation with HisPur Cobalt Resin (Thermo Scientific) which had been pre-washed with Wash buffer (50 mM Hepes pH 7.8, 120 mM KCl, 20 mM NaCl, 10 mM Imidazole). Resin was added to a

gravity column that was allowed to empty through gravity flow. The resin was washed with Wash buffer until no more protein was eluted off the column as determined by a Bradford assay. A second wash was performed with Wash buffer containing 300 mM NaCl as in the previous wash step. Bound protein was eluted in 50 mM Hepes pH 7.8, 120 mM KCl, 20 mM NaCl, 250 mM Imidazole. Protein was dialyzed overnight in 50 mM Hepes pH 7.8, 120 mM KCl, 20 mM NaCl and 10% glycerol, with two buffer exchanges. Dialyzed protein was concentrated in a Corning Spin-X concentrator and assayed for activity using the IMAP FP Progressive Screening Expression kit (Molecular Devices, catalog # R8127) following the manufacturer's protocol.

Human PKG, cloned into a pENTR221 vector, was obtained from DNASU.org. (HsCD00351766). It was cloned into a mammalian expression plasmid, Gateway pDEST27 (Invitrogen), for expression as a GST fusion protein, using LR Clonase II Plus enzyme (Invitrogen). The hPKG – pDEST27 plasmid was amplified in DH5 $\alpha$  Max Efficiency Competent Cells and purified with a PureYield Plasmid Midiprep System (Promega) following the manufacture's protocol. Expi293 cells were transfected with hPKG-pDEST27 using the Expifectamine 293 Transfection Kit (Gibco). After 18 hours, enhancing reagent (Gibco) was added. Cells were then collected 48 hours post-enhancing, centrifuged at 2000 x g for 10 min, washed in ice cold PBS and frozen as a pellet at -80°C until protein purification. The cell pellet was lysed with Mammalian Protein Extraction Reagent (Thermo Fisher) for 10 – 15 min. The lysate was centrifuged at 21,000 x g for 15 minutes at 4°C. The supernatant was incubated for 1 hour at 4°C with glutathione resin that was pre-washed 10 times with ice cold Wash Buffer (50 mM Hepes pH 7.8, 120 mM KCl, 20 mM NaCl, 10% glycerol). The resin was loaded onto a column and washed with resin wash buffer by gravity flow until no more protein was detectable in the washes by a Bradford assay. Protein was eluted with 10 mg/ml glutathione in Wash buffer. The protein was concentrated using a 30K MWCO Corning Spin X concentrator and assayed for activity.

## 2. PKG Assay

*Plasmodium falciparum* PKG (*Pf*PKG) and human PKG (hPKG) kinase activity was assayed using a commercial immobilized metal ion affinity-based fluorescence polarization (IMAP) assay according to the manufacture's protocol (Molecular Devices). Briefly, kinase assays (20  $\mu$ l in black half volume 96 well microtiter plates) contained the following: 10 mM Tris-HCl, pH 7.2, 10 mM MgCl<sub>2</sub>, 0.05% NaN<sub>3</sub>, 0.01% Tween®20, 10  $\mu$ M ATP, 1  $\mu$ M cGMP and 21 ng of recombinant enzyme per well. Compounds were preincubated with enzyme at 25°C for 15 minutes and reactions were initiated with the addition of 120 nM fluorescent peptide substrates, FAM-PKA tide for *Pf*PKG and FAM-IP3R for hPKG (Molecular Devices). Fluorescent polarization was measured using a Synergy 2 Microplate reader (BioTek, Winooski, VT). Fluorescent polarization was read in parallel and perpendicular with an excitation wavelength of 485 nm and an emission wavelength of 528 nm. IC<sub>50</sub> data was analyzed using a four-parameter logistic curve fit using Microsoft Excel Solver.



## VI. REFERENCES

1. Beale, J. J.; Block, J., *Wilson and Gisvold's Textbook of Organic, Medicinal and Pharmaceutical Chemistry Twelfth Edition* **2011**. Ed. Lippincott Williams & Wilkins; pp 242-257.
2. Falagas, M.; Pappas, G.; Kiriaze, I., Insights into infectious disease in the era of Hippocrates. *International Journal of Infectious Diseases* **2008**, *12*, 347-350.
3. Lalchandama, K., The Making of Modern Malariology: From Miasma to Mosquito-Malaria Theory. *Science Vision* **2014**, *14* (1), 2-8.
4. Malaria. World Health Organization. Available at <https://www.who.int/news-room/fact-sheets/detail/malaria>
5. Suh, K. N.; Kain, K. C.; Keystone, J. S., Malaria. *Canadian Medical Association Journal* **2004**, *170* (11), 1693.
6. Rang, H. P.; Dale, M. M.; Ritter, J. M.; Flower, R. J.; Henderson, G., *Rang and Dale's Pharmacology Seventh Edition* **2011**. Elsevier: pp 655-664.
7. Diagnosis of Malaria. In *Guidelines for the Treatment of Malaria*, 3 ed.; World Health Organization: **2018**.
8. Malaria. Centers for Disease Control and Prevention. Available at <https://www.cdc.gov/parasites/malaria/index.html>
9. Sharma, G.; Yogi, A.; Gaur, K.; Dashora, A., A Review on Antimalarial Drugs. *International Journal of Basic Clinical Pharmacy and Research* **2015**.
10. Pennisi, E., Genetic Change Wards Off Malaria. *Science* **2001**, *294* (5546), 1439.
11. Van den Bossche, H., Chemotherapy of parasitic infections. *Nature* **1978**, *273* (5664), 626-630.
12. Warhurst, D. C.; Craig, J. C.; Adagu, I. S., Lysosomes and drug resistance in malaria. *The Lancet* **2002**, *360* (9345), 1527-1529.
13. Ashley, E. A.; Dhorda, M.; Fairhurst, R. M.; Amaratunga, C.; Lim, P.; Suon, S.; Sreng, S.; Anderson, J. M.; Mao, S.; Sam, B.; Sopha, C.; Chuor, C. M.; Nguon, C.; Sovannaroeth, S.; Pukrittayakamee, S.; Jittamala, P.; Chotivanich, K.; Chutasmit, K.; Suchatsoonthorn, C.; Runchaoen, R.; Hien, T. T.; Thuy-Nhien, N. T.; Thanh, N. V.; Phu, N. H.; Htut, Y.; Han, K.-T.; Aye, K. H.; Mokuolu, O. A.; Olaosebikan, R. R.; Folaranmi, O. O.; Mayxay, M.; Khanthavong, M.; Hongvanthong, B.; Newton, P. N.; Onyamboko, M. A.; Fanello, C. I.; Tshefu, A. K.; Mishra, N.; Valecha, N.; Phyto, A. P.; Nosten, F.; Yi, P.; Tripura, R.; Borrmann, S.; Bashraheil, M.; Peshu, J.; Faiz, M. A.; Ghose, A.; Hossain, M. A.; Samad, R.; Rahman, M. R.; Hasan, M. M.; Islam, A.; Miotto, O.; Amato, R.; MacInnis, B.; Stalker, J.; Kwiatkowski, D. P.; Bozdech, Z.; Jeeyapant, A.; Cheah, P. Y.; Sakulthaew, T.; Chalk, J.; Intharabut, B.; Silamut, K.; Lee, S. J.; Vihokhern, B.; Kunasol, C.; Imwong, M.; Tarning, J.; Taylor, W. J.; Yeung, S.; Woodrow, C. J.; Flegg, J. A.; Das, D.; Smith, J.; Venkatesan, M.; Plowe, C. V.; Stepniewska, K.; Guerin, P. J.; Dondorp, A. M.; Day, N. P.; White, N. J., Spread of Artemisinin Resistance in Plasmodium falciparum Malaria. *New England Journal of Medicine* **2014**, *371* (5), 411-423.

14. Menard, D.; Dondorp, A., Antimalarial Drug Resistance: A Threat to Malaria Elimination. *Cold Spring Harbor Perspectives in Medicine* **2017**, 1-24.
15. Lell, B.; Kremsner, P. G., Clindamycin as an Antimalarial Drug: Review of Clinical Trials. *Antimicrobial Agents and Chemotherapy* **2002**, 46 (8), 2315.
16. Treatment of uncomplicated *P. falciparum* malaria. In *Guidelines for the Treatment of Malaria*, World Health Organization: **2018**; pp 31-58.
17. Treatment of uncomplicated malaria caused by *P. vivax*, *P. malariae*, *P. ovale* or *P. knowlesi*. In *Guidelines for the Treatment of Malaria*, World Health Organization: **2018**; pp 59-70.
18. Treatment of Severe Malaria. In *Guidelines for the Treatment of Malaria*, World Health Organization: **2018**; pp 71-88.
19. Kafy, H. T.; Ismail, B. A.; Mnzava, A. P.; Lines, J.; Abdin, M. S. E.; Eltaher, J. S.; Banaga, A. O.; West, P.; Bradley, J.; Cook, J.; Thomas, B.; Subramaniam, K.; Hemingway, J.; Knox, T. B.; Malik, E. M.; Yukich, J. O.; Donnelly, M. J.; Kleinschmidt, I., Impact of insecticide resistance in *Anopheles arabiensis* on malaria incidence and prevalence in Sudan and the costs of mitigation. *Proceedings of the National Academy of Sciences* **2017**, 114 (52), E11267.
20. World Malaria Report **2018**. World Health Organization.
21. Graewe, S.; Stanway, R. R.; Rennenberg, A.; Heussler, V. T., Chronicle of a death foretold: Plasmodium liver stage parasites decide on the fate of the host cell. *FEMS Microbiology Reviews* **2012**, 36 (1), 111-130.
22. Alonso, P. L.; Sacarlal, J.; Aponte, J. J.; Leach, A.; Macete, E.; Aide, P.; Sigauque, B.; Milman, J.; Mandomando, I.; Bassat, Q.; Guinovart, C.; Espasa, M.; Corachan, S.; Lievens, M.; Navia, M. M.; Dubois, M.-C.; Menendez, C.; Dubovsky, F.; Cohen, J.; Thompson, R.; Ballou, W. R., Duration of protection with RTS,S/AS02A malaria vaccine in prevention of Plasmodium falciparum disease in Mozambican children: single-blind extended follow-up of a randomised controlled trial. *The Lancet* **2005**, 366 (9502), 2012-2018.
23. Govindasamy, K.; Jebiwott, S.; Jaijyan, D. K.; Davidow, A.; Ojo, K. K.; Van Voorhis, W. C.; Brochet, M.; Billker, O.; Bhanot, P., Invasion of hepatocytes by Plasmodium sporozoites requires cGMP-dependent protein kinase and calcium dependent protein kinase 4. *Mol Microbiol* **2016**, 102 (2), 349-363.
24. Coppi, A.; Pinzon-Ortiz, C.; Hutter, C.; Sinnis, P., The Plasmodium circumsporozoite protein is proteolytically processed during cell invasion. *The Journal of Experimental Medicine* **2005**, 201 (1), 27.
25. Coppi, A.; Tewari, R.; Bishop, J. R.; Bennett, B. L.; Lawrence, R.; Esko, J. D.; Billker, O.; Sinnis, P., Heparan Sulfate Proteoglycans Provide a Signal to Plasmodium Sporozoites to Stop Migrating and Productively Invade Host Cells. *Cell Host & Microbe* **2007**, 2 (5), 316-327.
26. Brochet, M.; Collins, M. O.; Smith, T. K.; Thompson, E.; Sebastian, S.; Volkmann, K.; Schwach, F.; Chappell, L.; Gomes, A. R.; Berriman, M.; Rayner, J. C.; Baker, D. A.; Choudhary, J.; Billker, O., Phosphoinositide Metabolism Links cGMP-Dependent Protein Kinase G to Essential Ca<sup>2+</sup> Signals at Key Decision Points in the Life Cycle of Malaria Parasites. *PLOS Biology* **2014**, 12 (3), e1001806.

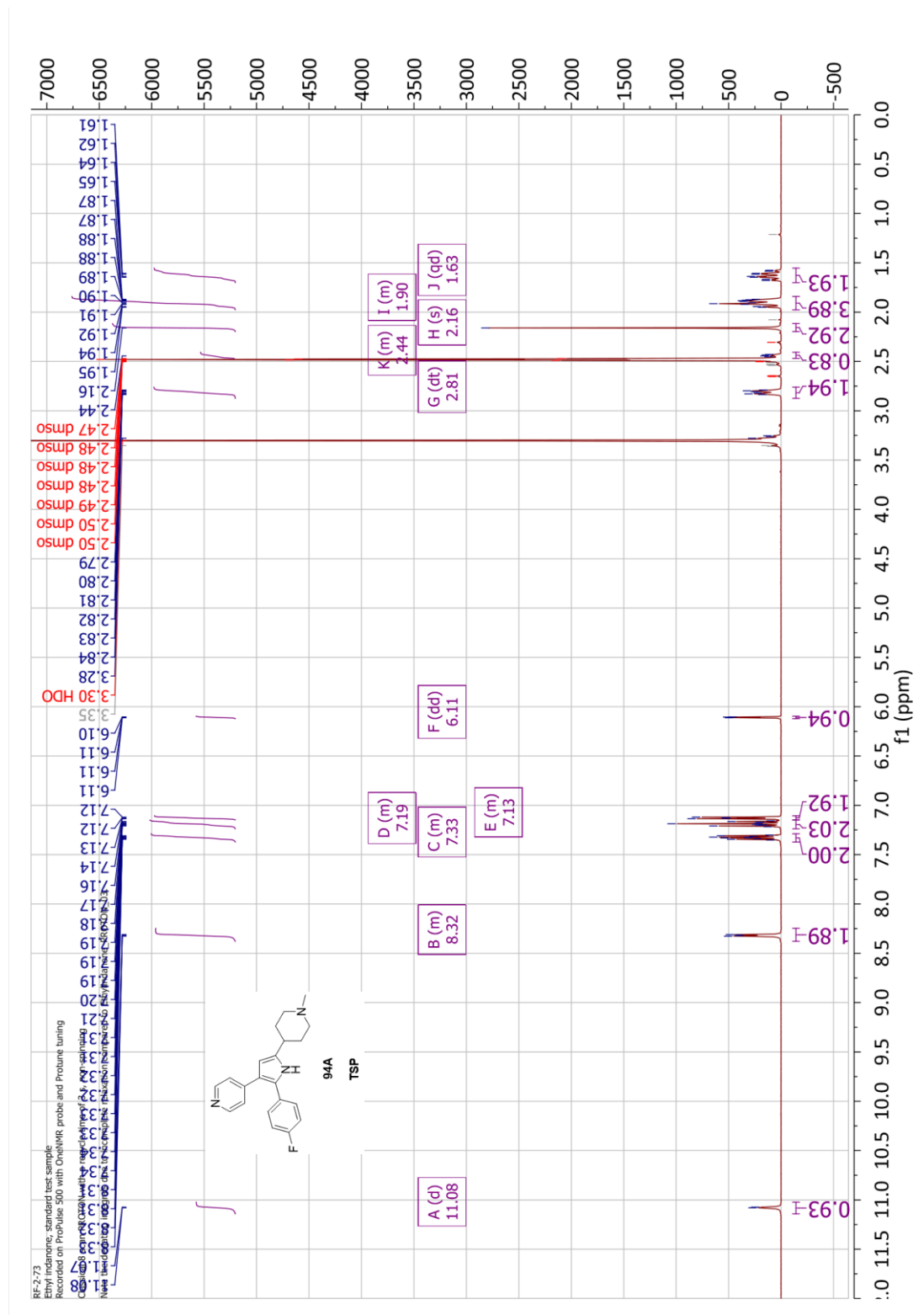
27. Donald, R. G. K.; Allocco, J.; Singh, S. B.; Nare, B.; Salowe, S. P.; Wiltsie, J.; Liberator, P. A., Toxoplasma gondii Cyclic GMP-Dependent Kinase: Chemotherapeutic Targeting of an Essential Parasite Protein Kinase. *Eukaryotic Cell* **2002**, *1* (3), 317.
28. McRobert, L.; Taylor, C. J.; Deng, W.; Fivelman, Q. L.; Cummings, R. M.; Polley, S. D.; Billker, O.; Baker, D. A., Gametogenesis in Malaria Parasites Is Mediated by the cGMP-Dependent Protein Kinase. *PLOS Biology* **2008**, *6* (6), e139.
29. Taylor, H. M.; McRobert, L.; Grainger, M.; Sicard, A.; Dluzewski, A. R.; Hopp, C. S.; Holder, A. A.; Baker, D. A., The Malaria Parasite Cyclic GMP-Dependent Protein Kinase Plays a Central Role in Blood-Stage Schizogony. *Eukaryotic Cell* **2010**, *9* (1), 37.
30. Sebastian, S.; Brochet, M.; Collins, Mark O.; Schwach, F.; Jones, Matthew L.; Goulding, D.; Rayner, Julian C.; Choudhary, Jyoti S.; Billker, O., A Plasmodium Calcium-Dependent Protein Kinase Controls Zygote Development and Transmission by Translationally Activating Repressed mRNAs. *Cell Host & Microbe* **2012**, *12* (1), 9-19.
31. Gurnett, A. M.; Liberator, P. A.; Dulski, P. M.; Salowe, S. P.; Donald, R. G. K.; Anderson, J. W.; Wiltsie, J.; Diaz, C. A.; Harris, G.; Chang, B.; Darkin-Rattray, S. J.; Nare, B.; Crumley, T.; Blum, P. S.; Misura, A. S.; Tamas, T.; Sardana, M. K.; Yuan, J.; Biftu, T.; Schmatz, D. M., Purification and Molecular Characterization of cGMP-dependent Protein Kinase from Apicomplexan Parasites: A Novel Chemotherapeutic Agent. *Journal of Biological Chemistry* **2002**, *277* (18), 15913-15922.
32. Panchal, D.; Bhanot, P., Activity of a Trisubstituted Pyrrole in Inhibiting Sporozoite Invasion and Blocking Malaria Infection. *Antimicrobial Agents and Chemotherapy* **2010**, *54* (10), 4269.
33. Gilson, P. R., Malaria Parasites Do the Stick-and-Slip Shuffle. *Cell Host & Microbe* **2009**, *6* (6), 499-501.
34. Wiersma, H. I.; Galuska, S. E.; Tomley, F. M.; Sibley, L. D.; Liberator, P. A.; Donald, R. G. K., A role for coccidian cGMP-dependent protein kinase in motility and invasion. *International Journal for Parasitology* **2004**, *34* (3), 369-380.
35. Collins, C. R.; Hackett, F.; Strath, M.; Penzo, M.; Withers-Martinez, C.; Baker, D. A.; Blackman, M. J., Malaria Parasite cGMP-dependent Protein Kinase Regulates Blood Stage Merozoite Secretory Organelle Discharge and Egress. *PLOS Pathogens* **2013**, *9* (5), e1003344.
36. Baker, D. A.; Stewart, L. B.; Large, J. M.; Bowyer, P. W.; Ansell, K. H.; Jiménez-Díaz, M. B.; El Bakkouri, M.; Birchall, K.; Dechering, K. J.; Boulloc, N. S.; Coombs, P. J.; Whalley, D.; Harding, D. J.; Smiljanic-Hurley, E.; Wheldon, M. C.; Walker, E. M.; Dessens, J. T.; Lafuente, M. J.; Sanz, L. M.; Gamo, F.-J.; Ferrer, S. B.; Hui, R.; Bousema, T.; Angulo-Barturén, I.; Merritt, A. T.; Croft, S. L.; Gutteridge, W. E.; Kettleborough, C. A.; Osborne, S. A., A potent series targeting the malarial cGMP-dependent protein kinase clears infection and blocks transmission. *Nature Communications* **2017**, *8* (1), 430.
37. Donald, R. G. K.; Zhong, T.; Wiersma, H.; Nare, B.; Yao, D.; Lee, A.; Allocco, J.; Liberator, P. A., Anticoccidial kinase inhibitors: Identification of protein kinase targets secondary to cGMP-dependent protein kinase. *Molecular and Biochemical Parasitology* **2006**, *149* (1), 86-98.

38. Tsagris, D. J.; Birchall, K.; Boulloc, N.; Large, J. M.; Merritt, A.; Smiljanic-Hurley, E.; Wheldon, M.; Ansell, K. H.; Kettleborough, C.; Whalley, D.; Stewart, L. B.; Bowyer, P. W.; Baker, D. A.; Osborne, S. A., Trisubstituted thiazoles as potent and selective inhibitors of *Plasmodium falciparum* protein kinase G (PfPKG). *Bioorganic & Medicinal Chemistry Letters* **2018**, 28 (19), 3168-3173.
39. Jones, R. A., *The Chemistry of Heterocyclic Compounds* **1990**; Vol. 48.
40. Zhang, M.; Fang, X.; Neumann, H.; Beller, M., General and Regioselective Synthesis of Pyrroles via Ruthenium-Catalyzed Multicomponent Reactions. *Journal of the American Chemical Society* **2013**, 135 (30), 11384-11388.
41. Zheng, J.; Huang, L.; Huang, C.; Wu, W.; Jiang, H., Synthesis of Polysubstituted Pyrroles via Pd-Catalyzed Oxidative Alkene C–H Bond Arylation and Amination. *The Journal of Organic Chemistry* **2015**, 80 (2), 1235-1242.
42. Rajasekar, S.; Anbarasan, P., Rhodium-Catalyzed Transannulation of 1,2,3-Triazoles to Polysubstituted Pyrroles. *The Journal of Organic Chemistry* **2014**, 79 (17), 8428-8434.
43. Rapoport, H.; Bordner, J., Synthesis of Substituted 2,2'-Bipyrroles1a. *The Journal of Organic Chemistry* **1964**, 29 (9), 2727-2731.
44. Bordner, J.; Rapoport, H., Synthesis of 2,2'-Bipyrroles from 2-Pyrrolinones1a. *The Journal of Organic Chemistry* **1965**, 30 (11), 3824-3828.
45. de Laszlo, S. E.; Visco, D.; Agarwal, L.; Chang, L.; Chin, J.; Croft, G.; Forsyth, A.; Fletcher, D.; Frantz, B.; Hacker, C.; Hanlon, W.; Harper, C.; Kostura, M.; Li, B.; Luell, S.; MacCoss, M.; Mantlo, N.; O'Neill, E. A.; Orevillo, C.; Pang, M.; Parsons, J.; Rolando, A.; Sahly, Y.; Sidler, K.; Widmer, W. R.; O'Keefe, S. J., Pyrroles and other heterocycles as inhibitors of P38 kinase. *Bioorganic & Medicinal Chemistry Letters* **1998**, 8 (19), 2689-2694.
46. Lee, J. C.; Laydon, J. T.; McDonnell, P. C.; Gallagher, T. F.; Kumar, S.; Green, D.; McNulty, D.; Blumenthal, M. J.; Keys, J. R.; Land vatter, S. W.; Strickler, J. E.; McLaughlin, M. M.; Siemens, I. R.; Fisher, S. M.; Livi, G. P.; White, J. R.; Adams, J. L.; Young, P. R., A protein kinase involved in the regulation of inflammatory cytokine biosynthesis. *Nature* **1994**, 372 (6508), 739-746.
47. Biftu, T.; Feng, D.; Ponpipom, M.; Girotra, N.; Liang, G.-B.; Qian, X.; Bugianesi, R.; Simeone, J.; Chang, L.; Gurnett, A.; Liberator, P.; Dulski, P.; Leavitt, P. S.; Crumley, T.; Misura, A.; Murphy, T.; Rattray, S.; Samaras, S.; Tamas, T.; Mathew, J.; Brown, C.; Thompson, D.; Schmatz, D.; Fisher, M.; Wyvratt, M., Synthesis and SAR of 2,3-diarylpyrrole inhibitors of parasite cGMP-dependent protein kinase as novel anticoccidial agents. *Bioorganic & Medicinal Chemistry Letters* **2005**, 15 (13), 3296-3301.
48. Liang, G.-B.; Qian, X.; Biftu, T.; Feng, D.; Fisher, M.; Crumley, T.; Darkin-Rattray, S. J.; Dulski, P. M.; Gurnett, A.; Leavitt, P. S.; Liberator, P. A.; Misura, A. S.; Samaras, S.; Tamas, T.; Schmatz, D. M.; Wyvratt, M., Hydroxylated N-alkyl-4-piperidinyl-2,3-diarylpyrrole derivatives as potent broad-spectrum anticoccidial agents. *Bioorganic & Medicinal Chemistry Letters* **2005**, 15 (20), 4570-4573.
49. Qian, X.; Liang, G.-B.; Feng, D.; Fisher, M.; Crumley, T.; Rattray, S.; Dulski, P. M.; Gurnett, A.; Leavitt, P. S.; Liberator, P. A.; Misura, A. S.; Samaras, S.; Tamas, T.; Schmatz, D. M.; Wyvratt, M.; Biftu, T., Synthesis and SAR Studies of diarylpyrrole anticoccidial agents. *Bioorganic & Medicinal Chemistry Letters* **2006**, 16 (10), 2817-2821.

50. Liang, G.-B.; Qian, X.; Feng, D.; Fisher, M.; Crumley, T.; Darkin-Rattray, S. J.; Dulski, P. M.; Gurnett, A.; Leavitt, P. S.; Liberator, P. A.; Misura, A. S.; Samaras, S.; Tamas, T.; Schmatz, D. M.; Wyvratt, M.; Biftu, T., N-Alkyl-4-piperidiny-2,3-diarylpyrrole derivatives with heterocyclic substitutions as potent and broad spectrum anticoccidial agents. *Bioorganic & Medicinal Chemistry Letters* **2008**, *18* (6), 2019-2022.
51. Biftu, T.; Feng, D.; Fisher, M.; Liang, G.-B.; Qian, X.; Scribner, A.; Dennis, R.; Lee, S.; Liberator, P. A.; Brown, C.; Gurnett, A.; Leavitt, P. S.; Thompson, D.; Mathew, J.; Misura, A.; Samaras, S.; Tamas, T.; Sina, J. F.; McNulty, K. A.; McKnight, C. G.; Schmatz, D. M.; Wyvratt, M., Synthesis and SAR studies of very potent imidazopyridine antiprotozoal agents. *Bioorganic & Medicinal Chemistry Letters* **2006**, *16* (9), 2479-2483.
52. Feng, D.; Fisher, M.; Liang, G.-B.; Qian, X.; Brown, C.; Gurnett, A.; Leavitt, P. S.; Liberator, P. A.; Mathew, J.; Misura, A.; Samaras, S.; Tamas, T.; Schmatz, D. M.; Wyvratt, M.; Biftu, T., Synthesis and SAR of 2-(4-fluorophenyl)-3-pyrimidin-4-ylimidazo[1,2-a]pyridine derivatives as anticoccidial agents. *Bioorganic & Medicinal Chemistry Letters* **2006**, *16* (23), 5978-5981.

## APPENDIX

### <sup>1</sup>H NMR of TSP



$^{13}\text{C}$  NMR OF TSP